Pneumolysin: the state of pore-formation in context to cell trafficking and inflammatory responses of astrocytes

Pneumolysin: Einfluss der Porenbildung auf zelluläre Transportprozesse und inflammatorische Antworten in Astrozyten

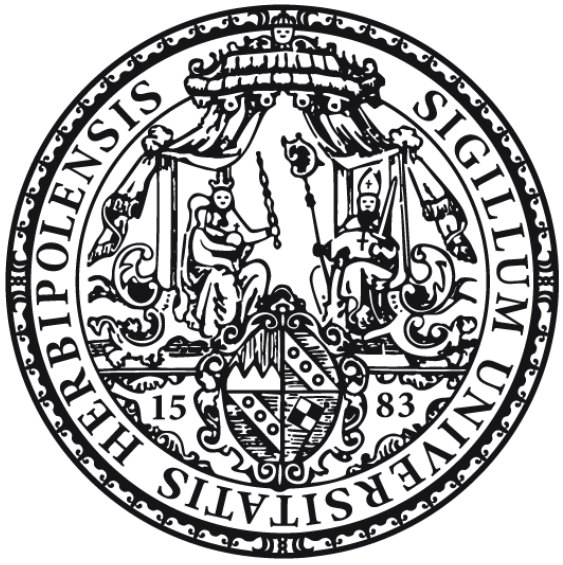

Christina Förtsch

from Leipzig

Graduate School of Life Sciences University of Würzburg

Section Biomedicine

Würzburg, January 2012

Submitted on ……

At the Graduate School of Life Sciences, University of Würzburg

Office stamp:

Members of the Thesis Comitee

Chairperson: Prof. Dr. Thomas Dandekar

1. Supervisor Dr. Asparouh I. Iliev

2. Supervisor Prof. Dr. Dr. h.c. (Barcelona) Dr. h.c. (Umeå) Roland Benz

3. Supervisor Prof. Timothy Mitchell

Date of public defense……

I hereby declare, that the following thesis entitled “Pneumolysin: the state of pore-formation in context to cell trafficking and inflammatory responses of astrocytes” is the result of my own work. I did not receive help or support from commercial consultants. All sources and/ or materials applied are listed and specified in the thesis.
Furthermore, I confirm that this thesis has not yet been submitted as part of another examination process neither in identical nor in similar form.

Würzburg, January 10th 2012

For my parents and siblings

If the brain were so simple that we could understand it, we would be so simple we couldn't. – Emeron M. Pugh

List of publications

Changes in astrocyte shape induced by sublytic concentrations of the cholesterol-dependent cytolysin pneumolysin still require pore-forming capacity

Christina Förtsch*, Sabrina Hupp*, Jiangtao Ma, Timothy J. Mitchell, Elke Maier, Roland Benz, and Asparouh I. Iliev

Toxins, 3, 43-62, 2011.

Extracellular calcium reduction strongly increases the lytic capacity of pneumolysin from *Streptococcus pneumoniae*

Carolin Wippel*, **Christina Förtsch***, Sabrina Hupp*, Elke Maier, Roland Benz, Jingtao Ma, Timothy J. Mitchell, and Asparouh I. Iliev

Journal of Infectious Diseases, 204, 930-936, 2011.

Astrocytic tissue remodeling by the meningitis neurotoxin pneumolysin facilitates pathogen tissue penetration

Sabrina Hupp, Carolin Wippel, Vera Heimeroth, **Christina Förtsch**, Jiangtao Ma, Timothy J. Mitchell, Asparouh I. Iliev

Glia, 60, 1, 137-146, 2012.

(*: shared first author)

INDEX

ABBREVIATIONS

Ø	diameter
A, Ala	alanine
ACSF	artificial cerebrospinal fluid
BBB	blood brain barrier
BCA	bicinchoninic acid
BL	black
BSA	bovine serum albumine
ca.	circa
CDC	cholesterol dependent cytolysin
CFR	case fatality rates
CNS	central nervous system
CSF	cerebrospinal fluid
cy	cyanine
DAMP	damage-associated molecular patterns
DMEM	dulbecco's Modified Eagle's Medium
EC	epithelial cells
EDTA	ethylenediaminetetraacetic acid
e.g.	for example
ELISA	enzyme linked immunosorbent assay
F, Phe	phenylalanine
Fig.	figure
FCS	fetal calf serum
FITC	fluorescein isothiocyanate
g	gravitational force
GAP	GTPase activating protein
GDP	guanosindiphosphate
GEF	guanine nucleotide exchange factor
GFP	green fluorescent protein
GTP	guanosine triphosphate
h	hour
HRP	horseradish peroxidase
IL	interleukin
ILY	intermediolysin
kDa	kilo dalton
LDH	lactate dehydrogenase
min	minutes

MOPS	3-(N-morpholino)propanesulfonic acid
NAD/H	nicotinamidadenindinucleotide
NHS	*N*-Hydroxysuccinimid
NLR	NOD-like receptors
NOD	nucleotide-binding and oligomerisation domain
p	postnatal
PAF	platlet activating factor
PAMP	pathogen-associated molecular patterns
PBS	phosphate buffered saline
PC	phosphatidyl-choline
PFA	paraformaldehyde
PFO	perfringolysin O
PI	propidium-iodide
PLB	planar lipid bilayer
PLY	pneumolysin
PMA	primary mouse astrocytes
PRR	pattern recognition receptors
PVDF	Polyvinylidenfluorid
R, Arg	arginine
RLR	retinoic acid inducible gene like receptors
ROCK	Rho associated serin- threonin kinase
ROS	reactive oxygen species
RT	room temperature
SD	sprague dawley
SDS PAGE	sodiumdodecylsulfate polyacrylamid gelelectrophoresis
SEM	standard error of the mean
TLR	toll-like receptor
TMB	tetramethylbenzidine
TNF α	tumor necrosis factor alpha
V	volt
v/v	volume per volume
W, Trp	tryptophan
WHO	world health organisation
WT	wildtype
w/v	weight per volume

ABSTRACT

English

Pneumolysin, a protein toxin, represents one of the major virulence factors of *Streptococcus pneumoniae*. This pathogen causes bacterial meningitis with especially high disease rates in young children, elderly people and immunosuppressed patients. The protein toxin belongs to the family of cholesterol-dependent cytolysins, which require membrane cholesterol in order to bind and to be activated. Upon activation, monomers assemble in a circle and undergo conformational change. This conformational change leads to the formation of a pore, which eventually leads to cell lysis. This knowledge was obtained by studies that used a higher concentration compared to the concentration of pneumolysin found in the cerebrospinal fluid of meningitis patients. Thus, a much lower concentration of pneumolysin was used in this work in order to investigate effects of this toxin on primary mouse astrocytes. Previously, a small GTPase activation, possibly leading to cytoskeletal changes, was found in a human neuroblastoma cell line. This led to the hypothesis that pneumolysin can lead to similar cytoskeletal changes in primary cells. The aim of this work was to investigate and characterise the effects of pneumolysin on primary mouse astrocytes in terms of a possible pore formation, cellular trafficking and immunological responses. Firstly, the importance of pore-formation on cytoskeletal changes was to be investigated. In order to tackle this question, wild-type pneumolysin and two mutant variants were used. One variant was generated by exchanging one amino acid in the cholesterol recognising region, the second variant was generated by deleting two amino acids in a protein domain that is essential for oligomerisation. These variants should be incapable of forming a pore and were compared to the wild-type in terms of lytic capacities, membrane binding, membrane depolarisation, pore-formation in artificial membranes (planar lipid bilayer) and effects on the cytoskeleton. These investigations resulted in the finding that the pore-formation is required for inducing cell lysis, membrane depolarisation and cytoskeletal changes in astrocytes. The variants were not able to form a pore in planar lipid bilayer and did not cause cell lysis and membrane depolarisation. However, they bound to the cell membrane to the same extent as the

wild-type toxin. Thus, the pore-formation, but not the membrane binding was the cause for these changes.

Secondly, the effect of pneumolysin on cellular trafficking was investigated. Here, the variants showed no effect, but the wild-type led to an increase in overall endocytotic events and was itself internalised into the cell. In order to characterise a possible mechanism for internalisation, a GFP-tagged version of pneumolysin was used. Several fluorescence-labelled markers for different endocytotic pathways were used in a co-staining approach with pneumolysin. Furthermore, inhibitors for two key-players in classical endocytotic pathways, dynamin and myosin II, were used in order to investigate classical endocytotic pathways and their possible involvement in toxin internalisation. The second finding of this work is that pneumolysin is taken up into the cell via dynamin- and caveolin-independent pinocytosis, which could transfer the toxin to caveosomes. From there, the fate of the toxin remains unknown. Additionally, pneumolysin leads to an overall increase in endocytotic events.

This observation led to the third aim of this work. If the toxin increases the overall rate of endocytosis, the question arises whether toxin internalisation favours bacterial tissue penetration of the host or whether it serves as a defence mechanism of the cell in order to degrade the protein. Thus, several proinflammatory cytokines were investigated, as previous studies describe an effect of pneumolysin on cytokine production. Surprisingly, only interleukin 6-production was increased after toxin-treatment and no effect of endocytotic inhibitors on the interleukin 6-production was observed. The conclusion from this finding is that pneumolysin leads to an increase of interleukin 6, which would not depend on the endocytotic uptake of pneumolysin. The production of interleukin 6 would enhance the production of acute phase proteins, T-cell activation, growth and differentiation. On the one hand, this activation could serve pathogen clearance from infected tissue. On the other hand, the production of interleukin 6 could promote a further penetration of pathogen into host tissue. This question should be further investigated.

Deutsch

Das Protein-Toxin Pneumolysin ist einer der entscheidenden Virulenzfaktoren von *Streptococcus pneumoniae*. Dieser Erreger verursacht bakterielle Meningitis, die vor allem Kleinkinder, ältere Menschen und immungeschwächte Patienten betrifft. Dieses Protein-Toxin gehört zur Familie der cholesterinabhängigen Zytolysine, die Membrancholesterol für ihre Aktivierung und Bindung benötigen. Nach der Membranbindung ordnen sich die Toxinmonomere kreisförmig an und ändern ihre Konformation, wodurch eine Pore entsteht, die dann zu einer Lyse der Zelle führt. Studien, die diese Erkenntnisse brachten, nutzen eine höhere Konzentration des Toxins, als in der zerebrospinalen Flüssigkeit von Meningitispatienten gefunden wurde. Aus diesem Grund wurde in vorliegender Arbeit genau diese Konzentration von Pneumolysin genutzt, um die Effekte dieses Toxins auf primäre Mausastrozyten zu untersuchen. Vor kurzem wurde nach Pneumolysinbehandlung in einer humanen Neuroblastomzelllinie eine Aktivierung kleiner GTPasen gefunden, die für zytoskelettale Veränderungen entscheidend sind (z.B. Zellbewegungen). Deshalb wurde die Hypothese aufgestellt, dass Pneumolysin diese zytoskelettalen Veränderungen auch in primären neuronalen Zellen auslösen könnte.

Das Ziel dieser Arbeit war, die Effekte von Pneumolysin auf primäre Mausastrozyten im Hinblick auf Porenbildung, zelluläre Transportprozesse und immunologische Antworten zu untersuchen. Im ersten Teil wird die Bedeutung der Porenbildung auf zytoskelettale Veränderungen untersucht. Hierfür wurden der Wildtyp und zwei Varianten des Pneumolysin genutzt. Die erste Variante wurde hergestellt, indem ein Aminosäureaustausch in einem Proteinbereich hergestellt wurde, der für die Membrancholesterolerkennung durch das Toxin entscheidend ist. Die zweite Variante wurde hergestellt, indem zwei Aminosäuren in der Proteinregion deletiert wurden, die entscheidend für die Oligomerisierung der Monomere ist. Diese beiden Pneumolysinvarianten sollten also nicht in der Lage sein eine Pore in der Zellmembran zu bilden und wurden mit dem Wildtyp verglichen. Hierbei wurden lytische Fähigkeiten, Membranbindung, Membrandepolarisation, Porenbildung im künstlichen Bilayer und Effekte auf das Zytoskelett untersucht. Sowohl der Wildtyp als auch die Varianten zeigten die gleiche Stärke an Membranbindung. Diese Untersuchungen weisen darauf hin, dass die Porenbildung für die Zell-Lyse, Membrandepolarisation und zytoskelettale

Veränderungen in Mausastrozyten wichtig ist und führt zu der Schlussfolgerung, dass nicht die Membranbindung, sondern die Porenbildung entscheidend für die beobachteten zytoskelettalen Veränderungen ist.

Im zweiten Teil dieser Arbeit wurde der Effekt des Pneumolysin auf zelluläre Transportprozesse untersucht. Erneut zeigten die Pneumolysinvarianten keine Wirkung, während der Wildtyp die Gesamtrate der Endozytose erhöhte. Weiterhin wurde nur der Wildtyp internalisiert. Um einen möglichen Mechanismus für die Internalisierung des Toxins vorschlagen zu können, wurde Pneumolysin als GFP-markiertes Toxin genutzt. Weiterhin wurden einige Marker für unterschiedliche endozytotische Transportprozesse genutzt um eine Ko-lokalisation mit Pneumolysin-GFP zu ermöglichen. Des Weiteren wurden Inhibitoren für zwei Schlüsselproteine endozytotischer Vorgänge, Dynamin und Myosin II, genutzt. Die Ergebnisse dieser Untersuchungen zeigten, dass Pneumolysin wahrscheinlich durch dynamin- und caveolin-unabhängige Pinozytose in die Zelle aufgenommen wird. Dieser Mechanismus führt zu der Bildung von Caveosomen, deren weiterer Transport, und somit das Schicksal des internalisierten Toxins, bis heute noch nicht aufgeklärt ist.

Die Beobachtung, dass Pneumolysin die Gesamtrate an Endozytose erhöht, führte zum dritten Teil dieser Arbeit. Wenn das Toxin die Gesamtrate an Endozytose erhöht, stellt sich die Frage, ob dieser Vorgang der Zerstörung des Toxins – also einer Abwehr der Zelle – dient, oder ob diese Internalisierung eine Strategie des Pathogens ist, um tiefer in das Wirtsgewebe einzudringen. Aktuelle Studien belegen, dass Pneumolysin einen Einfluss auf inflammatorische Antworten des Immunsystems hat. Aus diesem Grund wurden unterschiedliche proinflammatorische Zytokine untersucht. Überraschenderweise zeigte sich nur eine Erhöhung des Interleukin 6 nach der Toxinbehandlung. Weiterhin hatten die Endozytoseinhibitoren keinen Effekt auf die Produktion dieses proinflammatorischen Zytokins. Pneumolysin führt also zu einem Anstieg der Interleukin 6 Produktion, diese Produktion ist jedoch unabhängig von der Internalisierung dieses Toxins. Die Produktion dieses Interleukins würde zur Produktion der Akute-Phase Proteine, der Aktivierung der T-Zell Antwort, zu Wachstum und Zelldifferenzierung führen. Einerseits könnte diese Aktivierung die Infektion durch das Pathogen bekämpfen. Andererseits könnte *S. pneumoniae* die erhöhte Produktion durch PLY an Interleukin 6

nutzen um weiter in das Wirtsgewebe vordringen zu können. Diese Frage sollte noch durch weitere Experimente untersucht werden.

1 INTRODUCTION

1.1 Pneumococcal meningitis

The meninges are responsible for the protection of the central nervous system (CNS) from infections (Kim 2010). In bacterial meningitis these are infected. The meninges consist of three connective tissue membranes: *pia mater, arachnoid mater* and *dura mater*. The *pia* is a very thin membrane, which is closest to the brain and even covers small invaginations of the brain. The *arachnoid*, meaning "spider like", is a web-like structure and similar to the *pia* concerning the regions which it covers. The *dura* is a hard inelastic covering that is close to the inner surface of the skull (Squire and Zigmond 2003).

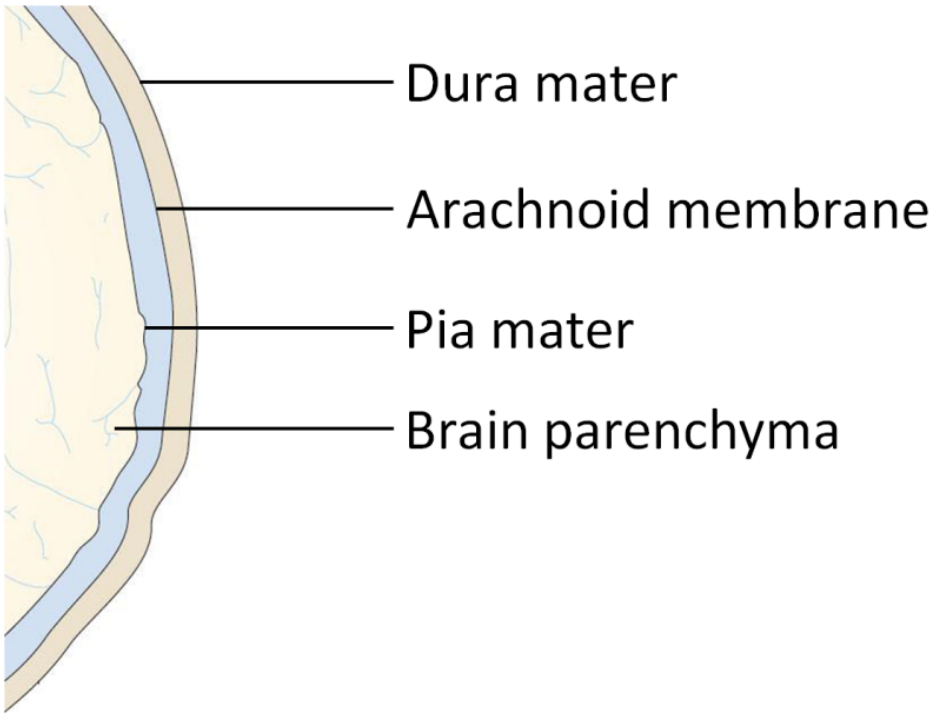

Fig 1: The meninges of the brain. Modified from Kristensson (Kristensson 2011). Visible are the three meninges surrounding the brain under the skull. The *dura mater* being the outermost and hardest meninges located directly under the skull. The *arachnoid,* representing the meninges under the *dura mater* and the *pia mater,* being the softest and thinnest meninges being closest to the brain.

The infection of the meninges has critical effects on the brain, such as remaining neurological sequelae e.g. as cognitive deficits and behavioural problems (Ortqvist, Hedlund et al. 2005; Herrmann, Kellert et al. 2006). If this barrier is damaged, for example

after surgical treatments or infection, pathogens could enter into the brain in an invasive manner and reach regions that otherwise would be well protected.

According to the World Health Organisation (WHO) bacterial meningitis represents the most-feared infectious disease in children (O'Brien, Wolfson et al. 2009). *Neisseria meningitidis*, *Haemophilus influenza* and *Streptococcus pneumonia* are the most common causes of bacterial meningitis (Hart, Cuevas et al. 1993; Ciana, Parmar et al. 1995). Here, *S. pneumonia* and *H. influenzae* represent the leading cause of death in young children in the developing countries.

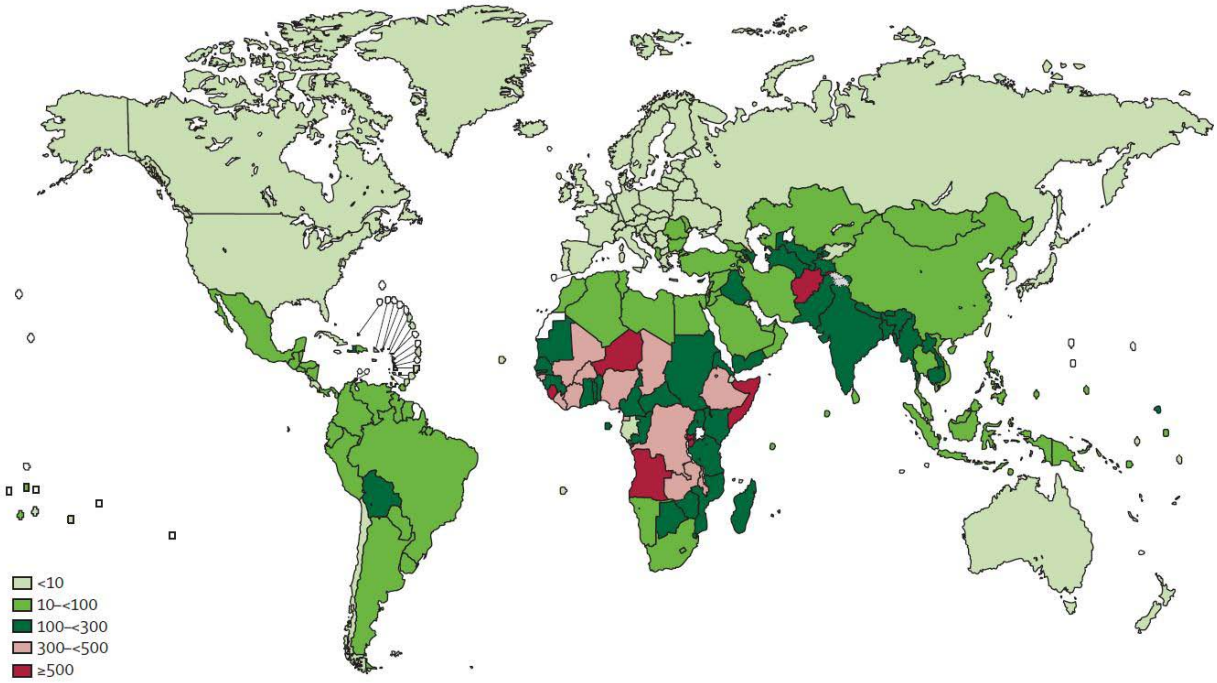

Fig 2: Overview of occurences of bacterial meningitis worldwide from O'Brien and Wolfson *et al.* (O'Brien, Wolfson et al. 2009). The map shows pneumococcal deaths in children at the age of 1-59 month per 100 000 children. It has to be noted that HIV-positive children are excluded. The high incidence in developing countries becomes clear.

In 1999 the WHO estimated that five million neonatal deaths occur per year (Lazo, Tamura et al. 2001). The high prevalence in infants and the focus on developing countries can be explained by the following risk factors: low birth weight, low socioeconomic status of the mother and prematurity (Lazo, Tamura et al. 2001). Nevertheless, precise studies are almost impossible, as a tight monitoring of meningitis is difficult to be carried out in those countries. In his review Furyk describes the following statistics: 14 out of 23 studies on neonatal meningitis were performed in Africa, three were a multicentre study carried

out by the WHO, four were from the Middle East, two were carried out in Latin America and in Asia. All these studies were carried out under different conditions leading to a difficult comparability until today (Furyk, Swann et al. 2011).

S. pneumonia causes the most common form of bacterial meningitis (Ortqvist, Hedlund et al. 2005) and causes diseases such as otitis media and pneumonia (Kadioglu, Weiser et al. 2008). Disease rates are very high in young children, elderly people and immunosuppressed patients (Ortqvist, Hedlund et al. 2005). Majorily, developing countries are affected (Lazo, Tamura et al. 2001.). After infection with bacterial meningitis, 15-20% of patients survive with neurological sequelae such as hearing loss, seizures and mental retardation (Baraff, Lee et al. 1993; Ciana, Parmar et al. 1995; Qazi, Khan et al. 1996). These sequelae could be explained by the brain regions that are damaged, for example the the hippocampal formation, where also neural stem cells can be found that might serve a stimulation of neuronal outgrowth after damage of that region (Zhang and Barres 2010). Coverage of vaccination and antibiotic treatment turn out to be difficult, as *S. pneumonia* shows 90 (or more) serotypes and pneumococci show a reduced susceptibility to penicillin (Ortqvist, Hedlund et al. 2005). Nevertheless, *S. pneumonia* infection not only represents a threat to developing countries but also to highly developed ones as well (Jedrzejas 2001).

In developed countries *S. pneumoniae* is the most common pathogen causing meningitis in adults (Kastenbauer and Pfister 2003). Here again infection mostly occurs after invasive surgical procedures. Bacterial meningitis occurs much more often in infants (Kim 2010). In developed countries the case fatality rates (CFR) for bacterial meningitis lie in the range of 4.5% and at 15-50 % in developing countries (O'Brien, Wolfson et al. 2009). The mortality rate caused by *S. pneumonia* lies at 40.000 per year in the USA and is thus larger than the mortality rate caused by any other bacterial pathogen (Jedrzejas 2001). So, understanding mechanisms of this disease in order to develop ideas for possible cures is a tempting task.

1.2 Cell types in the brain and their function

As an infection of the meninges can spread further into the brain, it is important to understand the effect of the infection on the brain and on brain cells. In the brain nerve cells and their extensions, dendrites and axons are closely surrounded by glial cells. For maintenance of learning and memory a proper functioning of neurons in the brain is required. This functioning and the homeostasis in the brain depend on functional glial cells including astrocytes, oligodenrocytes and microglia.

1.2.1 Neurons

The neuron cannot be defined into only one phenotypical form. Textbook knowledge states that the neuron is a highly polarised cell, which in its development forms distinct cellular domains. In general, a neuron consists of a cell body, the perykaryon, which contains the nucleus and the major cytoplasmatic organelles, which produce all proteins and membranes of the neuron. From this perikaryon several dendrites emanate, varying in size and shape. Thirdly, an axon emerges from the perikaryon. The axon extends farther from the cell body than the dendrites (Squire and Zigmond 2003). The Axon is a structure required for the transmission of actionpotentials. At the cell soma dendrites are found which can also represent the postsynapse. Generally, neurons are assembled by the same components compared to any other cell type. Nevertheless, neurons show diverse phenotypes (Fig 3). Four major classifications can be named: interneurons, sensory neurons, motor neurons and pyramidal cells. Interneurons, which show a bipolar phenotype, are composed of a branched axon and serve the interconnection between other neurons. The dendrites of interneurons show a non-spiny phenotype (Squire and Zigmond 2003). Sensory neurons convert external stimuli into internal stimuli, meaning that they send information to the brain. Motoneurons, in contrast, convert internal signals and send those to muscles. Pyramidal cells facilitate the development of neuronal circuits within the brain. Here, a spiny phenotype of dendrites can be found (Squire and Zigmond 2003).

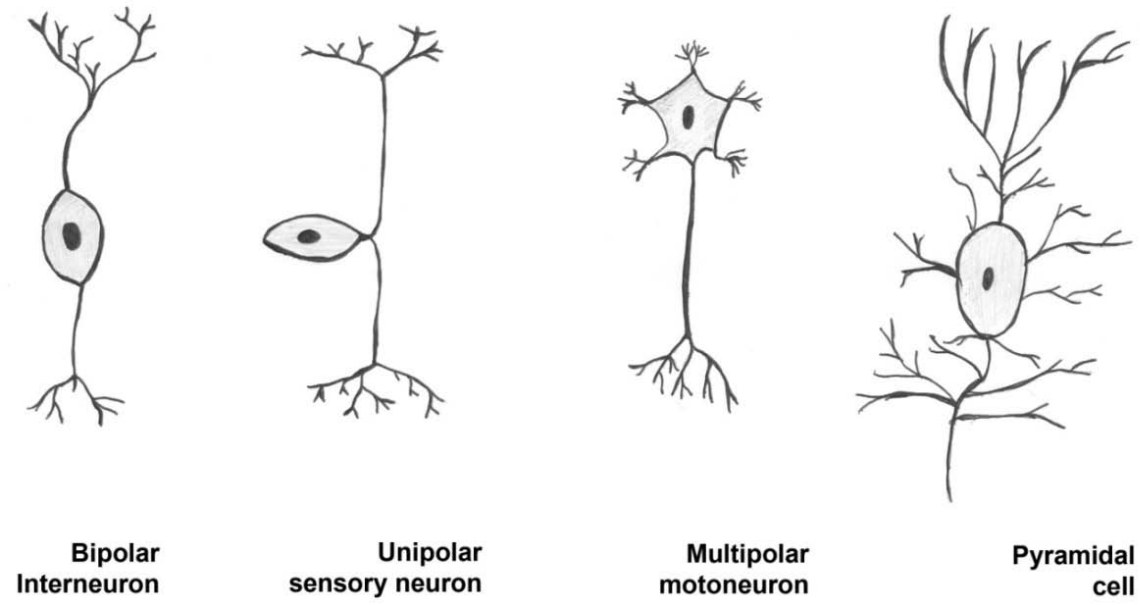

Fig 3: Basic neuron types. Modified from Kuffler and Martin *et al.* (Kuffler, Martin et al. 1984). Roughly, four basic neuron types can be described. Mostly, interneurons show a bipolar phenotype. Sensory neurons show an unipolar phenotype. Motoneurons show a multipolar phenotype and pyramidal cells a highly branched phenotype.

Neurons can have excitatory, inhibitory or modulatory functions. Again, the role of a neuron can be found by looking at the cellular phenotype of these cells. Assymetric synapses are responsible for the transmission of excitatory inputs, whereas symmetric synapses are responsible for an inhibitory transmission. Furthermore, these functions are mastered by the use of neurotransmitters. The main excitatory neurons in the cerebral cortex are pyramidal cells and the excitatory neurotransmitters found here are glutamate and possibly aspartate (Squire and Zigmond 2003).

Most neurotransmitters, acetylcholin being the only exception, are amino acids, derivates from amino acids, nucleotides and ATP. Classically, one neuron only produces one neurotransmitter. These exit the cell via exocytosis into the synaptic cleft. The next neuron, on the other side of the synaptic cleft, usually produces the receptors for those neurotransmitters. Some neurons also release neuropeptides into the synaptic cleft. Nevertheless, those are stored in different vesicles. Neuropeptides establish their signalling over a longer period of time (up to days) compared to neurotransmitters (Siegel, Albers et al. 2006).

1.2.2 Glia

The major population of cells found in the brain are glial cells. Rudolf Virchow gave these cells their name in 1859, as he found neuroglia as a tissue that held neurons together functioning as a connective tissue (Squire and Zigmond 2003). They make up half of the volume of the human brain (Barres 2008). Ramón y Cajal and del Rio-Hortega managed to classify neuroglial types phenotypically into three types: oligodendrocytes, astrocytes and microglia (Squire and Zigmond 2003). Here, microglia and astrocytes will be discussed in further detail.

1.2.2.1 Microglia

For a long time, the brain has been seen as an immunological compromised site (Squire and Zigmond 2003). However, microglia represent macrophage-like cells and thus immune cells in the brain and make up about 10% of CNS glial cells (Barres 2008). One of the hallmarks of microglia is that they can become reactive and respond to pathological challenges (Squire and Zigmond 2003). At the point of infection they can follow a chemotactic gradient and reach the site of insult in the tissue. They are evenly dispersed throughout the brain and are highly motile. Thus, they have the capacity to move, proliferate and phagocytose (Kettenmann, Hanisch et al. 2011). Microglia may secrete cytokines or growth factors (Block, Zecca et al. 2007). They are found in all regions of the brain. They have small rod shaped somas from which many processes emanate. Cell-cell contacts, however, have not been described so far (Squire and Zigmond 2003).

1.2.2.2 Astrocytes

The name of astrocytes is based on the Greek word for star giving a hint at the shape, namely a star-like cell shape. Nevertheless, astroglia show many phenotypes. Markers for immunocytochemical staining are the glial fibrillary acidic protein (GFAP), S-100, which is a calcium-binding protein, and glutamine synthetase (Squire and Zigmond 2003). Especially Astrocytes play an essential role in the maintenance of neuronal functions. They surround or “fence in” neurons by extending long processes which range

to the *pia mater* (Squire and Zigmond 2003). Astrocytes regulate the recycling of neurotransmitters and play an essential role in repair of injury of neurons (Barreto, Gonzalez et al. 2011). If neurotranmsmitters stay in the synaptic cleft, new signalling could be disturbed. Thus, astrocytes take up neurotransmitters for a clearance of the synaptic cleft (Squire and Zigmond 2003). Furthermore, astrocytes play an important role in neural development. They can either represent stem cells that become neurons, they can promote neurite outgrowth, guide axon projections and much more (Barres 2008; Zhang and Barres 2010).

Astrocytes are interconnected by gap junctions, which enable those cells to exchange ions and small molecules (Squire and Zigmond 2003).

In the case of neuronal damage the astrocyte responds with a reactive gliosis. Initially this process turns out to be neuroprotective (Barreto, Gonzalez et al. 2011). On the other hand, the reaction of the astrocyte can cause damage to the neurons by producing a toxic edema leading to neuroinflammatory processes (Barreto, Gonzalez et al. 2011).

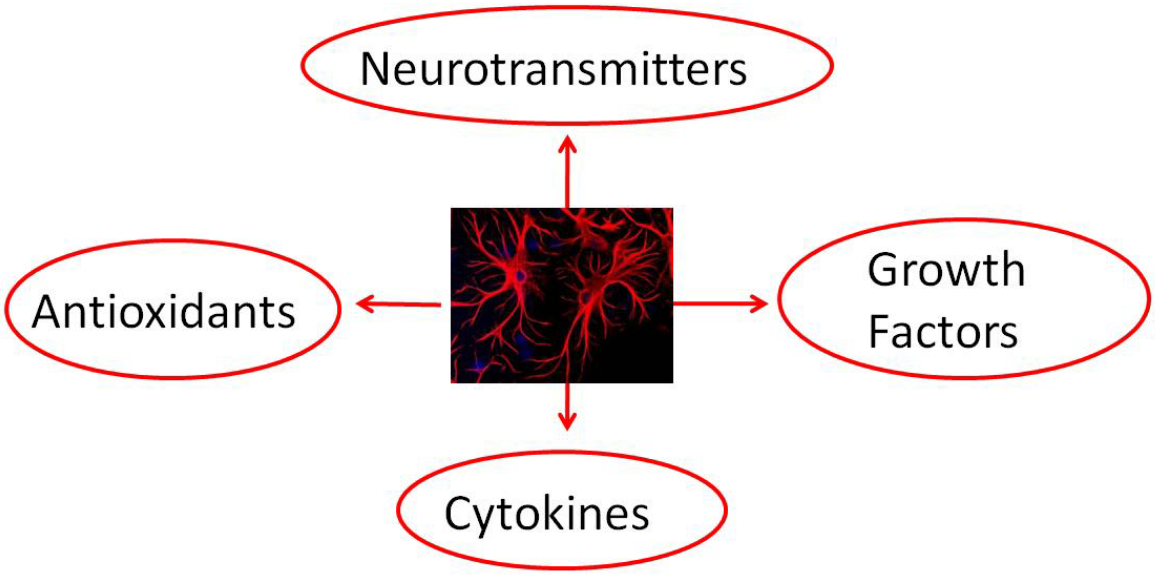

Fig 4: Reactive astrocytes in brain injury. Modified from Barreto and Gonzalez *et al.* (Barreto, Gonzalez et al. 2011). Astrocytes can produce neurotransmitters, cytokines, growth factors and antioxidants upon activation.

Astrocytes are known to release and recycle neurotransmitters essential for neurons. Upon brain damage, glutamate receptors in astrocytes can decrease in number leading to an excitotoxic effect on the neurons (Barreto, Gonzalez et al. 2011). On the

other hand, astrocytes downregulate glutamate production after brain injury and thus decrease excitotoxicity (Zou, Wang et al. 2010). For a long time it was believed that astrocytes physically form the blood brain barrier (BBB), but now it is known, that astrocytes form and maintain the tight junctions in endothelial cells, that form the BBB. Astrocytes also play a role in migration and guidance of neurons in early brain development, by producing for example growth factors (Squire and Zigmond 2003).

1.2.3 Maintenance of the blood brain barrier

The blood brain barrier (BBB) consists of an epithelial cell layer that is surrounded by astrocytes (Kristensson 2011). This layer protects the CNS from a non-selective passage of molecules and toxins, while metabolites are able to pass (Kristensson 2011). The BBB consist of four cellular elements: endothelial cells (ECs), astrocytes end-feet, microglial cells and pericytes. In some regions of the CNS, the BBB is replaced by cerebrospinal fluid (CSF) (Correale and Villa 2009).

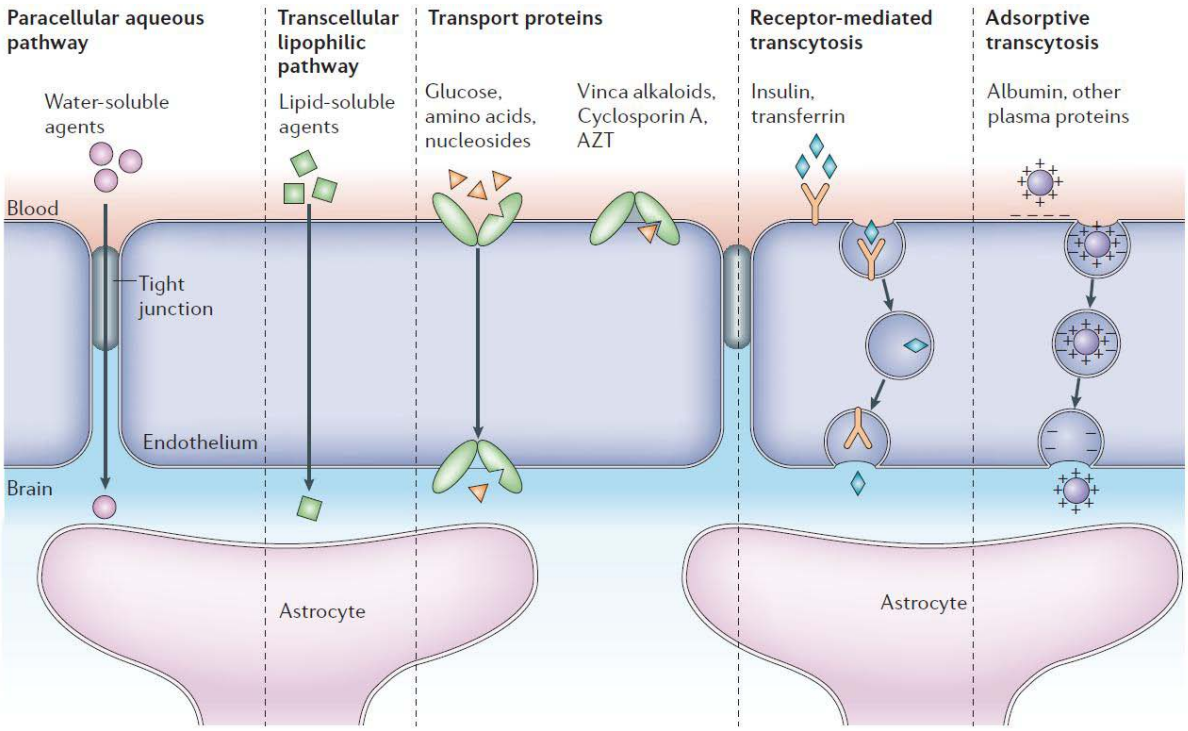

Fig 5: The Blood Brain Barrier. From Abbott and Ronnback *et al.* (Abbott, Ronnback et al. 2006). The different mechanisms are visible that facilitate transport of nutrients across the blood brain barrier. Possible mechanisms are the paracellular aqueous pathway, the transcellular lipophilic pathway, transport via transport proteins, receptor mediated transcytosis and adsorptive transcytosis.

As depicted in Fig 5 small water-soluble agents can pass the endothelial layer through gap-junctions whereas lipid-soluble agents can diffuse through endothelial cells. Transport proteins are moved across the BBB via active transport through receptors. Other proteins pass the BBB via receptor-mediated or adsorptive-transcytosis (Abbott, Ronnback et al. 2006), which will be explained in a later chapter. The BBB is disrupted in the course of bacterial meningitis. This is due to the fact, that meningeal vessels are more permeable than vessels in the brain parenchyma, which will eventually lead to a passage of pathogens across the BBB (Kristensson 2011). The exact mechanism used by *S. pneumoniae* is not yet clarified (Mook-Kanamori, Geldhoff et al. 2011). One way used to cross the BBB could be the binding of pneumococcal phosphorylcholine to the platlet activating factor (PAF) and thus leading to transcytosis entering the PAF-receptory cycling pathway. Other possibilities are utilising the IgG recycling pathway or the release of reactive oxygen species (ROS) leading to tissue damage, that increases the permeability of the BBB (Mook-Kanamori, Geldhoff et al. 2011). Nevertheless, the invasive strategy of *S. pneumoniae* is shown by the increase of proinflammatory cytokines in hippocampal and cortical tissue of young rats after infection with *S. pneumonia* shown by the distribution of evans blue into the brain 12-24 h after infection (Barichello, Pereira et al. 2011).

1.2.4 Cytoskeleton of cells in the brain

The cytoskeleton is composed of the actin-cytoskeleton, microtubili and intermediate filaments. These components enable the cell to move and to adhere (Alberts 2008). In addition, the cytoskeletal components provide a structural organisation for the cell e.g. by allowing a separation into different intracellular compartments. Furthermore, they serve as tracks for intracellular transport-mechanisms (Siegel, Albers et al. 2006). In terms of cellular movement the cell requires a remodelling of the actin cytoskeleton. In order to migrate, the cell extends a lammellipodium at the front of the cell. This process is followed by the contraction of the cell body and by the loosening of the tail adherence (Ridley 2001). This process involves actin polymerisation which is possible due to the signalling of Rho GTPases, such as Rho, Rac1 and CDC42 (Ridley 2001).

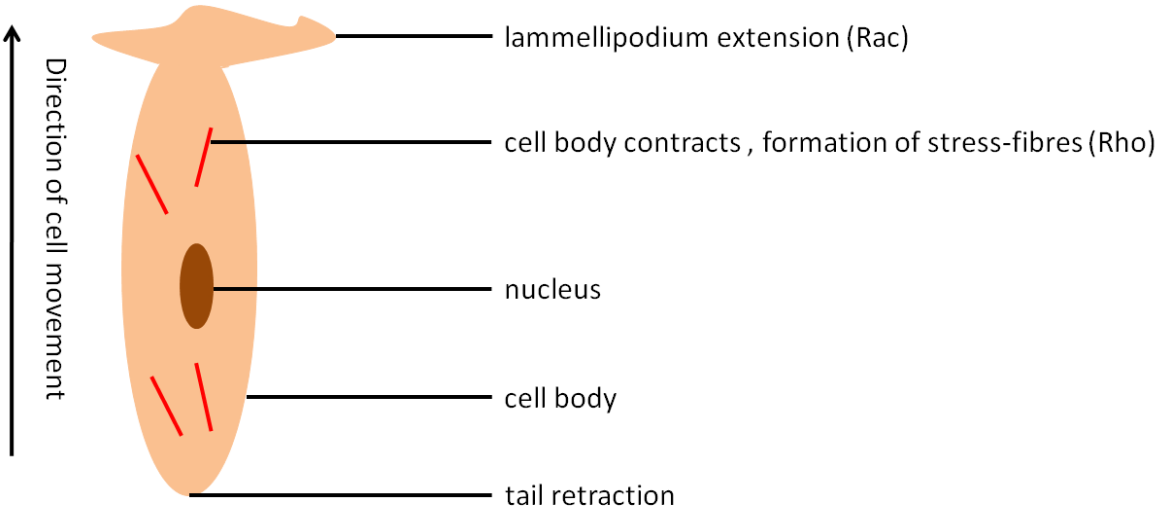

Fig 6: Function of Rho GTPases in cellular movement. Modified from Ridley (Ridley 2001). Upon stimulation, the cell forms lammellipodia at the front of the cell. The cell body contracts, facilitated by the formation of stress-fibres, and the tail of the cell retracts. This provides directionality to the movement of the cell.

The small GTPases Rho and Rac lead to the downstream regulation of many proteins involved in actin polymerization e.g. Arp2/3 or depolymerisation e.g. cofilin. The activity of the small GTPases depends on their state of GTP/ GDP-binding. The exchange of GDP to GTP is enabled by guanine nucleotide exchange factors (GEFs), which eventually leads to an activation of the small GTPase. An inactivation is enabled by GTPase activating proteins (GAPs), which catalyse a GTP hydrolysis. In an activated state the small GTPases bind to their downstream targets, in the case of Rho to ROCK (Rho associated serin-threonine kinase) and in the case of Rac to PAK (p21-activated kinase). ROCK and PAK can then activate LIMKs, which are essential for the regulation of Cofilins (Ridley 2006).

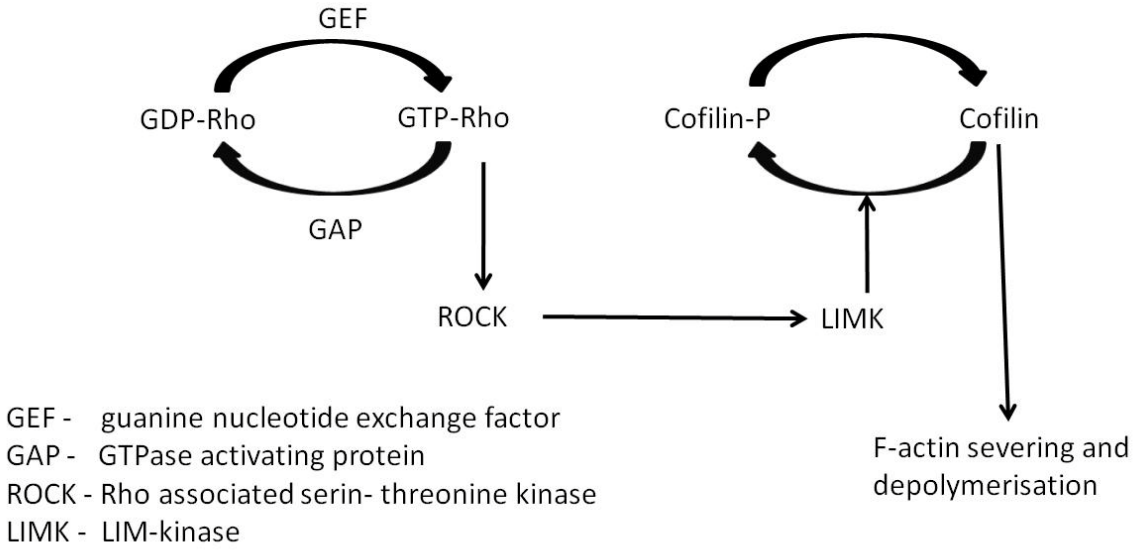

Fig 7: Functions of small GTPases modified from Ridley (Ridley 2006). Small GTPases facilitate a regulation of cytoskeletal processes such as actin polymerisation and depolymerisation. These functions are supported and mediated by GEFs and GAPs.

Via these highly regulated mechanisms the cell preserves the capability to react to external stress and to move away from stressors or towards chemotactic gradient.
Previously, it has been shown that bacteria have evolved different strategies to modulate the actin cytoskeleton by their toxins (Aspenstrom 1999; Aktories and Barbieri 2005). For pneumolysin it has been shown, that it activates RhoA and Rac1 GTPases and thus leads to a formation of filopodia, lammelipodia and stress fibers in a human neuroblastoma cell line (Iliev, Djannatian et al. 2007). The question remains to what extent the toxin achieves these modulations and what the biological significance of these changes is.

1.3 The family of the cholesterol dependent cytolysins

Cholesterol dependent cytolysins (CDCs) represent a family of protein toxins, which require membrane cholesterol in order to bind and to be activated (Solovyova, Nollmann et al. 2004; Tweten 2005). These toxins are produced by Gram positive bacteria such as *C. perfringens*, *S. intermedius*, *L. monocytogenes* and *S. pneumoniae.* CDCs bind to membrane cholesterol, oligomerise in a pre-pore and, after undergoing conformational change, punch a huge pore into the membrane of the cell leading to cell lysis (Alouf 2000;

Aktories and Barbieri 2005). The members of this family show a significant amino acid identity and similarity. Most structural studies and crystal structures have been obtained on perfringolysin O (PFO) from *C. perfingens* and intermediolysin (ILY) from *S. intermedius (Rosado, Buckle et al. 2007)*. Rossjohn *et al.* solved the structure of perfingolysin O (Rossjohn, Polekhina et al. 2007). This structure serves as a suggestion for the structure of other CDCs based on the assumption that they might share a high structural similarity.

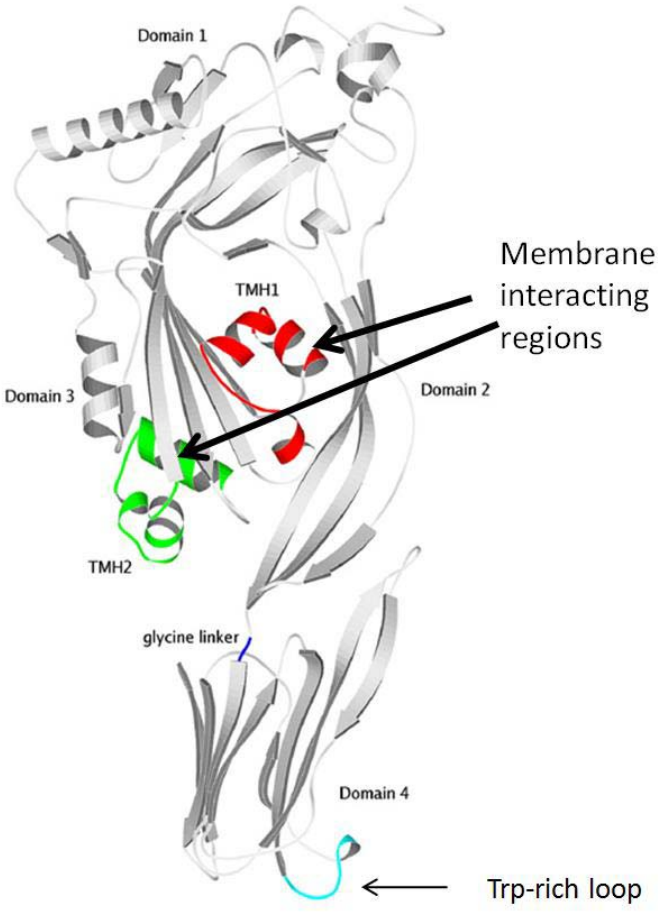

Fig 8: Struture of perfringolysin O as a structural suggestion for PLY. Modified from Rossjohn and Polekhina *et al.* (Rossjohn, Polekhina et al. 2007). PLY consists of four domains showing a slightly curved, but not globular shape.

1.3.1 Pneumolysin

Pneumolysin (PLY) is a major virulence determinant for *S. pneumoniae* and also shows many effects on host immune components at sub-lytic concentrations (Kadioglu, Weiser et al. 2008). It plays a distinct role in the early pathogenesis of infection (Ortqvist, Hedlund et al. 2005). PLY belongs to the family CDCs, meaning that the toxin preferably

forms pores in cholesterol-rich regions of the plasma membrane (Marriott, Mitchell et al. 2008) and has the capability to bind cholesterol (Jedrzejas 2001). Pneumolysin is produced by virtually all clinical isolates of *S. pneumoniae* (Kanclerski and Mollby 1987). PLY is a cytosolic protein, released predominantly upon bacterial auto-lysis (Berry, Yother et al. 1989), although other mechanisms are also suggested e.g. via a secretion mechanism (Balachandran, Hollingshead et al. 2001).

Several studies show that the toxin oligomerises in a circle and forms lytic pores after undergoing conformational change and thus penetrating the membrane of the cell (Korchev, Bashford et al. 1998; Marriott, Mitchell et al. 2008). Most of the structural biology studies use PLY concentrations of 10 µg/ml to 200 µg/ml, as either artificial liposomes, artificial membranes or erythrocytes were used (Korchev, Bashford et al. 1998; Kirkham, Kerr et al. 2006; Sonnen, Rowe et al. 2008). In pathological conditions, such as *S. pneumoniae* meningitis, the concentration on PLY in the cerebrospinal fluid (CSF) of patients never exceeds 0.2 µg/ml (Malmgren, Olsson et al. 1978) and thus is much lower (20-1000-fold) than used in those studies (El-Rachkidy, Davies et al. 2008). In this work the term “sub-lytic” shall be used, as only 10 % of the cells die *in vitro* and the toxin at this concentration causes changes in actin cytoskeleton (Fortsch, Hupp et al. 2011).

1.3.2 Structural aspects of pneumolysin

Pneumolysin is a protein-toxin with a size of 53 kDa and an amino acid length of 471. It consists of four domains showing a slightly curved, but not globular shape (Marriott, Mitchell et al. 2008). In solution PLY itself stays monomeric and in rare cases forms dimers.

1.3.3 Mechanism of pore-formation and membrane interaction

The solved structure of PFO serves as a model for the monomeric form of PLY (Fig 8). Both toxins have a secquence identity of 46% and a secquence similarity of 67% (Tilley, Orlova et al. 2005). Tilley *et al.* describe the pore-formation, exemplary on PFO, of PLY (Tilley, Orlova et al. 2005). The four domains of the toxin, mainly showing a β-sheet structure, also show a hydrophilic surface. Domains 1, 2 and 4 are arranged in a linear

manner, whereas domain 3 is attached loosely to domain 2 via a glycin-linker. Domain 4 contains the cholesterol recognition site. This task is facilitated via a tryptophan-rich motif. Domain 3 is composed of a central β-sheet flanked by 2 groups of α-helices, which can refold into β-hairpins and thus insert into the membrane. If 50 oligomers form a pore, punching through the membrane with these β-hairpins, a hughe barrel-like structure would be formed creating a large pore of 350-450 Å (Solovyova, Nollmann et al. 2004).

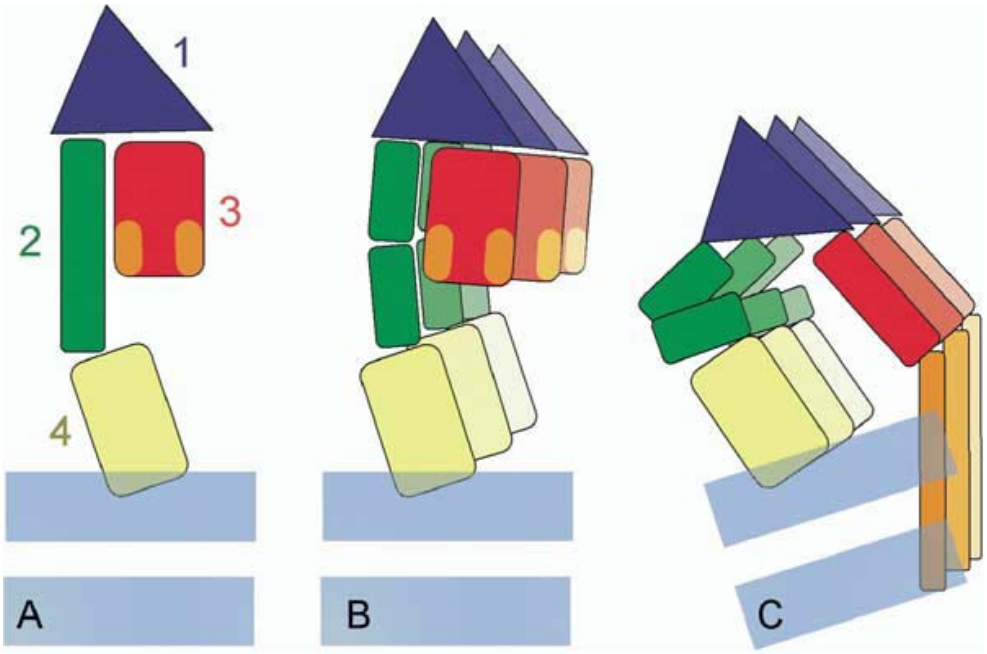

Fig 9: Mechanism of pore-formation (Tilley, Orlova et al. 2005). Domains 1, 2 and 4 of PLY are arranged in a linear manner, whereas domain 3 is attached loosely to domain 2 via a glycin linker. Domain 4 contains the cholesterol recognition site. This task is facilitated via a tryptophan-rich motif. Domain 3 is composed of a central β-sheet flanked by 2 groups of α-helices, which can refold into β-hairpins and thus inserts into the membrane.

Next to its homology within the CDC-group, it has to be mentioned, that perfringolysin O shares structural characteristics with the membrane attack complex perforin (MACPF) of the complement system (Rosado, Kondos et al. 2008). The MACPF is used by the immune system as a defense against bacterial infection (Janeway, Travers et al. 1997). Thus, bacteria producing CDCs use the same structure for the attack of mammalian cells that is used by mammals for eliminating a bacterial infection. Here, the structural characteristics of the MACPF show a high structural similarity to the structure of the CDCs. Furthermore, a common size of the fold has been found (Rosado, Kondos et al. 2008).

1.3.4 Variants

In order to accomplish experiments characterising the importance of pore-formation in this work, negative controls are required. Two variants of PLY were used as non-pore forming variants of this CDC. These variants were developed in order to study the effect of PLY on the immune system (Berry, Alexander et al. 1995; Kirkham, Kerr et al. 2006). The first variant shows an amino acid exchange at position 433. Here a tryptophan was replaced by a phenylalanin and this variant will be named PLY-W433F. The tryptophan in position 433 must have an essential functioning in the lytic capacity of the toxin. Thus, this variant only shows 1% of the lytic capacity, tested on erythrocytes, compared to the wildtype (Korchev, Bashford et al. 1998).

The second variant used in this work will be named PLY-Δ6. PLY-Δ6 is incapable of forming pores as the mutation is located between domain 1 and 3, thus losing the capability to oligomerise (Garcia-Suarez Mdel, Cima-Cabal et al. 2004; Kirkham, Kerr et al. 2006). Here two amino acids are deleted, A146 and R147 (Kirkham, Kerr et al. 2006). However, it remains unclear whether lytic pore formation and micropore formation (possessing ion channel-like properties), both of which are properties of the CDCs, are mechanistically similar or different phenomena.

1.4 Cell trafficking

In order to move, to achieve a metabolic exchange and to enable cellular signalling, the cell requires many components. The ones involved in movement, cellular reorganisation and transport are the previously mentioned cytoskeletal components, intermediate filaments, microtubules and the actin cytoskeleton. When it comes to transport into or through the cell more elements are required. Some of these mechanisms are not only important for transport and signalling, but also for the reaction to damages and subsequently for repair.

1.4.1 Endocytosis

Endocytosis describes the process in which cells remove plasma membrane components and bring them to internal components into the cell. In this way an endosome is created. From these endosomes, internalised components can be degraded or recycled. Thus, new internal membranes are built from the plasma membrane lipid bilayer (Doherty and McMahon 2009). These transport mechanisms must be selective and tightly regulated. They can be classified into and biosynthetic-secretory and into an endocytotic pathway. Furthermore, classifications in mechanism are described by cellular components involved in these pathways. Reviewed by Doherty in 2006 ten possible mechanisms could be named: Clathrin mediated-, caveolin-dependent-, CLIC (Clathrin independent carrier)/GEEC (GPI-AP-enriched early endosomal compartment)-, IL2βpathway, Arf6 dependent-, flotilin-dependent endocytosis, as well as phagocytosis, macropinocytosis, circular dorsal ruffles and entosis (Doherty and McMahon 2009). For this work these mechanisms shall be summarised into four groups: caveolin- and clathrin-dependent endocytosis as well as pinocytosis and phagocytosis.

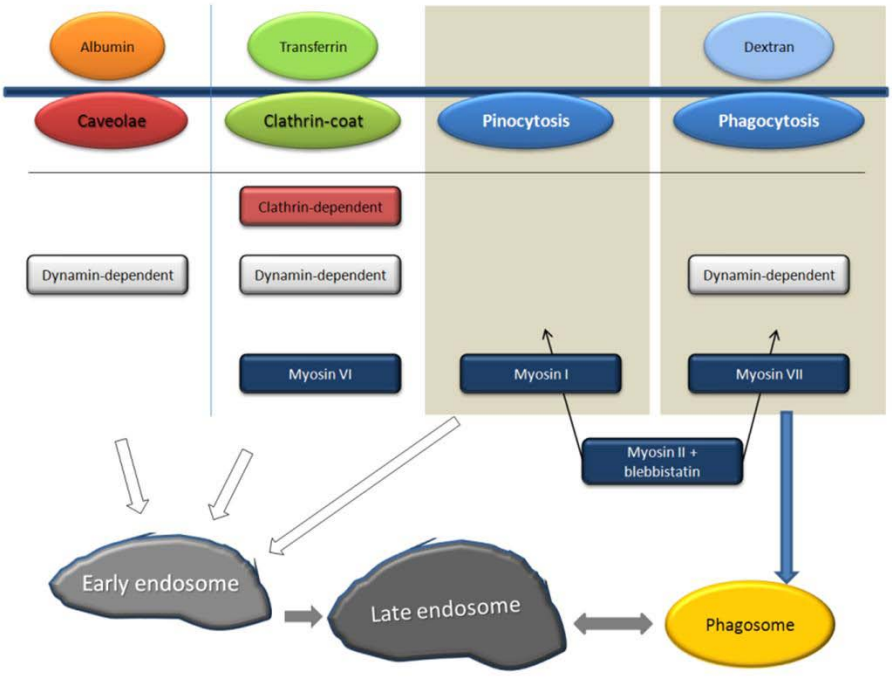

Fig 10: Summary of endocytotic mechanisms. Roughly, endocytotic processes can be divided in four groups: caveolin-dependent, clathrin-dependent, phagocytosis and pinocytosis. Several of these pathways depend on dynamin or different myosins. Albumin, transferrin and dextran are shown as potential markers for classical endocytotis pathways. Albumin is taken up via caveolin-dependent endocytosis (Bento-Abreu, Velasco et al. 2009), transferrin is taken up via clathrin-dependent pathways (Pearse and Robinson 1990) and dextran is internalised via phagocytosis (Costantini, Gilberti et al. 2011).

Summarised, it can be said, that endocytosis mediated by either clathrin or caveolin is receptor mediated (Clague 1998). Caveolin can be found in regions of the membrane that are rich in cholesterol, whereas clathrin forms crystal-like structures at the inner site of the plasmamembrane. Fluid-phase endocytosis/macropinocytosis describes the uptake of suspended or cell adherent particles, whereas phagocytosis is triggered by specific receptors (for mannose, complement, Fc, phosphatidylserine and scavenger) (Alberts 2008). Both, pinocytosis and phagocytosis require an actin-cytoskeleton reorganisation in a RhoA GTPase dependent manner (Erridge 2010). Methodologically, these mechanisms can be recognised in live imaging by using fluorescence labelled structures that the cell takes up specifically. Albumin, for example, is taken up in a caveolae specific manner (see Fig 10) (Bento-Abreu, Velasco et al. 2009). Transferrin, an iron-binding protein, is internalised in a clathrin dependent manner (Pearse and Robinson 1990). Dextran is phagocytosed, meaning that the endosome fuses with an incoming phagosome during or shortly after internalisation (Costantini, Gilberti et al. 2011). By using these components experimentally, labelled with fluorescent dyes, one could follow their internalisation via live-imaging and differentiate between the several endocytic mechanisms.

By using endocytotic actions the cell can escape for example from an attack by large- and small-pore forming toxins that trigger or enhance endocytic responses (Idone, Tam et al. 2008; Husmann, Beckmann et al. 2009; Tam, Idone et al. 2010; Thiery, Keefe et al. 2010; Los, Kao et al. 2011). In contrast, the pathogen could use this defence by the cell as a shuttle to cause further harm to the cell. For example, listeriolysin (another CDC) from *Listeria monocytogenes* enables listeria to escape from the phagolysosome after internalisation and to infect the cell from the cytoplasm. Endo- and also exocytosis can also serve as mechanisms to repair the cell membrane after injury (Bi, Alderton et al. 1995; Idone, Tam et al. 2008).

1.4.2 Exocytosis

Excocytosis describes the process of vesicles fusing with the plasma membrane. Thus, it serves as a secretory pathway leading to the cell exterior. The cell can promptly secrete substances via exocytosis when it is triggered to do so. Furthermore, exocytosis can serve as a mechanism to enlarge the surface of the cell e.g. in fast growing cells or as

a repair mechanism after cell damage or injury. If a cell is wounded, a sudden increase in calcium triggers exocytosis by rushing into the cell (Alberts 2008).

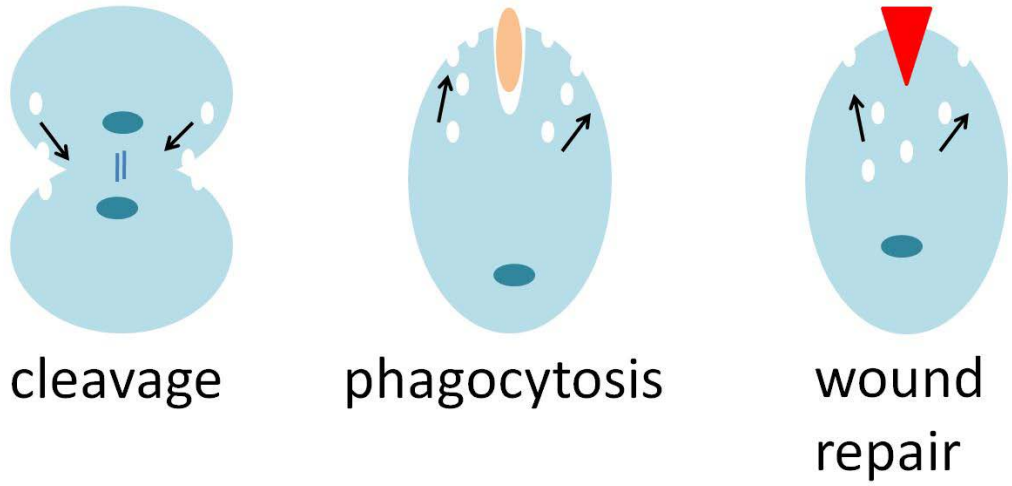

Fig 11: Exocytosis as a mechanism of membrane repair. Modified from Alberts (Alberts 2008). The cell can react with an increased exocytosis to wounding or to a decrease in overall membrane area e.g. by phagocytosis or cleavage.

Several publications show that a calcium-regulated exocytosis is required for a resealing of the cell membrane after injury (Bi, Alderton et al. 1995), after challenge with the CDC Streptolysin O (Tam, Idone et al. 2010) or as a reaction of challenge with the α-toxin from *Staphylococcus aureus* (Husmann, Beckmann et al. 2009). The argumentation is, that the exocytosis resealing process occurs within the first 30 seconds after toxin challenge, which indicates that the mechanism cannot be due to an automatic resealing by the bilayer. Here, the duration would be between 30 minutes to hours. This spontaneous resealing could be driven by the thermodynamic force that favours the bilayer (Bi, Alderton et al. 1995).

1.4.3 Transcytosis

Transcytosis serves the purpose to transport molecules across epithelial cells. A nice example described in a textbook (Alberts 2008) is that of a rat newborn. It takes up antibodies from the mother rat via milk and in the acidic pH of the gut these antibodies bind to certain receptors enabling a transport across the gut epithel. There, the process of endocytosis occurs enabling a further transport of the antibody. Transcytosis is not a

direct process but uses a route via endocytotic mechanisms to reach the target (Alberts 2008). By crossing the BBB two mechanisms of transcytosis are used: vesicle mediated transcytosis and adsorptive mediated transcytosis. Vesicle mediated transcytosis describes the transfer of substances across the cell after the binding to a specific receptor leading to an internalisation via endocytosis. Adsorptive mediated transcytosis describes the transport of substances across the cell after a non-specific binding of a ligand to the cell surface charges and thus leading to an internalisation via endocytosis (Abbott, Ronnback et al. 2006).

1.5 Neuroinflammation

Inflammatory processes induced by an activated immune system play a role in CNS diseases. Here, microglia are activated within the CNS parenchyma (Lehnardt 2010). Innate immunity and neuroinflammation are mediated by Toll-like-receptors, which lead to an increase of proinflammatory cytokines (e.g. TNF-α) that cause neuronal injury in bacterial meningitis (Lehnardt, Massillon et al. 2003). The activation of innate immunity via Toll-like receptor 4 (TLR 4) might either trigger neurodegeneration (Lehnardt, Massillon et al. 2003) or increase neurogenesis, e.g. after experimental *S. pneumonia* meningitis (Gerber, Bottcher et al. 2003) or in *postmortem* brain sections of humans who died from meningitis (Gerber, Tauber et al. 2009). Nevertheless, activation of innate immunity via TLR 4 in meningitis remains controversial (Srivastava, Henneke et al. 2005; McNeela, Burke et al. 2010). Astrocytes have also been recognised as contributors to inflammatory responses by inducing a cytokine production and thus leading to an invasion of leukocytes into the brain. Furthermore, it has been shown that astrocytes express TLR 2,4, 5 and 9 (Shepard, Heuck et al. 1998).

Some TLRs, such as TLR9, signal and thus activate inflammatory cytokines via endosomes (Krieg and Vollmer 2007). In contrast, other TLRs, such as TLR 2 and 4, are believed to signal via mechanisms on the plasmamembrane (McGettrick and O'Neill 2010). Moreover, large- and small- pore forming toxins trigger or enhance endocytic responses (Idone, Tam et al. 2008; Husmann, Beckmann et al. 2009; Tam, Idone et al. 2010; Thiery, Keefe et al. 2010; Los, Kao et al. 2011). Furthermore, an activation of TLRs

leads to a release of reactive oxygen species (ROS), such as NO and peroxide leading to oxidative stress (Steinborn, Seelos et al. 1999).

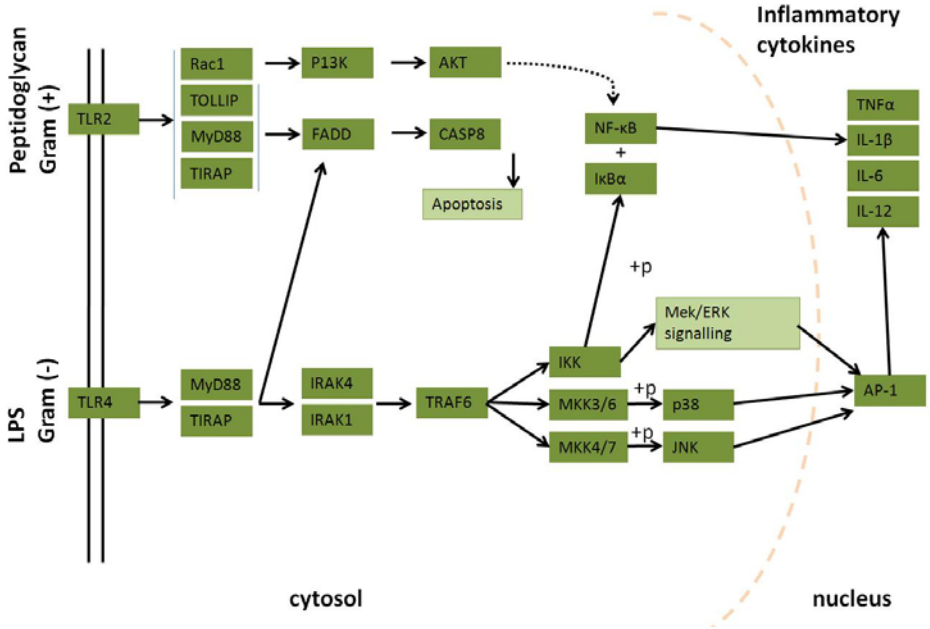

Fig 12: Toll-like receptor signalling. From KEGG Pathways (http://www.genome.jp/kegg-bin/show_pathway?org_name=mmu&mapno=04620&mapscale=1.0&show_description=show). TLR 2 can be activated by peptidoglycan (Gram+ bacteria) and TLR 4 can be activated by LPS (Gram- bacteria). Signalling can lead to apoptotic pathways or to the activation of stress-kinases (Mek/ ERK), which eventually leads to a production of proinflammatory cytokines such as TNF-α, IL-1β, IL-6 and IL-12 (p40).

1.5.1 Innate immunity and Toll-like receptors

The innate immune response serves as a precursor to adapted immunity (Janeway, Travers et al. 1997). The main task here is to lead phagocytosing cells and effector molecules to the site of infection (Baccala, Gonzalez-Quintial et al. 2009). The functionality of this immune response depends on specific receptors, which can be classified into three systems, which are summarised in the term of pattern recognition receptors (PRR). PRRs subdivide into Toll-like receptors (TLRs), retioid acid inducible gene like receptors (RLR) and cytosolic nucleic acid sensors and nucleotide-binding and oligomerisation domain (NOD) like receptors (NLRs). These three types can be found ubiquitously and show a high diversity. They recognise PAMPs (pathogen-associated molecular patterns) and DAMPs (damage-associated molecular patterns). In this work the focus will be laid onto TLRs (Baccala, Gonzalez-Quintial et al. 2009).

TLR serve as a sensor in recognising infection with viruses and bacteria (Beutler 2009). On the other hand the recent findings state that TLR are essential for an adaptive

immune response (Beutler 2009), whereas others line out evidence that adaptive immunity can be encountered without the signalling of TLRs (Blasius and Beutler 2010). TLRs can accomplish the signalling either intracellularly (TLR 3, 7, 8, 9, 13) or via actions on the membrane (TLR 2 and 4) (Beutler 2009; Blasius and Beutler 2010). Other TLRs are expressed on the cell surface, but the route and possible intracellular signalling cannot be explained for sure until today (Beutler 2009). TLRs can bind many factors, such as cell wall components of bacteria, RNA and DNA, but in terms of bacterial infection TLR2 and 4 shall be named here (Beutler 2009). TLR 2 serves the recognition of infection with Gram negative bacteria by recognising cell wall LPS of the pathogen. TLR 4 serves in the recognition with Gram positive bacteria by recognising peptidoglycan (Beutler 2009). Nevertheless, all possible studies in terms of a TLR signalling should be handled with care, as most protein purifications can be a source of LPS contamination and thus lead to false data concerning a signalling mechanism (Erridge 2010).

1.5.2 Proinflammatory cytokines

The activation of either TLR 2 or 4 will subsequently lead to a production of proinflammatory cytokines. These execute the function of leading phagocytic cells and effector molecules to the site of infection. Exemplary, the interleukines IL- 1, IL- 6, IL- 8, IL- 12 and TNF- α (Tumor necrosis factor α) shall be named. They fulfill local and systemic functions. IL-1 activates lymphocytes, leads to a local destruction of tissue and enables better access for effector cells. Subsequently, the production of IL-1 leads to a fever and production of IL-6. The production of TNF-α increases the permeability of vascular endothel and to results in an inflow of IgG and complement. This reaction leads to fever, shock and a mobilisation of metabolites. IL-12 activates natural killer cells and promotes differentiation of CD4-t-cells to t_H1 cells. Futhermore, these pro-inflammatory cytokines activate the immune raction of the acute phase (Janeway, Travers et al. 1997; Borish and Steinke 2003).

2 AIMS OF THIS WORK

After challenge with Pneumolysin at sub-lytic concentrations small GTPases are activated and and microtubule-bundling is initiated. However, the possibility of a micropore formation with ion-channel like properties and a clustering of toxin molecules on the cell surface and thus leading to the observed effects could not be excluded. Thus, various Pneumolysin mutants should be investigated. First, one mutant, which is capable of membrane binding but incapable of pore-formation and membrane insertion called PLY-Δ6. A second variant, PLY-W433F, would be able to penetrate the cell membrane, but bind to a lesser extent to the membrane. Here, the role of pore-formation on the changes in the model of primary mouse astrocytes should be investigated. The part of a possible pore-/micro-pore formation on the shape-changes in astrocytes, the ability to bind to the cell-membrane, and electrophysiological properties should be characterised. The objective was to determine the role of pore-formation on cytoskeletal remodelling (in terms of cell movement) and membrane depolarisation properties. For answering these questions, biochemical approaches, such as membrane fractionation and western blotting were to be used. In addition, the technique of the Planar Lipid Bilayer (PLB) should be used for an electrophysiological characterisation of possible pores in an artificial membrane. Membrane/cell movement was to be studied via various live-cell imaging approaches and immunocytochemistry.

Furthermore, functional and pathophysiological aspects should be studied. The question of the toxin-fate after membrane interactions remains open. The impact of toxin and toxin-mutant treatments on cellular trafficking were of special interest. If the toxin would be internalised into the cell, where would it go and how would the fate of the cell be influenced. Again, live-cell imaging approaches with various dyes specific for endocytic events should be used. For a further clarification of cellular modifications, that could impact whole tissue, proinflammatory effects should be investigated via ELISA. In order to link the actions of the toxin to disease relevant and brain-tissue modulatory effects this second project was tackled.

3 MATERIALS AND METHODS

3.1 Materials

3.1.1 Chemicals

All chemicals were supplied by Roth from Karlsruhe Germany. Chemicals used from other suppliers are listed in the table below.

Table 1: List of used chemicals and providers.

Chemical	Manufacturer
acetazolamid	Sigma
acetic acid	Merck
agarose	MoBitec
bafilomycin A	Sigma
boric acid	Sigma
cholesterol	Sigma
complete EDTA free	Roche
DAPI	Invitrogen
dimethylformamid (N,N)	Merck
diphytanoyl phosphatidylcholine	Avanti Polar Lipids
immobilon P, PVDF membrane	Milipore
PLO	Sigma
propidium iodide	Invitrogen
saccharose D(+)	Applichem

3.1.2 Buffers and solutions

3.1.2.1 Buffers

All buffers were prepared as aqueous solutions.

Table 2: Used buffers.

Buffers I	Buffers II
toxin labeling with Atto dyes: 100 mM Tris-Cl 1M, pH 9, Bicine	**crude membrane fractionation:** 200 mM sucrose Protease inhibitior added 1:100 before use
planar lipid bilayer assay 150 mM NaCl 10 mM Hepes pH 7.4	**coating buffers (ELISA)** a.) 0.2 M Sodium phosphate, pH 6.5 b.) 0.1 M Sodium carbonate, pH 9.5

Buffers I	Buffers II
Laemmli 4x sample buffer 0.25 M Tris-Cl (pH 6.8) 8% SDS w/v 30% Glycerol (v/v) Spatula tip bromphenol-blue	**imaging buffers for Ca-imaging** with and without calcium (in brackets) 135 mM NaCl (2 mM $CaCl_2$) 2 mM $MgCl_2$ 4 mM KCl 5 mM Hepes pH 7.4
Trp-fluorescence 50 mM Tris-Acetate 100 mM K-Acetat pH 7.2	**NuPAGE SDS running buffer** 20x (Invitrogen) 50 mM MOPS 50 mM Tris Base 0.1% SDS 1 mM EDTA pH 7.7
Phosphate buffered saline (10x) 1.3689 M NaCl, 26.8 mM KCl, 101.4 mM Na_2HPO_4, 17.6 mM KH_2PO_4	**lysis buffer** 0.1% Triton-X-100 in PBS

3.1.2.2 Solutions

Table 3: Used solutions.

Solutions I	Solutions II
blocking solution for western blot: 3% w/v milk powder 1x PBS 0.1% v/v tween in 1x PBS	ECL plus **western blotting detection** reagents GE healthcare 1:40 (solution A:B)
coomassie protein staining solution: 10% v/v acetic acid 50 % v/v methanol 0.1 % w/ v coomassie R250 in water	**coomassie destaining solution:** 10% v/v acetic acid 50 % v/v methanol in water
immunocytochemistry 0.1 % v/v Triton-x 100 4% PFA 4% w/v BSA in PBS	**poly-L-ornithine (PLO)** 0.025% w/v in 0.15 M Boric acid
cholesterol in ethanol 100 mg/ 10 ml	**assay diluent (ELISA)** 10 % v/v FCS in PBS
Bovine Serum Albumine (BSA) 4% in 1x PBS (w/v)	**Artificial cerebrospinal fluid** (ACSF) Volume = 1 L 7.26 g NaCl, 0.186 g KCl, 0.242 g $MgSO_4$, 0.17 g KH_2PO_4, 2.18 g $NaHCO_3$, 1.802 g Glucose, 1.37 g Saccharose, 0.368 g $CaCl_2$

3.1.3 Antibodies

3.1.3.1 Primary antibodies

Table 4: List of used primary antibodies.

Epitop	Species	Distributor	Dilution
Actin	mouse	Santa Cruz	1:1000
Pneumolysin	mouse	Santa Cruz	1:200 1:1000 (western blot)
Vinculin	mouse	Genetex	1:400

3.1.3.2 Secondary Antibodies

Table 5: List of used secondary antibodies.

Species directed against	Species (origin)	Company	Conjugates
mouse	goat	Jackson Immuno research	cy3, cy5, FITC and 1:200 peroxidase

3.1.4 Reagents for cytochemistry and live imaging

3.1.4.1 Dyes

Table 6: List of dyes used for live imaging and immunocytochemistry.

Dye	Distributor	dilution/ concentration
Albumin 555	Invitrogen, Molecular probes	0.1 mg/ ml
Atto 488 NHS Ester	Atto-tec GmbH	In labelling 4:1 (Atto dye:toxin)
BSA 488	Invitrogen, Molecular probes	1:10
Dextran conjugates	Roth	2 mg/ ml
$DiBAC_4$	Invitrogen, Molecular probes	500 nM
FM 1-43	Invitrogen, Molecular probes	200 µg/ ml; 5 µg/ml
Hoechst	Invitrogen, Molecular probes	1:1000
Phalloidine 488	Invitrogen, Molecular probes	5 µl/ ml PBS
Propidium iodide	Invitrogen Molecular Probes	1:1000
Transferrin 555	Invitrogen Molecular probes	20 µg/ ml

3.1.4.2 Inhibitors

Table 7: List of inhibitors used in live imaging experiments and immunocytochemistry.

Inhibitor (Target)	Distributor	dilution/ final concentration
Blebbistatin (myosin II)	Calbiochem	2 µM
Dynasore (dynamin)	Calbiochem	60 µM
Polymyxin B sulphate (LPS)	Calbiochem	30 µM
Protease Inhibitor (proteases)	Roche	1:100

3.1.5 Kits

Table 8: Used kits and supplier.

Purpose	Kit	Distributor
Cytotoxicity Assay (LDH release)	Cytotox 96® Non-radioactive cytotoxicity assay LDH Cytotoxicity Detection Kit	Promega Clontech
Quantification of IL-1β, IL-6, IL-12 (p40), MCP-1, TNF-α	ELISA	BD

3.1.6 Tools

Surgical tools for tissue preparation:	Roth and Hartenstein
Binocular:	Motic Microscopes, Roth
Cell culture microscope:	Leica
Vibratome:	Vibroslice NVSL, World Precision Instruments, (Berlin, Germany)

3.1.7 Protein Biochemistry

3.1.7.1 SDS-PAGE and western blot

Table 9: Materials for sodium dodecylsulphate polyacrylamide gel electrophoresis and western blotting.

Material	Distributor
4-12% Bis Acrylamid gradient Gels Running Buffer	Invitrogen
4-12 % Bis Acrylamid Gels Running Buffer	Anamed
Polyvinylidene fluoride (PVDF) Membrane	Milipore Immobilon P

Material	Distributor
x-ray film, Fujifilm Super RX	Hartenstein
fixer, Kodak	Hartenstein
developer, Kodak	Hartenstein

3.1.7.2 Columns and tubes

Table 10: Other materials.

Purpose	Kit	Distributor
Size exclusion chromatography	Econo Pac 10 DG desalting column	Bio Rad
Membrane fractionation	Polycarbonate tubes	Laborgeräte Beranek, Weinheim

3.1.7.3 Protein purification (Glasgow)

Escherichia coli XL-1 cells: Stratagene, Cambridge, UK

HySoy J media: Sigma-Aldrich, Dorset, UK

Dialysis buffer: 0.2 g/L KCl, 0.24 g/L KH_2PO_4, 1.44 g/L Na_2HPO_4, Sigma-Aldrich

Amicon ultra-15 centrifugal filter tubes: Millipore, Watford, UK

BioCAD® 700E workstation: Applied Biosystems Ltd, Warrington, UK

Limulus Amebocyte Lysate Kinetic-QCL® Kit: Cambrex, Nottingham, UK

3.1.8 Cell culture

3.1.8.1 Media and antibiotics

Leibovitz L 15, DMEM and BME-media were purchased from Invitrogen.

Penicillin/ Streptomycin was purchased from Invitrogen.

3.1.8.2 Solutions and materials

Table 11: Solutions and materials used in cell culture.

Solution/ Material	Distributor
Trypsin EDTA 0.05%	Invitrogen
FCS (fetal calf serum)	Pan Biotec
cell culture flask	Sardtedt
dishes (60, 100 mm, 6-well, 12-well, 24-well)	Sardtedt
hepes buffer solution 1M	Invitrogen
PLO (Poly-L-Ornithine)	Sigma
chambered slides	BD
cover glass chambered slides	VWR

3.1.9 Machines

Microscopes: Confocal System: Leica TCS SP5 II

Epifluorescent System: Olympus Cell^M

96-well-plate reader: Biotek Instruments GmbH

Chambers for SDS PAGE: Invitrogen

Table 12: Materials used for planar lipid bilayer.

Tool	Supplier
Amplifier	fabrication of Prof. Benz's lab
Electrodes	Metrohm
Electrometer	Keithley 614
Magnetic stirrer	Hanna Instruments
Oscilloscope	OWON
Recoder	Rikadenki
Teflon chamber	fabrication of Prof. Benz's lab
Telescope	Spindler und Hoyer
Voltage Source	fabrication of Prof. Benz's lab

Centrifuges: Beckmann ultracentrifuges, Optima™

TLX Ultracentrifuge

Rotor TLA 120.2

Luminescence Spectrometer : Perkin Elmer, LS50B

3.1.10 Software

Program	Supplier
GraphPad	GraphPad Software Inc., La Jolla, CA, USA
imageJ	version 1.43 for Windows, National Institute of Health, Bethesda, Maryland, USA
Photoshop CS6	Adobe Systems Inc., USA
spekwin32	Dr. Menges, Jena, Germany

3.1.11 Animals

SD rats were purchased from Charles River, mice (C57Bl/6) were purchased from Janvier.

3.1.12 Other materials

UV Cuvettes: Roth

Immersion-oil: Hartenstein

Carbogen-gas: Westfalia

3.2 Methods

Parts of this section have already been published in (Fortsch, Hupp et al. 2011) and (Wippel, Fortsch et al. 2011).

3.3 Biochemical assays

3.3.1 Pneumolysin preparation

PLY and variants of the toxin were kindly supplied by Professor Mitchell. PLY-W433F (partially non-lytic (1% of wild-type) mutant) was expressed in *Escherichia coli* XL-1 cells in HySoy J media and purified by hydrophobic interaction chromatography as described previously (Bakhiet, Olsson et al. 1993). Eluted fractions were run on SDS-PAGE and coomassie stained using standard protocols. Fractions containing >98% pure PLY were pooled and dialyzed overnight in phosphate buffer, prior to concentration using Amicon ultra-15 centrifugal filter tubes. The concentrated sample was then further purified by anion exchange with Poros® HQ20 Micron chromatography media using the BioCAD® 700E workstation and introducing a 0 M to 1 M NaCl gradient. Lipopolysaccharide (LPS) content of purified toxin was determined using the Limulus Amebocyte Lysate Kinetic-QCL® Kit run according to manufacturer's instructions. All purified proteins had <0.6 Endotoxin Units (EU)/μg protein. The purified toxin had an activity of ca. 5 x 104 hemolytic units (HU)/mg. One HU was defined as the minimum amount of toxin, needed to lyse > 90% of 1.5 x 108/ml human erythrocytes within 1 h at 37°C.

3.3.2 Protein content determination assay

For protein content determination the BCA assay was used . A calibration curve with bovine serum albumin ranging from 2000 μg/ml down to approximately 15 μg/ml in serial dilutions was prepared. Analogue to dilution of the calibration curve the protein samples were diluted in PBS. The principle of the BCA test is the Biuret reaction based on the fact, that proteins build a complex with Cu^{2+}-ions in an alkaline solution. Cu^{2+}-ions are most probably reduced to Cu^{+}-ions reacting to form a violet complex with bicinchoninic acid

and thus enabling a colorimetric determination of protein amount in a sample (Smith, Krohn et al. 1985).

3.3.3 Enzyme-linked immunosorbent assay

E nzyme-linked immunosorbent assay (ELISA) for IL-1β, IL-6, IL-12 (p40) and TNF-α were carried out as described by the manufacturer's manual.

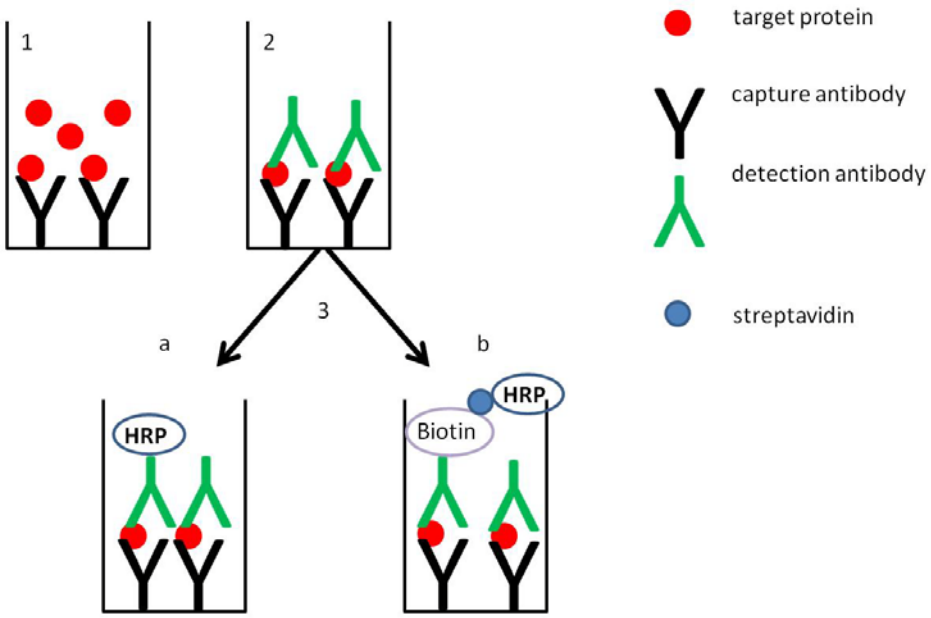

Fig 13: Description of sandwich enzyme-linked immunodorbent assay. The target protein binds in the first step to the immobilized capture antibody (1). After a washing step the detection antibody was added (2). In the last incubation step the Horseradish-Peroxidase (HRP) was able to bind either to the biotin-coupled (3b) detection antibody or it was already bound to the detection antibody (3a). In the very last step, the substrate of HRP was added leading to a colorimetric reaction.

A 96-well plate was covered with 50 µl of the capture antibody the night before at 4°C in coating buffer. The plate was blocked for 1 h in assay-diluent. Subsequently, the plate was washed three times in washing buffer (PBS-T). A standard calibration curve was prepared ranging from 2000 pg/ml or from 1000 pg/ml in serial dilutions down to 0 pg/ml. In total, eight calibration points were used, including maximum and minimum. 50 µl of the sample and of the standard was added to each well. Each sample was determined in double measurements. After an incubation of 2 h, the plate was washed for five times. 50 µl of detection antibody was added per well. Either the detection

antibody was combined or already tagged with a streptavidin-HRP tag. Here, an incubation of 1 h followed. In other cases, the detection antibody was added for 1 h and following this step a streptavidin-HRP conjugate was added for an extra time of 30 min. In any case, after incubation the plate was washed thoroughly for seven times. 100 µl of tetra-methyl-benzidine (TMB) was added as a substrate for HRP leading to a colorimetric reaction. After 30 min the reaction was stopped with 0.12 M H_2SO_4. The colorimetric product turned from blue to yellow. Thus, the absorbance was measured at 450 nm with the plate reader. By producing a calibration curve, the amount of the different pro-inflammatory cytokines could be calculated.

3.3.4 Membrane binding properties of PLY-wildtype and variants

Cells were treated with toxins at set concentrations (0.1-0.2 µg/ml) in 100 mm dishes. After treatment cells were washed with PBS. With the help of a cell scraper cells were harvested in 200 µl crude membrane fractionation buffer. Homogenisation was done, strictly at 4°C, via a syringe (Ø of 0.7 and 0.4 mm) by pipetting the cell lysate up and down for 20 times in the larger syringe and 10 times in the smaller syringe. Centrifugation at 900 x *g* for 10 minutes at 4°C removed cell debris. The pellet was discarded and the supernatant subjected to ultracentrifugation at 110.000 x *g* for 75 min at 4°C. The cytosol-containing supernatant was transferred into a new tube, the pellet was inverted on cellulose paper and dried o.N. at 4°C and resuspended in lysis buffer the following day. Samples were stored at -20°C until SDS-PAGE and western blot were carried out.

3.3.5 Cytotoxicity (LDH-release) assay

The lactate dehydrogenase detection kit (Roche Diagnostics GmbH, Mannheim, Germany) was used in some experiments according to the manufacturer's instructions to assess toxicity and cell lysis. After treatment of cells with toxin, lysis buffer (as a positive control) and medium as a negative control, medium was transferred into a new tube and cell debris was centrifuged down at 900 x *g*. The supernatant was assessed in the cytotoxicity assay. In triple measurements, 50 µl were added per well on a 96-well-plate. The substrate-mix was reconstituted in a dilution of 1:25. 50 µl of the substrate was

added to the samples and incubated for 30 min at RT. The reaction was stopped by adding 50 µl of 1 M HCl. The colorimetric reaction was measured via a plate-reader at a wavelength of 490 nm.

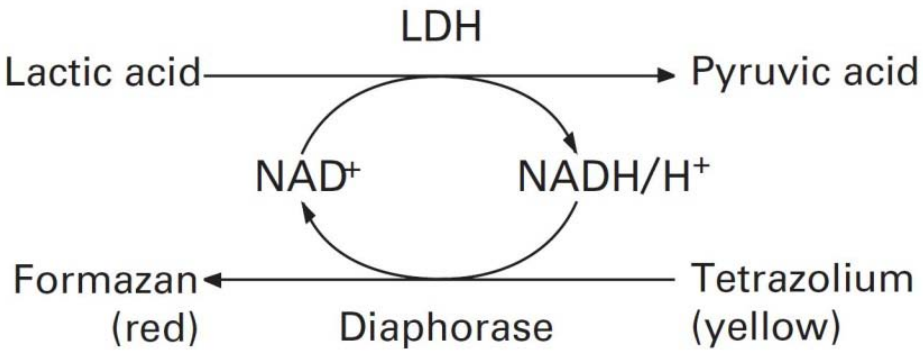

Fig 14: Lactate dehydrogenase assay. From the clontech manual.

3.3.6 Labeling of toxin with dye

For the coupling reaction an NHS-Ester bond was selected, as no free amino-groups in the cholesterol binding loop were found (based on the pdb-file on Cα atoms of PLY). By labeling free amino-groups, an accidental inhibition of toxin-activity should be avoided. NHS-esters readily react with amino groups of proteins. The optimum pH range for NHS-ester coupling is pH 8.0 – 9.0. At this pH amino-groups of proteins, i.e. the ε-amino groups of lysines are unprotonated to a high degree and highly reactive towards dye-NHS-ester. The dye was conjugated in 0.1 M Bicine buffer, pH 9, in and 4-fold molar excess to the toxin for 30 min at room temperature. The coupling reaction was stopped with 1/10 100 mM Tris-Cl, pH 8 in order to add an excess of free amines. After the coupling reaction the protein was separated from the free dye by using size-exclusion chromatography. Here, the coupled protein will travel faster through the gel-filtration column compared to unlabeled dye. This is due to the selected pore-size of the matrix made of branched dextranes. As these dextranes show a high content of hydroxyl-groups, the polymer is hydrophilic and swells due to the mobile phase (Kleber, Schlee et al. 1990). Molecules that are larger than the resulting pores, e.g. the protein labeled with the dye, cannot enter the gel-matrix, whereas the dye itself can enter. For the elution it is possible to see

to distinct bands passing during elution with PBS. The first fraction will be the labeled protein, the second band will be the uncoupled dye. Fractions were collected. Via SDS-PAGE the labeled fractions were verified, by analyzing the Gel under a UV-Light transilluminator. Labelled fractions were pooled. Protein amount was verified by BCA protein assay and remaining cytotoxic activity was investigated by using LDH-assay.

3.3.7 SDS-PAGE

Under denaturating conditions, Sodium dodecyl sulfate is an anioinic detergent binding to hydrophobic areas of proteins and thus leading, next to a boiling of samples, to denaturation. The protein charges are covered by a strong negative charge, so that the proteins can be separated by size only in an electric field (Laemmli 1970).

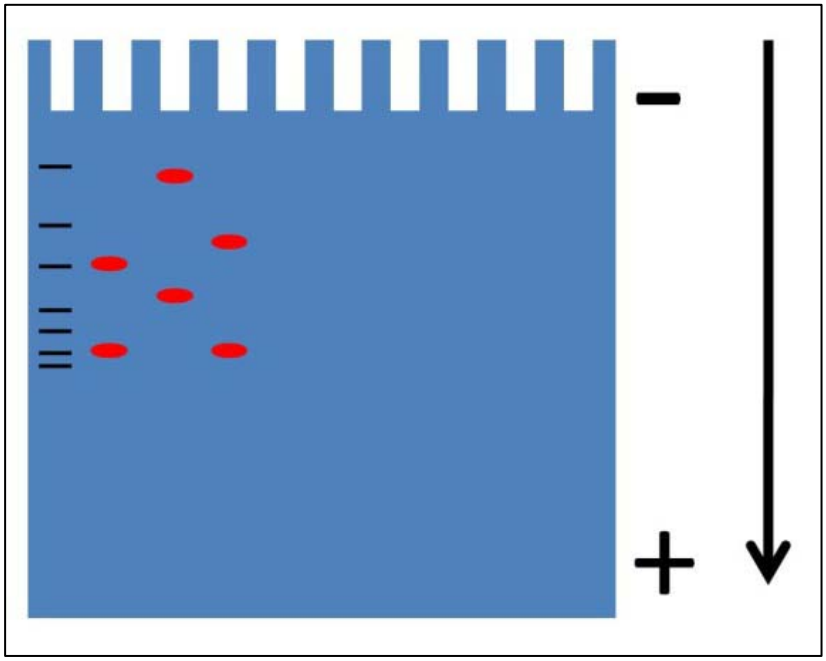

Fig 15: Description of protein migration in electric field during SDS-PAGE. The negatively charged proteins migrate in the electric field to the cathode.

Gradient gels of 4-12% polyacrylamid were purchased from Invitrogen. The protein samples were boiled for 3 min at 95°C in order to denaturate the proteins. Subsequently, samples were stored on ice to avoid renaturation. Laemmli buffer was added for the purpose of covering the own charges of proteins with negative charges. When the samples were applied to the gel, an electric field was applied in order to separate the proteins migrate to the cathode. Electrophoresis was carried out at 200 V for 2 h.

3.3.8 Western blot

Western blotting serves the purpose to transfer proteins after finished SDS-PAGE onto a PVDF Membrane. This enables the experimenter to detect proteins specifically with the help of antibodies, as a PVDF membrane exhibits higher stability compared to a fragile gel. Here, the method of semi-dry blotting was used.

Again the proteins were transferred to the cathode. After protein-transfer, membranes were blocked in 3-5% milk-powder in PBS-T. Subsequently, membranes were incubated with primary antibody for 1 h at room-temperature in blocking solution and, after tree times washing in PBS-tween, incubated with secondary antibody for 1 h at room-temperature in blocking solution. The secondary antibody was linked to HRP which uses luminol as a substrate and leads to a chemiluminescence reaction. This chemoluminescence is captured on a x-ray film in a dark-room and after exposure subsequently developed and fixed.

Fig 16: Semi-dry western blotting. Proteins separated on the polyacrylamide gel are transferred onto the PVDF membrane in the direction of the cathode. Gel and membrane are enclosed by blotting paper and all are soaked in transfer buffer. Again, the negatively charged proteins migrate in the electric field from the gel onto the PVDF membrane.

3.3.9 Preparation of cells

Primary mouse astrocytes (PMA) were prepared from cortices of postnatal day 4-6 newborn C57/Bl6 mice. Mice were decaptivated and brains were put into dishes containing ice-cold 1x PBS. Meninges and the cerebellum were removed with surgical tools under a binocular. The remaining tissue was sheared into smaller pieces by using a pasteur pipette. The cells of 2 brains were seeded in 75 cm^2 poly-L-ornithine-coated cell culture flasks in DMEM.

3.3.10 Seeding of cells

Prior to treatment, the cells had to be reseeded into the reaction vessel. For live imaging coverslip chamber slides were used. In immunocytochemical assays chambered slides were used. For biochemical assays, either 100 mm dishes or 6-, 12-, or 24-well plates were used. 4-16 h prior to seeding, reaction vessels were covered with poly-L-ornithine at 37°C and 5% CO_2 in order to provide a matrix for the primary mouse astrocytes. Before seeding the astrocytes were rinsed wit 2 ml of Trypsin. Subsequently, the cells were incubated with 2 ml Trypsin until trypsination at 37°C and 5 % CO_2 was completed. Trypsination was stopped by adding 8 ml of full medium to the flask. After rinsing the cells via a pipette, the complete volume of 10 ml was collected in a 10 ml tube and cells were centrifuged at 240 x *g*. The cells were then seeded into the reaction dishes. Per 6-, 12- or 24-well plate one 75 cm^2 cell-culture flask of cells was used. In the case of chambered slides (containing 4 reservoirs) 1/8 of a flask was seeded.

3.3.11 Culture treatment

Cells were treated with pneumolysin and variants at final concentrations of 0.1-0.2 µg/ml. Inhibitors were used at the following final concentrations: 2 µM blebbistatin (inhibitor for myosin II), 60 µM dynasore (inhibitor for dynamin). Dyes were used according to Table 6.

3.3.12 Preparation of acute brain slices

Acute brain slices were prepared from postnatal day (PD) 4-6 newborn SD rats and C57Bl/6 mice by decapitation and vibratome sectioning (300 µm slices) in artificial cerebrospinal fluid (Wippel, Fortsch et al. 2011). Slices were continuously oxygenised with carbogen gas (95% O_2, 5% CO_2) at 4°C. The slices were allowed to adapt in carbogenated BME medium with 1% penicillin/streptavidin and 1% glucose at 37°C for 1 h before being challenged with PLY in the 5% CO_2-buffered medium (pH=7.3). Medium and toxin were mixed with 30 mM polymyxin B and pre-incubated at 37°C for 30 min. Toxin dilution and control solution, with and without polymyxin B, were added to brain slices for 5 h. Slices

were carbogenated during incubation. Samples were taken and either measured immediately via ELISA or stored at -80°C.

3.4 Live imaging experiments

For live imaging experiments, the cells were pre-incubated in pH-insensitive L-15 Leibovitz medium at 37°C without phenol-red and without FCS. This medium was selected as described previously (Goldman, Swedlow et al. 2010). After testing of primary mouse astrocytes in a 24 h imaging and confirmation of cell viability, this medium was selected. Compared to cultivation medium (DMEM) without phenol-red being buffered with hepes leibovitz's medium does not show toxicity compared to 15 mM Hepes buffered medium. The medium had to be free of any indicator as phenol red can interfere with the spectral properties of the dyes used for live imaging. Upon treatment the cells were visualised on an Olympus Cell^M imaging system using 10x and 20x dry objectives. The rate of endocytosis was visualised by cell incubation with the FM1-43 lipophilic styryl dye at a final concentration of 50 µg/ml using an Olympus Cell^M system. Additionally, the dependency of the dye on endosome acidification was tested by pre-treating cells with 10 nM Bafilomycin A in order to prevent endosomal acidification. Membrane depolarisation was visualized using $DiBAC_4$ at a final dilution of 1:10 000. This was optionally achieved by imaging on the confocal system. Here, one well after the other was imaged. In all experiments, cells and tissues were treated with PLY and inhibitors in serum-free medium. In live imaging experiments, the cells were starved for 60 min to 24 h before exposure to the toxin in order to deprive the medium of cholesterol. Cells were analysed by simultaneous observation of toxin-treated and mock-treated cells with automatic repositioning of the microscopic stage with a precision of 1 µm (according to manufacturer's instructions) per single move. All images were processed with ImageJ.

3.5 Immunofluorescent staining

PMA were cultivated in chamber slides and starved 60 min in advance to treatment. After co-treatment with 0.1-0.2 µg/ml of PLY-WT GFP and either albumin, dextran or transferrin for 4 min, cells were fixed in 4% PFA. Samples were preserved by covering in

mowiol and visualised with a Leica SP5 microscope, using a 63x oil immersion objective. Image processing and analysis was performed with ImageJ.

For visualisation of focal adhesions, cells were fixed in 4% PFA after treatment, permeabilized in 0.1% TritonX-100 and blocked in 4% BSA. Between these steps, slides were washed in PBS. After the blocking step, fixated cells were incubated for 1 h with FITC coupled Phalloidin and with the mouse anti-vinculin antibody. After incubation with the primary antibody and another washing step, the incubation with the goat anti-mouse cy3 coupled antibody followed. After three washing steps, the slide was preserved by covering with mowiol.

3.6 Planar lipid bilayer (PLB)

The planar lipid bilayer experiments were carried out as described previously (Benz, Stark et al. 1973; Benz, Janko et al. 1978). The properties of membranes, namely to prevent electric currents to pass the membrane, are used in this assay. If a pore is formed in the artificial membrane e.g. by a pore-forming toxin, the conductance across the membrane will increase. The formation of a pore can be observed as a conductance step in the electrophysiological recording. For this method, a teflon chamber consisting of two reservoirs is required. The wall between the two chambers shows a hole with an area of ca. 0.5 mm^2. This chamber is inserted in a metal box serving as a faraday cage and thus preventing an influx of external forces. Membranes were formed from a 1% (w/v) solution of diphytanoyl phosphatidylcholine (PC) in n-decane. 25% cholesterol (w/w) was added to simulate cholesterol content in an astrocyte membrane. The lipid was spread with a Teflon loop over the small hole in the wall between two chambers containing the aqueous buffer.

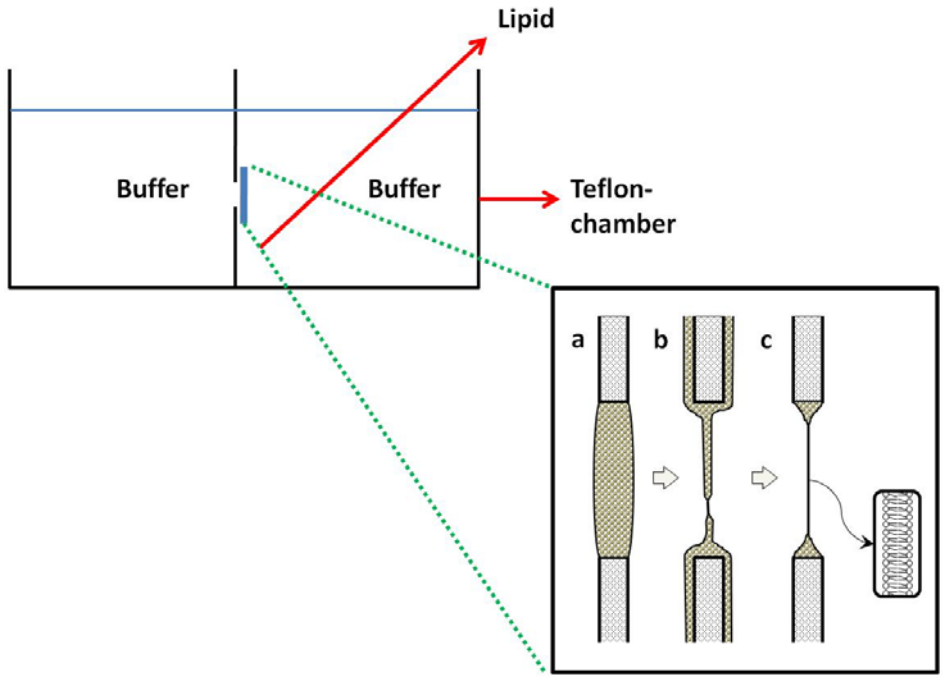

Fig 17: Formation of planar lipid bilayer. The top-panel shows the Teflon chamber with two reservoirs. The blue line represents the bilayer, which is magnified at the bottom-panel. At first Newton rings are visible (a). When the membrane turns black the lipid bilayer with a thickness of about 5 nm has formed (c).

The thin lamella shows at first the newton colours. After a time the membrane will turn black, indicating a formation of a lipid bilayer with a thickness of about 5 nm resembling the thickness of a biological membrane.

The toxin (0.1 µg/ml - 0.3 µg/ml) was added to the *cis*-side in the aqueous phase after the membrane had turned black. The membrane current was measured with a pair of Ag/AgCl electrodes with salt bridges switched in series with a voltage source and a highly sensitive current amplifier. The electrode at the *cis*-side was connected to the voltage source, whereas the electrode at the *trans*-side is connected to the amplifier. The temperature was maintained at 20°C throughout.

In order to answer the question, whether a pore from the toxin shows a certain selectivity for cations or anions, the ion-selectivity had to be determinded. Ion-selectivity depends on the charge distribution at the entrance to the pore. While testing for an ion-selectivity, a concentration gradient is established between the two reservoirs. If the pore shows a specificity for a certain sort of ion, it will be transported, or it will diffuse to the reservoir following the concentration gradient. Here a difference in potential can serve as an indicator for an ion-selectivity.

3.7 Evaluation and statistics

Image processing and image analysis were performed using ImageJ software. Statistical analysis was performed on GraphPad Prism 4.02 for windows. Statistical tests included Mann-Whitney U-test (comparing two groups differing with one parameter at a time) or one-way ANOVA with Bonferroni post test (comparing three or more groups, differing with one parameter at a time).

4 RESULTS

Parts of this section have already been published in (Fortsch, Hupp et al. 2011) and (Wippel, Fortsch et al. 2011).

4.1 Characterisation of wildtype and variants

4.1.1 Lytic capacities

The lytic capacities of PLY-WT, PLY-W433F and PLY-Δ6 were estimated by measuring the release of Lactate-Dehydrogenase (LDH) from primary mouse astrocytes (PMA) into the medium. The positive control, thus releasing 100% of LDH, was treated with the lysis buffer. All colorimetric measured quantities are shown as a percentage in relation to the positive control. Resulting, PLY-WT showed a lytic capacity in 4 trials of almost 100%, compared to PLY-W433F and PLY-Δ6, confirming previous data that these variants are incapable of forming a pore and thus cause cell lysis.

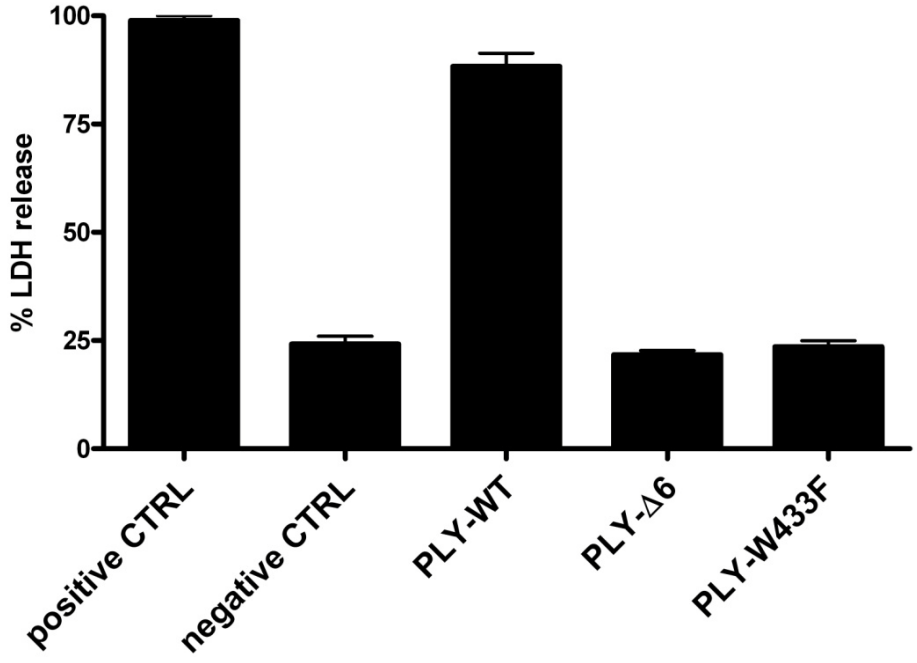

Fig 18: Comparison of LDH-release after toxin-challenge. Only PLY-WT causes a release of LDH, whereas the non pore-forming variants cause a release similar to that of untreated cells. Values represent mean +/- SEM.

Furthermore, a classification of lytic capacities was achieved via live-imaging. Thus, a definition for lytic and non-lytic abilities should be found. Here, cells were challenged with 0.1-0.5 µg/ml PLY-WT and co-stained with propidium-iodide. This chromatin stain with a molecular weight of 668 g/mol should easily enter through macropores and stain chromatin in the nucleus of lysed cells, but it cannot pass an intact biological membrane. The rate of permeabilisation was evaluated by judging the effectivity of PI-Staining. Permeabilisation of the cells occurred in an exponential manner, reaching a plateau at all concentrations not later than 40 min after PLY-WT challenge. As the concentration of PLY-WT rose, the half-time of cell permeabilisation dropped from ca. 22 min (0.05 µg/ml) to ca. 6 min (0.5 µg/ml). As soon as the plateau was reached, two defined populations of cells – permeabilized (PI-positive; accounting for about 10% of cells at 0.1 µg/ml PLY) and non-permeabilised (ca. 90% of the cells at 0.1 µg/ml PLY) were formed and remained unchanged with the time.

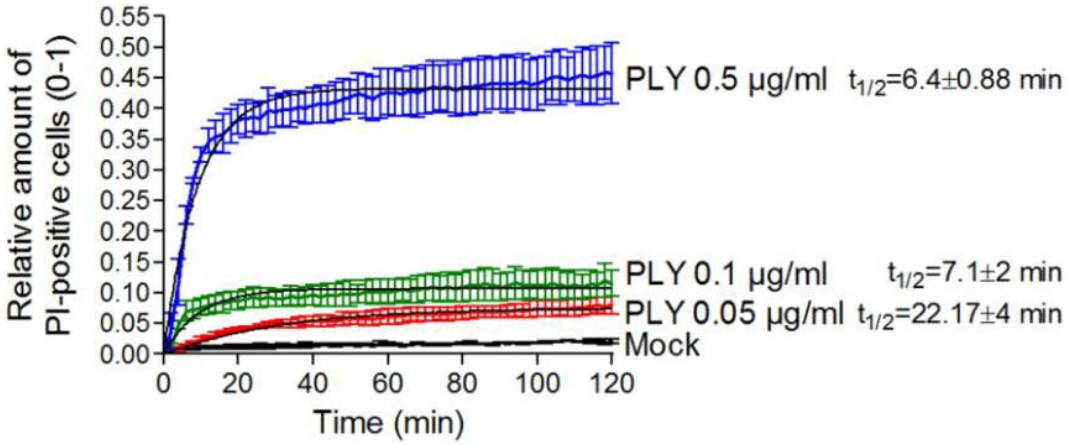

Fig 19: Evaluation of lytic capacity of PLY-WT by propidium iodide. In any case a plateau was reached. At the highest concentration of PLY-WT the plateau was reached in the shortest time. Values represent mean +/- SEM (Fortsch, Hupp et al. 2011).

4.1.2 Membrane binding properties of pneumolysin wildtype and variants

In order to see, whether the variants bind to the membrane in the same manner as the wildtype, an assay visualising the membrane binding was established. Here, 100 mm dishes were treated with the same concentrations of PLY-WT, PLY-W433F and PLY-Δ6. After cell harvest, cells were subjected to ultracentrifugation at 110.000 x *g* for 75 min at

4°C. This served the separation of cytosol from membrane. All fractions were separated via SDS-PAGE and transferred on a PVDF membrane via western blotting. The reactivity of a specific pneumolysin antibody served as mean value to visualise the binding. An antibody directed against actin served as a loading control. Even if the variants PLY-W433F and PLY-Δ6 are incabable of showing any lytic capacity, both can bind to the membrane. Nevertheless, it is worth mentioning, that PLY-W433F binds to a lesser extend, which can be explained by the site of mutation. The tryptophan in position 433 is located in the tryptophan-rich loop, which is supposed to be important for cholesterol recognition. Tryptophan 433 seems to be essential for this recognition and one could assume, that a mutation to a phenylalanin leads to a lesser depth of binding in the lipid bilayer due to the hydroxyl group and thus a slightly increased hydrophility.

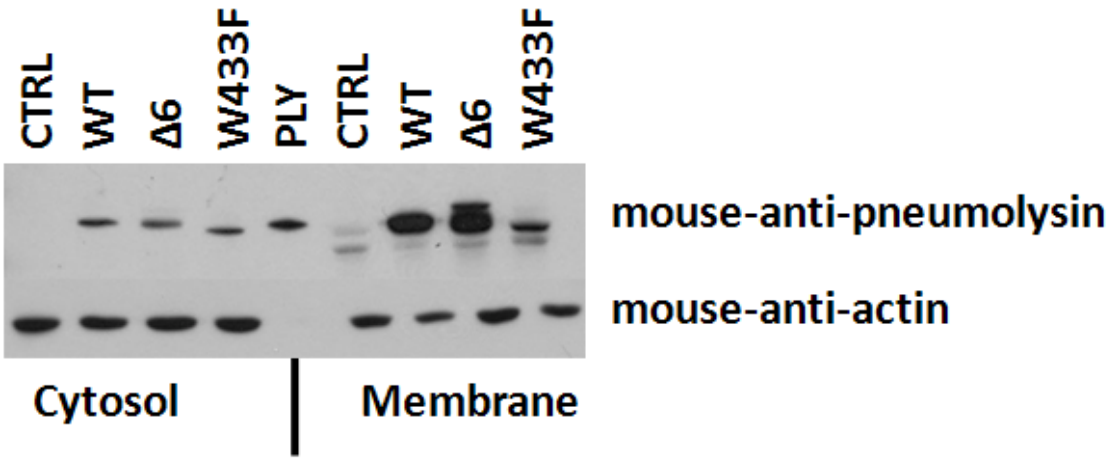

Fig 20: Membrane-binding capacities of PLY-WT, PLY-Δ6 and PLY-W433F at 0.1-0.3 µg/ml. The wildtype and the variants all bind to the membrane. Only PLY-W433F seems to bind to a lesser extent.

4.1.3 Membrane depolarisation

$DiBAC_4$, a voltage sensitive dye, serves as a marker for membrane depolarisation. A change in membrane potential is accompanied by changes in the optical properties of the dye. If the membrane is depolarised, the dye can enter the cell and interact with cytosolic proteins. This interaction leads to an increase in fluorescence. Large changes in fluorescence do not cause a mitochondrial uncoupling (Epps, Wolfe et al. 1994). Thus, if

the membrane potential changes, one could observe, if it is due to a membrane binding or a possible pore-formation.

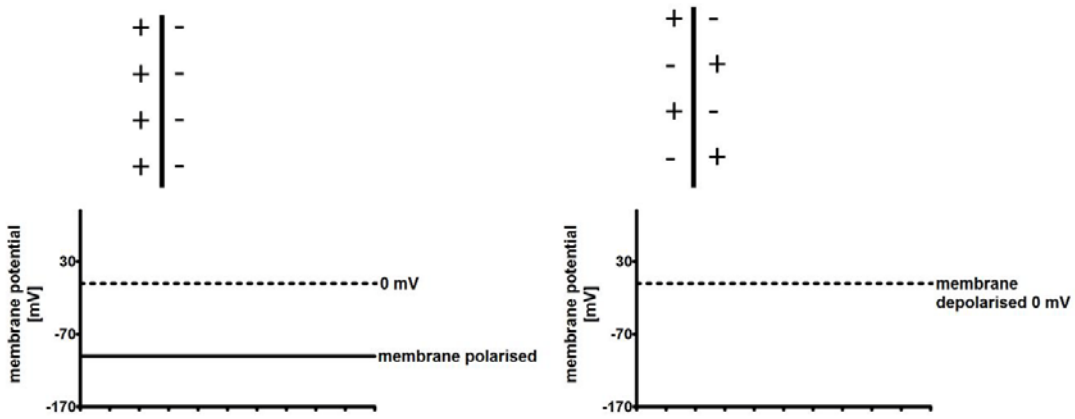

Fig 21: Schematic demonstration of the membrane potential. Left: intact membrane potential, $DiBAC_4$ would not be able to pass through the membrane. Right: depolarised membrane, $DiBAC_4$ can reach the cytosol and interact with cytosolic proteins, thus increasing fluorescence.

In fig 22 it is clearly visible, that only PLY-WT causes a depolarisation of the membrane indicated by the increase in fluorescence of $DiBAC_4$. The variants showed no change. All graphs were normalised to the untreated control. This data shows the independence of membrane depolarisation to membrane binding. Even if the PLY-variants bind to the cell membrane, the depolarisation cannot be caused by membrane binding. The option left to discuss would be a micro-pore formation of PLY-WT in contrast to the non pore-forming variants.

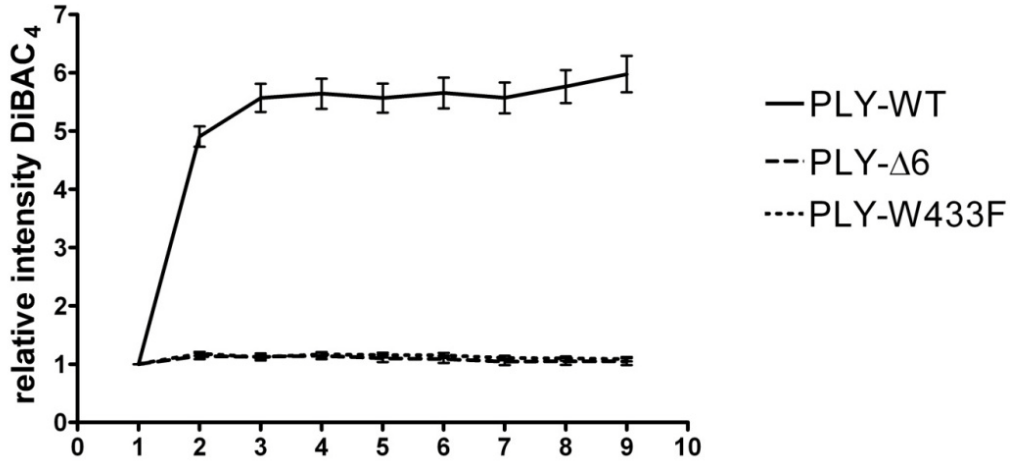

Fig 22: Membrane depolarisation induced by PLY-WT compared to PLY-Δ6 and PLY-W433F. Only PLY-WT caused a visible increase in membrane depolarisation. Values represent mean +/- SEM.

4.1.4 Tryptophan fluorescence

The methodology of measuring tryptophan fluorescence is known to show a change of absorbance spectra, if the polarity of protein environment changes (Vivian and Callis 2001). Thus, if Pneumolysin binds to membrane cholesterol in the membrane, a shift in Tryptophan fluorescence should be observed, as the protein dips from an aqueous phase into the membrane lipid bilayer. Furthermore, the variant PLY-W433F, lacking one tryptophan, should exhibit a different tryptophan fluorescence and spectral behavior. Fig 23 shows the different tryptophan spectra. PLY-WT, PLY-W433F and PLY-Δ6 were pre-incubated with cholesterol. Compared to the cholesterol-free spectrum, a shift of the maximum of 7-10 nm was observed showing that the pre-treatment with cholesterol abolishes the membrane binding capacity to membrane cholesterol. PLY-WT and the variants show the same shift. Due to the pre-treatment with cholesterol, the cholesterol binding site was saturated and the toxins could not bind to membrane cholesterol.

Fig 23: Shifts in tryptophan Fluorescence after challenge with PLY-WT, PLY-Δ6 and PLY-W433F. Dotted line shows treatment with PLY-WT pre-incubated with cholesterol, full line shows pre-treatment without cholesterol.

4.1.5 Planar lipid bilayer

The characterisation of the PLY-variants should also be carried out in an artificial system, in order to avoid cellular effects caused for example by endocytosis. Here, the pore-froming capability should be characterised in an artificial lipid bilayer system in aqueous buffer. Fig 24 shows that PLY-WT causes smaller oscillations (up to 25 pA at 170 mV) indicating an activity of the toxin at the artificial bilayer. PLY-W433F shows small and infrequent oscillations compared to PLY-WT. PLY-Δ6 showed no oscillations at all. All treatments were carried out at comparable concentrations. These data indicate that only the PLY-WT is capable of forming a pore.

The measurement of ion-selectivity is described in 3.6. Here, only PLY-WT has been measured, as the wildtype is the only variant capable of forming a pore. However, only a slight selectivity for cations could be determined as seen in Table 13.

Table 13: Determination of ion-selectivity for PLY-WT pores in PLB. A slight cation selectivity is visible.

Electrolyte	Values	MEAN
KCl	1.16 1.19 1.27 1.23	1.23 → slightly cation selective

Fig 24: Electrophysiology in planar lipid bilayer of PLY-WT, PLY-Δ6 and PLY-W433F. The arrow indicates one step-wise increase of ion-conductance. Each step represents one pore in the bilayer.

In order to further clarify, if pores formed depend on calcium, the conductance of PLY-WT pores under different calcium-conditions was investigated. It becomes clear that

the distribution of pores shows a comparable pattern under different calcium conditions (0 mM, 1 mM and 2 mM calcium).

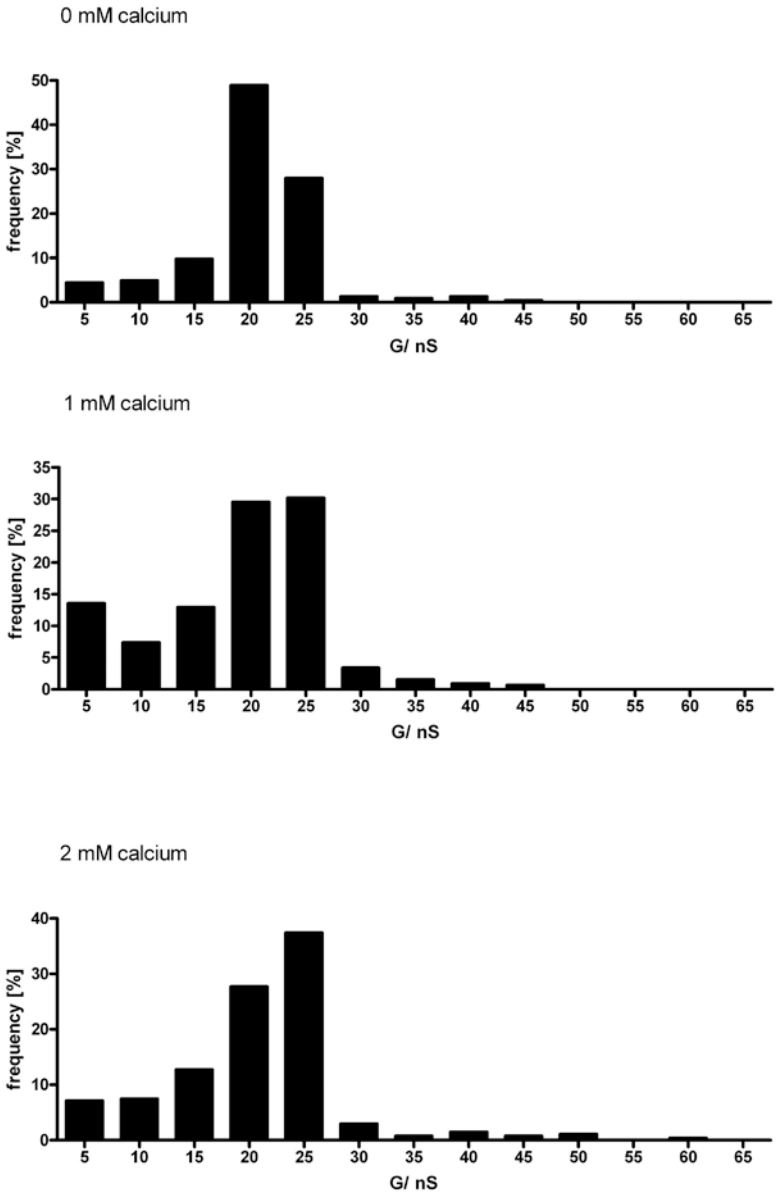

Fig 25: Distribution of PLY-WT pore-sizes in planar lipid bilayer under different calcium conditions. No dependency of pore-size/conductance changes across the artificial membrane on calcium could be observed. In addition, no different pore-sizes in different calcium concentrations could be observed. 0 mM calcium = 225 pores, 1 mM calcium = 325 pores, 2 mM calcium = 267 pores.

4.1.6 Cell displacement

In order to complete the comparison of PLY-WT, PLY-W433F and PLY-Δ6, the effect of these variants on the movement of the cells was followed in time-lapse live-imaging experiments. Both variants PLY-W433F and PLY-Δ6 did not show any ability to cause displacement after toxin challenge, whereas PLY-WT showed a significantly greater cell displacement. The cells were treated with PLY-WT or variants. The films were analysed with imageJ. For this the cell border of the initial time-point up to the last time point was tracked. These tracks are on top of the microscopy panel in Fig 26.

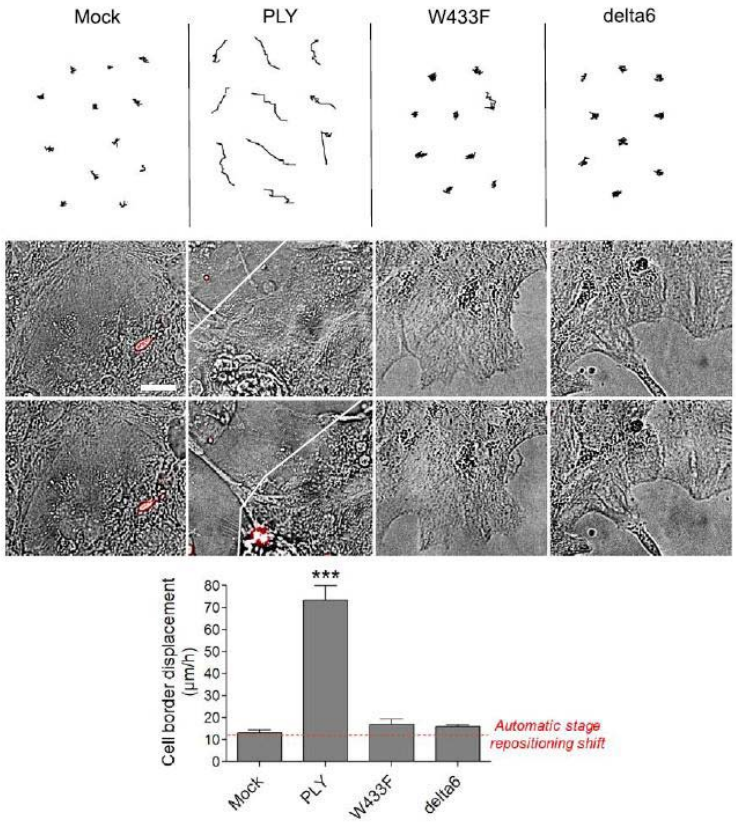

Fig 26: Cell retraction after PLY-WT treatment. It becomes clearly visible that only PLY-WT causes cell retraction, whereas in treatment with PLY-variants the cells stay calm comparable to untreated control cells. Values represent mean ± SEM, n = 40–60 cells of four experiments. The red line in the graph indicates automatic stage repositioning shift. Scale bars: 10 µm. Published in Fortsch and Hupp *et al.* (Fortsch, Hupp et al. 2011).

4.1.7 Cell adhesion

Effects of the PLY-WT and the variants on the movement of astrocytes should be described. Focal adhesions stand for cellular movement. If the cell retracts from or moves towards cellular stressors, on the end of the cell, adhesion points are loosened, whereas in front of the cell new adhesions are fromed pulling the cell forward. Considering previous data and experiments, a difference in cell movement or displacement should be observed comparing PLY-WT with the variants. Here, PLY-WT compared to the variants showed in most cases more and larger focal anhesions, confirming the data on cell dicplacement.

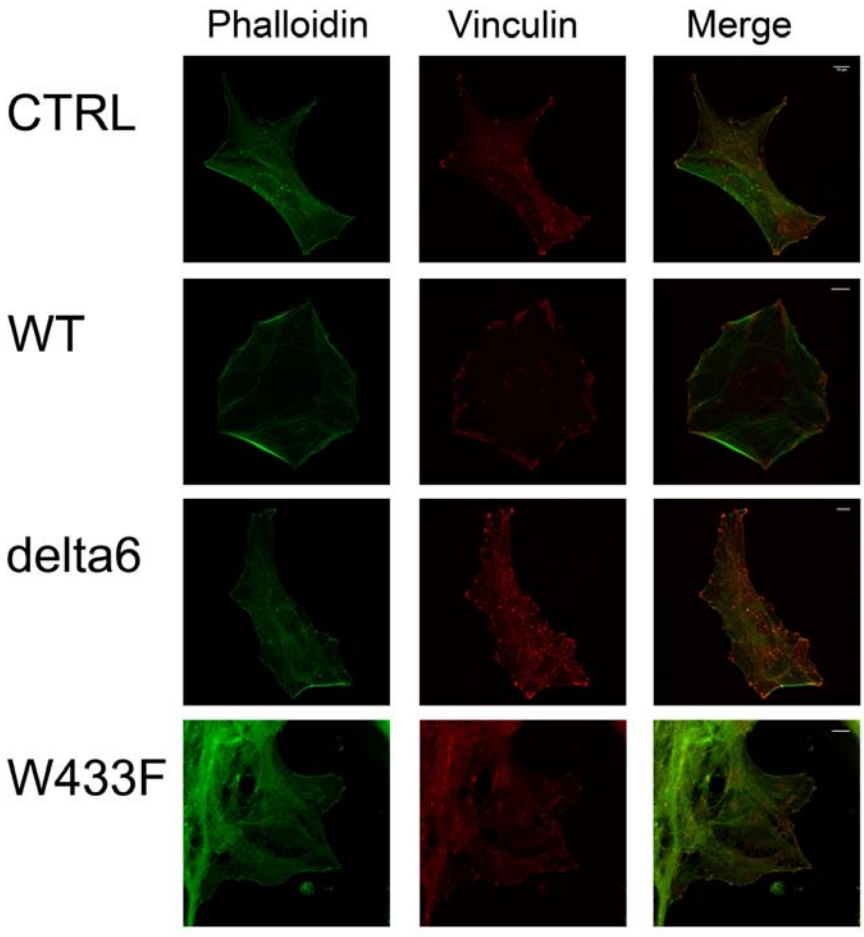

Fig 27: Staining of primary rat astrocytes with phalloidin-alexa 488 and vinculin-cy3 antibody for visualisation of focal adhesions. In PLY-WT treated cells long and strong focal adhesions are visible, whereas in the PLY-variant and control treated cells the focal adhesions have a far smaller appearance. Scale bar = 10 µm.

4.2 Effects on endocytosis

4.2.1 FM 1-43 dye

For a general observation of endocytotic events, FM-Lipophilic styryl dyes were used. These dyes insert into the outer leaflet of membranes and cannot flip-flop across the membrane due to a charged and thus polar head group. If endocytosis occurs, the dye is internalised in the endosome and after acidification of the endosome, the fluorescence of the dye increases. In order to evaluate, whether the increase in fluorescence depends on the acidification of the endosome, cells were imaged with FM 1-43 and a preincubation with bafilomycin A. This antibiotic prevents the acidification of the endosomes (Bowman, Siebers et al. 1988). It is visible, that the fluorescence intensity of FM 1-43 depends on the acidification of the endosome as no fluorescence increase of FM 1-43 after toxin treatment can be observed, when cells have been pre-treated with Bafilomycin A. All values have been normalised to the corresponding control.

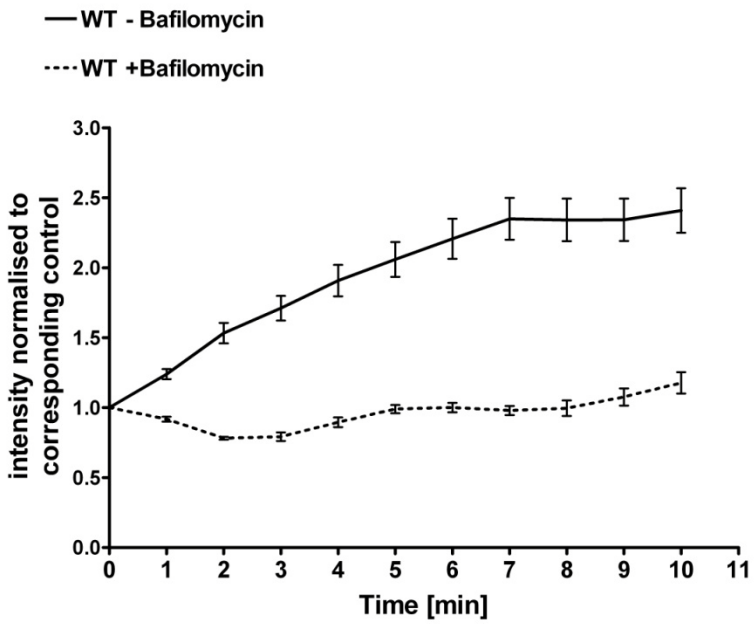

Fig 28: Inhibition of fluorescence caused by FM 1-43 after inhibition of endosomes acidification. Fluorescence intensity of FM 1-43 depends on endosomal acidification. Values represent mean +/- SEM.

4.2.2 Variants

Following the characterisation of the variants under different conditions, cellular effects should be described. Fig 29 shows the rate of endocytosis after toxin challenge. The FM 1-43 dye was applied to the cells 30 min prior to treatment in order to allow an equilibration of the dye in the course of normal rate endocytosis. At 3-5 min after treatment of the primary mouse astrocytes with 0.2 µg/ml of PLY-WT, PLY-W433F and PLY-Δ6 only the PLY-WT causes an increase in endocytotic rate. This reaches a plateau after 7-8 min. The graph shows the data of the variants normalised to untreated control cells.

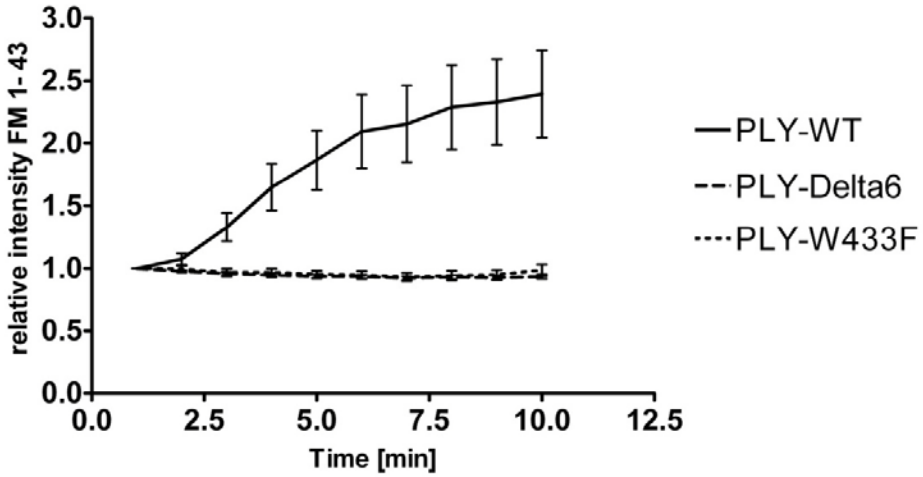

Fig 29: Real-time monitoring of endocytotic processes with FM1-43 dye. Comparison of PLY-WT, PLY-Δ6 and PLY-W433F. Only PLY-WT causes an increase in overall endocytosis. Values represent mean +/- SEM.

4.2.3 Effects of inhibitors on endocytosis

As effects on endocytotic behaviour of the cells were observed, a mechanistic explanation should be attempted. Here two inhibitors were used. The first inhibitior dynasore, inhibits the GTPase activity of dynamin. The second inhibitor blebbistatin inhibits seletively and potently nonmuscle myosin II. The inhibitors and the FM 1-43 dye were applied 30 min prior to toxin challenge at concentrations of blebbistatin at 2 µM and dynasore at 60 µM. The cells were challenged with 0.2 µg/ml of PLY-WT. Fig 30 depicts the effect of the two inhibitors on the endocytotic rate in co-treatment with PLY-WT. The wildtype alone causes an increase in overall endocytic rate, whereas treatment

with dynasore and both inhibitors lead to no change in the endocytotic rate. Co-treatment of cells with Blebbistatin and PLY-WT shows a much stronger increase in endocytic rate compared to the wildtype.

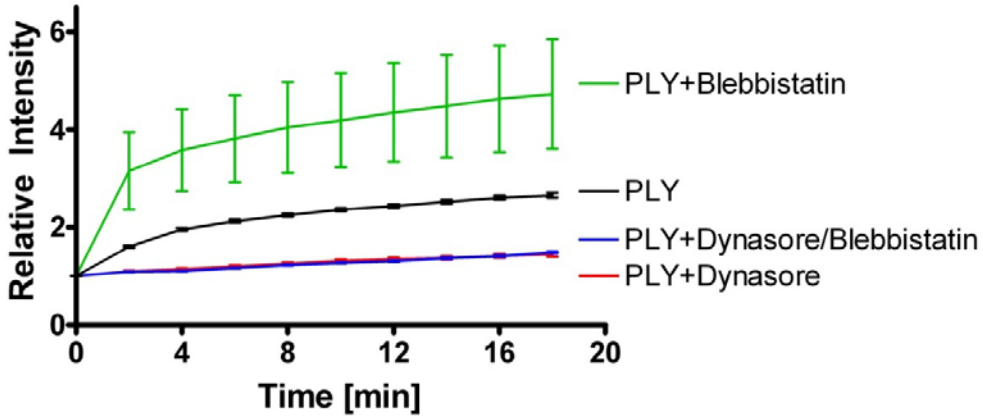

Fig 30: Real-time monitoring of endocytotic processes. Inhibition of dynamin, myosin II, both and no inhibitor are shown. Inhibition of myosin II leads to a stronger increase in overall endocytosis compared to PLY-WT treatment without inhibitor. Inhibition of dynamin and dynamin/myosin II leads to a decrease in overall endocytic rate compared to treatment with PLY-WT alone. Values represent mean ±SEM.

4.2.4 Effects of inhibitors on membrane depolarisation

As inhibitors of dynamin and myosin II showed effects on endocytosis the question remained what the effect on membrane depolarisation would be. If the endocytotic processes serve as a possible rescue mechanism of the cell, after pore or micro-pore formation, the depolarisation pattern could change. Again, cells were pre-treated with dynasore, blebbistatin, or both and after 30 min challenged with 0.2 µg/ml PLY-WT. In Fig 31 it is visible that the wildtype alone causes a depolarisation of the cell. This depolarisation is comparable to the treatment with both inhibitors. Cells pre-treated with dynasore alone show more depolarisation compared to the wildtype, whereas pre-treatment with blebbistatin alone leads to a smaller increase of depolarisation compared to the treatment without inhibitors. All values are normalised to untreated control cells.

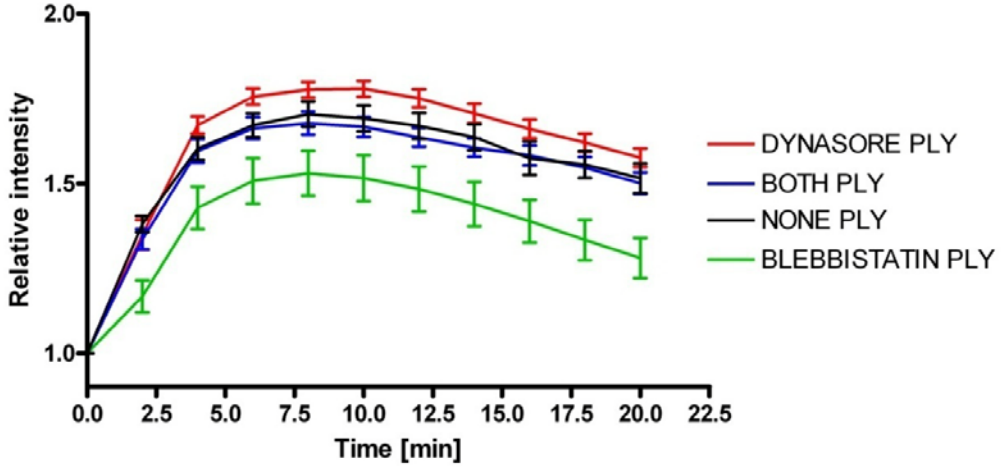

Fig 31: Real-time monitoring of membrane depolarisation. Dynasore and blebbistatin or both inhibitors were applied prior to toxin treatment. Membrane depolarisation is increased after inhibition of dynamin compared to cells treated with PLY-WT alone. Inhibition of myosin II led to a decrease of membrane depolarisation. Inhibiting dynamin and myosin II, the level of depolarisation is comparable to cells treated without inhibitor with PLY-WT alone. Values represent mean +/-SEM.

4.2.5 Calcium dependency

Before and during toxin challenge, cells were kept in medium either containing 2 mM calcium or in medium containing no calcium. Calcium, being possibly involved in membrane repair mechanisms, turned out not to make any difference in the pore-size distribution in the planar lipid bilayer Fig 25. Different calcium conditions were applied and release of LDH was measured in order to evaluate the impact of different calcium conditions on cytotoxic effects of PLY-WT. As shown in Fig 32 the depletion of calcium from the medium causes a much higher lytic capacity of PLY-WT. In further treatments without calcium, the toxin concentration was adapted to a concentration that would turn out to be non-lytic.

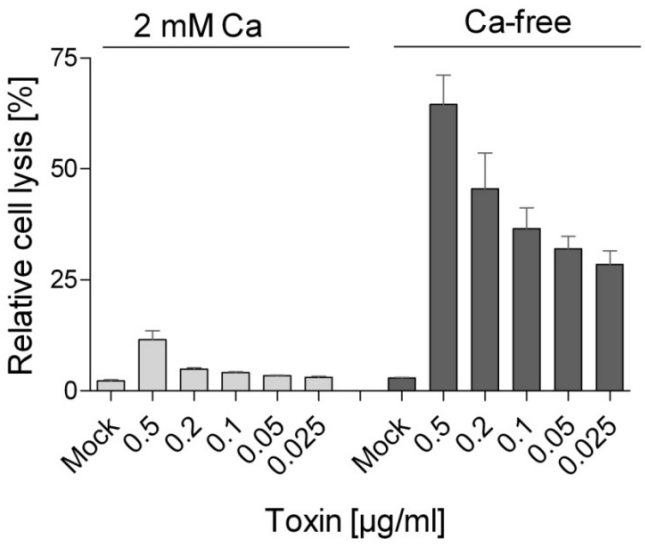

Fig 32: Measurement of cytotoxicity by measuring the release of Lactate-Dehydrogenase in different calcium conditions. +Ca = 2 mM, -Ca = 0 M Ca. Values represent mean +/-SEM. Figure also published in (Wippel, Fortsch et al. 2011).

By using different calcium concentrations in medium, at 2 mM or 0 mM calcium, the possible effect of calcium on the endocytotic rate of PLY-WT should be determined. As the toxin concentration in calcium-free conditions was adapted to a sub-lytic concentration, one can say that the observed effects are not due to a higher toxicity of PLY-WT. Under calcium-free conditions, the endocytic rate was three times higher than under calcium-containing conditions.

PLY-WT is thus not only more lytic in calcium-free conditions, but Ca^{2+} seems to play an inhibitory role of the rate of endocytosis induced by PLY-WT.

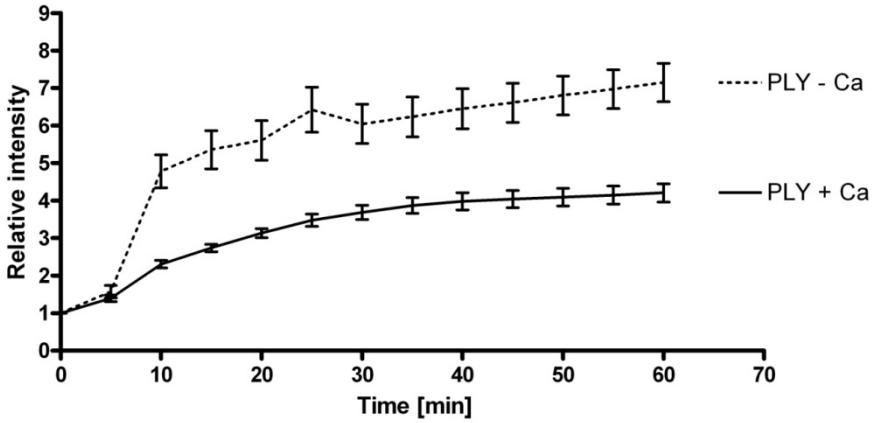

Fig 33: Real-time imaging of endocytotic processes by using FM 1-43 dye in the context to calcium dependency. $+Ca^{2+}$ = 2 mM, $-Ca^{2+}$ = 0 M. Endocytic rate is increased about 3-fold compared to treatment with PLY-WT with calcium. Values represent mean +/- SEM.

4.2.6 Endocytotic markers

4.2.6.1 Internalisation of PLY-WT

PLY tagged with GFP was visualised on a confocal system. In addition, several inhibitors on endocytotic adaptor proteins, dynamin and myosin II, were used as co-treatment. In Fig 34 it becomes visible that PLY-GFP is internalised to a higher extent, when the primary mouse astrocytes were pre-treated with dynasore or both inhibitors. If the cells are just treated with PLY-GFP or pre-treated with blebbistatin the level of internalisation is comparable.

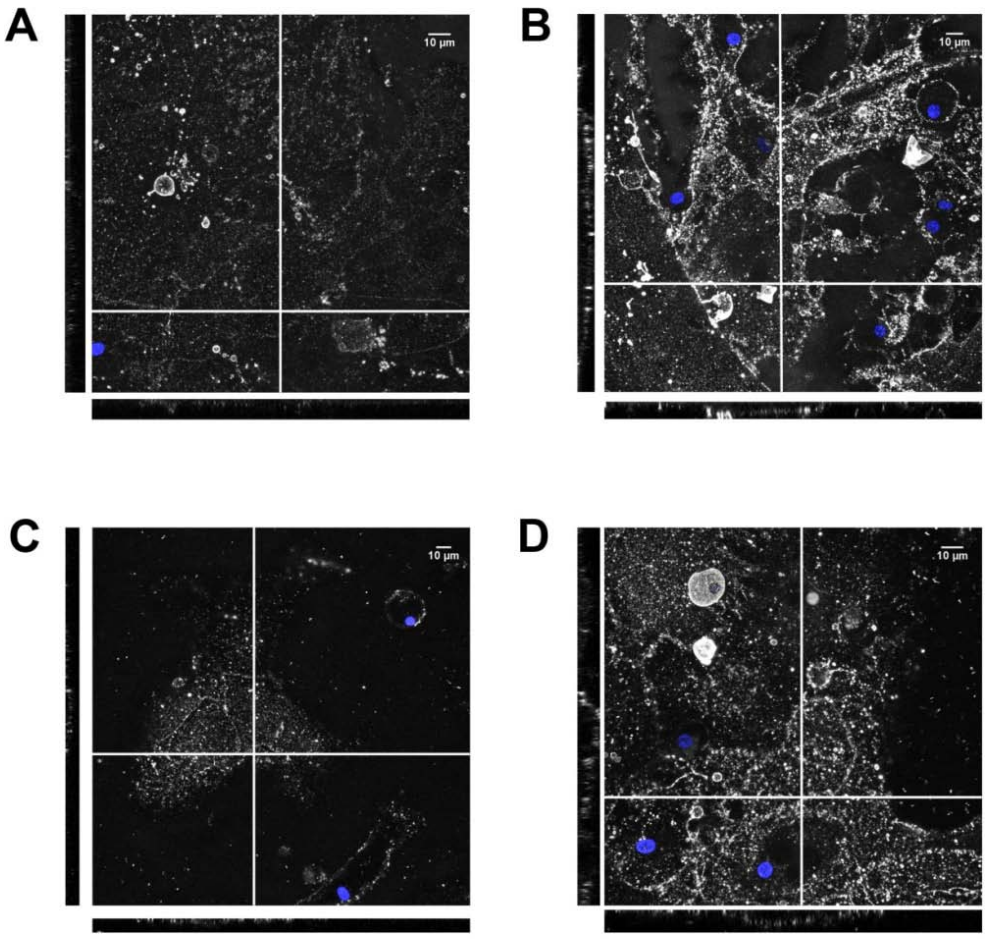

Fig 34: Internalisation of PLY-WT by using A) no inhibitor, B) dynasore C) blebbistatin and D) both inhibitors. The scale bar represents 10 µm. An orthogonal view was produces via imageJ. Vertical white line represents the XZ plane, whereas the horizontal white line represents the XZ plane. These planes are represented at the side (YZ) and at the bottom (XZ) of the stacks. Nuclei are stained with propidium iodide in blue. PLY-GFP is represented in gray values. Orthogonal views were produced in cells that are negative for PI staining and thus are not lysed.

4.2.6.2 Albumin, dextran and transferrin

Albumin is taken up via caveolin dependent mechanisms (Bento-Abreu, Velasco et al. 2009). Thus labelled albumin would serve as a marker for caveolin dependent endocytosis and in a co-staining with GFP-tagged PLY (PLY-GFP) a possible explanation for the internalisation of the toxin could be found. Dextran is taken up into the cell via phagocytosis (Costantini, Gilberti et al. 2011), as it consists of branched sugar molecules and has a high molecular weight. In a co-staining with PLY-GFP the mechanism of phagocytosis could be analysed and the question could be answered if it applied for the uptake of the toxin. Transferrin is a soluble protein that carries iron in the blood. If transferrin is endocytosed, it carries the bound iron to the endosomes (Pearse and Robinson 1990). If the endosome is acidified, transferrin releases the iron. Transferrin is endocytosed in a clathrin dependent manner. A staining with transferrin would highlight clathrin mediated endocytotic processes. Here, PLY tagged with green fluorescent protein (PLY-GFP) and transferrin labelled with Rhodamine were visualised to find a possible co-localisation.

In fig 35 it is visible that PLY-WT and all the above mentioned markers for endocytotic processes are internalised. However, PLY-GFP shows no co-localisation with either albumin, dextran or transferring, excluding these pathways as possible internalisation mechanisms for PLY-WT.

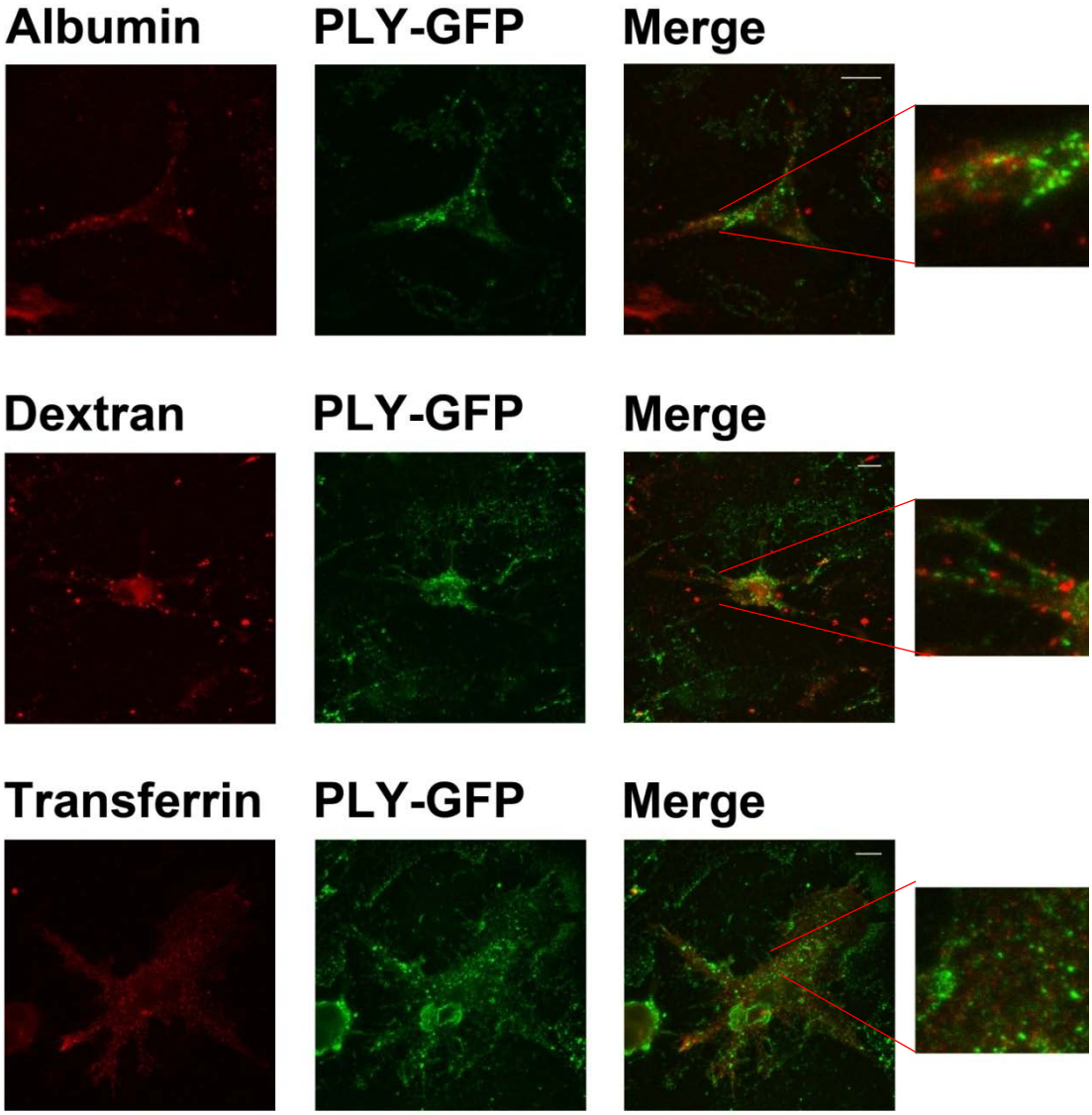

Fig 35: Internalisation of albumin, dextran and transferrin. Co-staining with PLY-WT tagged with GFP showed no co-localisation. The scale-bar represents 10 µm. Magnified pictures are shown in the right panel and are indicated via red lines.

4.3 Immunological aspects

The previously presented data showed that the cells respond in different manners to the PLY-variants and the wiltype. While PLY-WT causes an increase in overall endocytosis, the variants show no differences. The pathological meaning of the described effects shall be characterised by looking more closely at proinflammatory cytokines. IL-1β,

IL-6, IL-12 (p40) and TNF-α were investigated. Of all these proinflammatory cytokines only IL-6 showed an increase in primary mouse astrocytes.

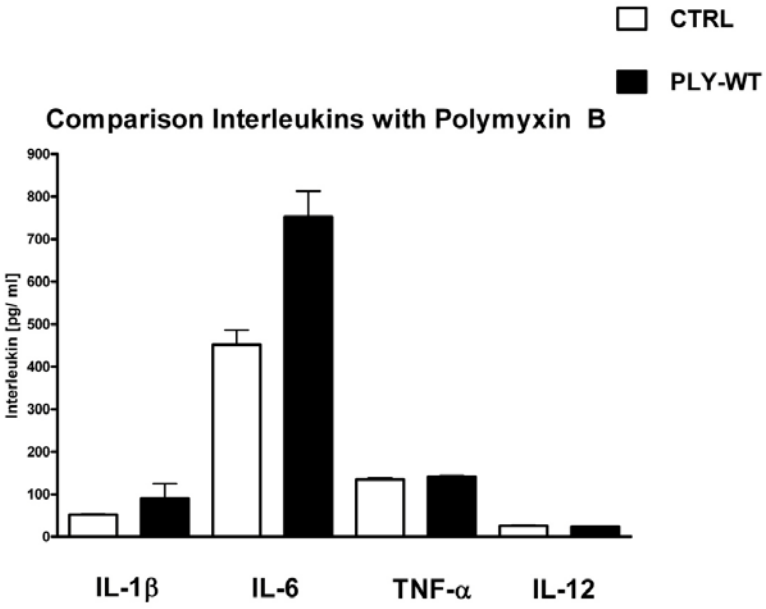

Fig 36: Comparison of all tested interleukins. No difference in IL-1β, TNF-α and IL-12 (p40) were found in measurements with and without Polymyxin B. Only IL-6 was investigated to a further extent. Values represent mean +/- SEM.

For all measurements, toxin dilutions were pre-incubated with polymyxin B in order to abolish an activation of TLR 4 by LPS. Cells that were treated with WT-PLY alone could show activations mediated by LPS and by the toxin. After pre-incubation with 30 µM polymyxin a possible activation of TLR 4 by LPS should be abolished. Pre-incubation with Cholesterol should inhibit any membrane binding and thus the pore-forming effect of PLY-WT. It becomes visible, that PLY-WT alone, after Polymyxin B pre-treatment, shows a higher activation of IL-6 compared to the untreated PLY-WT. After pre-treatment with Cholesterol the release of IL-6 is abandoned.

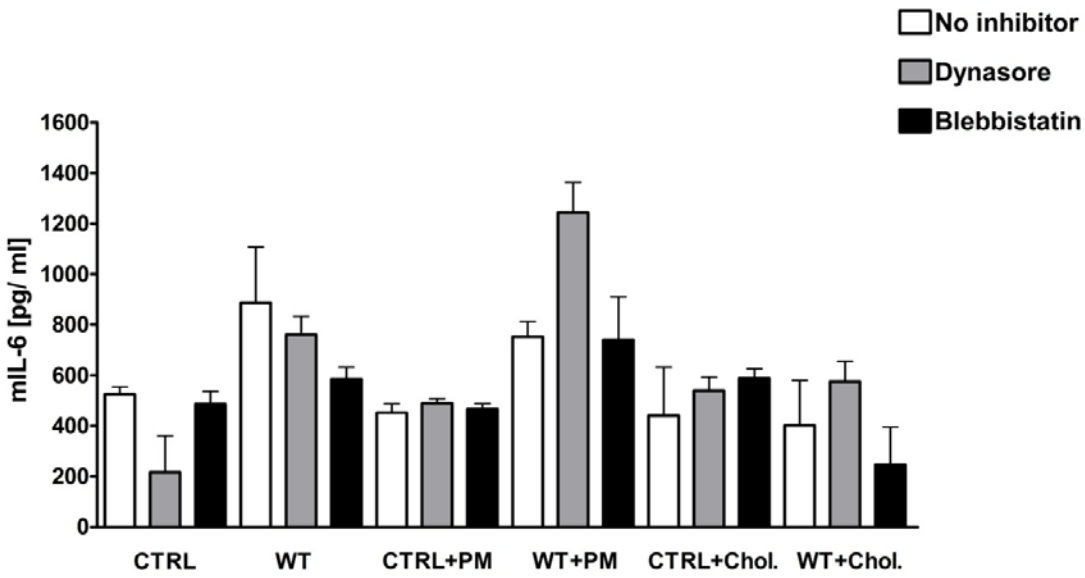

Fig 37: Treatment of primary mouse astrocytes with PLY-WT. Either cells were treated with PLY-WT and medium, with PLY-WT and 30 µM polymyxin B (PM) or with cholesterol (Chol.). Polymyxin B should abolish LPS from the toxin-dilution and thus only PLY-WT activation of IL-6 should be visible. Cholesterol should saturate the binding-site of PLY to membrane-cholesterol and thus only action by LPS should be visible. Values represent mean +/- SEM.

IL-6 is increased after treatment with PLY-WT compared to control cells. The PLY-variants show no increase. If the heat-killed *S. pneumonia* (HKSP) were added to the toxin treatment the production of IL-6 increased to a lesser extent (1.5-fold compared to the corresponding control. Again, the PLY-variants showed no increase. Furthermore, treatment with dynasore showed a smaller amount of IL-6 production, whereas treatment with blebbistatin led to a similar increase in IL-6 production compared to the treatment with PLY-WT alone. The fold-changes are shown in the appendix (Table 14).

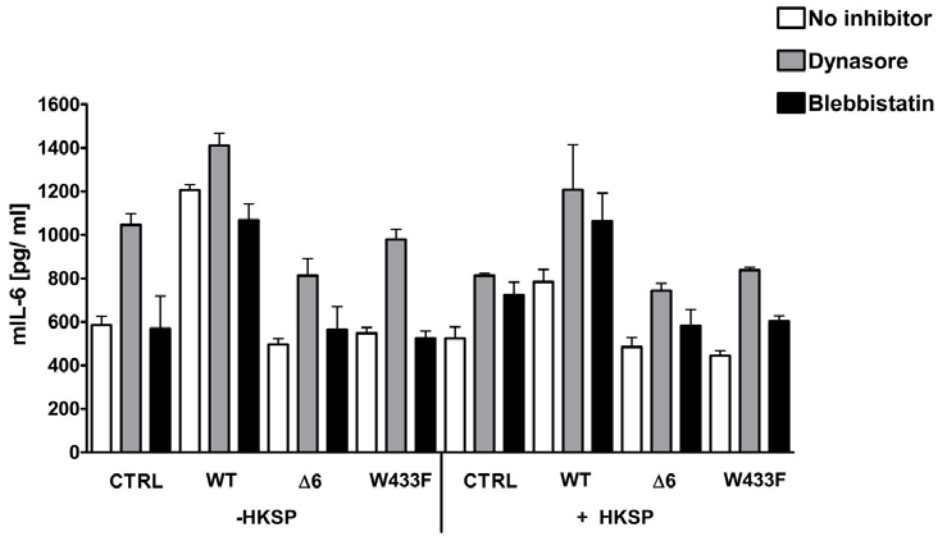

Fig 38: Quantification of IL-6 after treatment with PLY-WT, PLY-Δ6 and PLY-W433F either with or without HKSP. Toxin dilutions were pre-incubated with Polymyxin B in order to abolish an activation of IL-6 production by LPS. Values represent mean +/- SEM.

Furthermore, acute brain slices were incubated for 5 h with PLY-WT and with medium alone. The longer incubation time can be explained by the duration of the toxin needed in order to penetrate the tissue. In addition, the polymyxin B control was carried out as well. In Fig 39 it becomes visible that PLY-WT shows no significant LPS contamination. It is also visible that PLY-WT also leads to an increase in IL-6 production in acute brain slices and not only in the PMA monolayer.

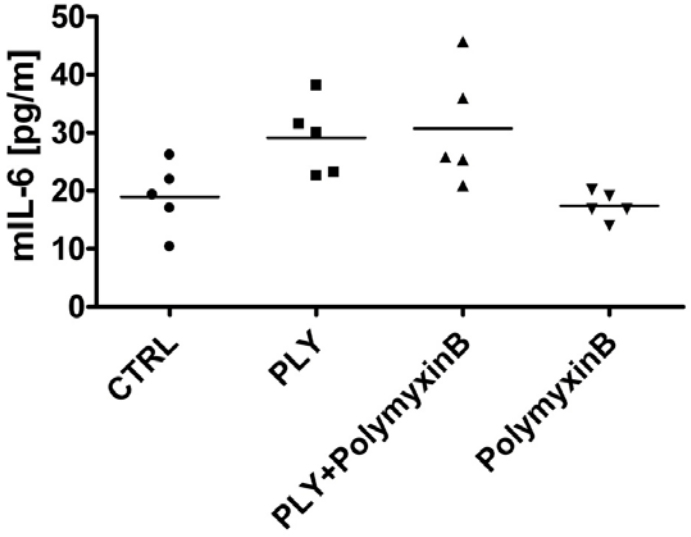

Fig 39: Treatment of acute brain slices from mice show an increase of IL-6 production compared to the control. Polymyxin B alone showed no increase of IL-6.

5 DISCUSSION

5.1 Properties of pneumolysin-wildtype and pneumolysin-variants at the cell membrane and effects on the actin cytoskeleton

Sections of this discuccion have been published in (Fortsch, Hupp et al. 2011) and in (Wippel, Fortsch et al. 2011).

Previously, a small GTPase-dependent actin remodeling in SH-SY5Y neuroblastoma cells by wildtype pneumolysin (PLY-WT) at sub-lytic concentrations has been demonstrated (Iliev, Djannatian et al. 2007). In this work the role of pore-formation on these observations was investigated. To this end, variants of Pneumolysin, which are incapable of forming pores, have been investigated. Treatment with PLY-WT led to cellular displacement compared to the variants that did not cause these changes (Fig 26). Active cellular retraction and displacement in a given direction should be accompanied by changes in the focal adhesion formation and size (Shemesh, Verkhovsky et al. 2009). The cell accomplishes this by establishing traction points (Mierke 2009). Here, focal adhesions were visualized by immuncytochemical staining for Vinculin, a marker for focal adhesions. Cells were challenged with PLY-variants, which are described in 1.3.4 with PLY-WT, PLY-Δ6 and PLY-W433 (Fig 27). After treatment of cells with PLY-WT for 30 min, astrocytes seemed to form more and more definded focal adhesions. The cells showed more stress fibers compared to cells treated with PLY-Δ6, PLY-W433F and medium only. This indicates a RhoA GTPase-like activation by PLY-WT, analogous to earlier experimental findings in neuroblastoma cells (Iliev, Djannatian et al. 2007). This shows that the cell shape changes represent active cytoskeleton reorganizing phenomena without a loss of surface attachment (Oliver, Lee et al. 1994). The presence of focal points in astrocytes under normal, untreated conditions indicated a capacity to be motile and thus to react to toxin stimulation with increased cell movement (Fortsch, Hupp et al. 2011).

These observations confirm that active cytoskeleton reorganising events follow PLY-WT challenge in primary astroglial cells, but not after challenge with non-pore forming variants. This finding supports the general idea that mammalian cellular motility depends on actin reorganisation phenomena reviewed by Pollard and Borisy (Pollard and Borisy 2003), Ridley et al. (Ridley 2001) and Pollard and Cooper (Pollard and Cooper 2009). One

aim of this work was to investigate the role of the pore-forming capacity of PLY as an initiation factor for the occurring actin cytoskeletal reorganisation phenomena. Toxin-induced actin-reorganising phenomena in glial cells seem to be more complex than those observed in human neuroblastoma cells and some non-small GTPase-dependent events might contribute to their occurrence.

Furthermore, a dose-dependent cell lysis was observed. As PLY-WT is a cytolysin, it was necessary to define the terms lytic/sublytic/non-lytic concentrations precisely for the used system. Primary mouse astrocytes were challenged with PLY-WT in the presence of PI (propidium iodide), using PLY-WT concentrations in the range from 0.05 to 0.5 µg/ml (Fig 19) (Fortsch, Hupp et al. 2011). Simultaneous staining with PI allowed an exclusion of permeabilised for subsequent experiments. PI iodide staining has been shown to be suitable for a discrimination of acutely lytic cells from non-lytic cells (Darzynkiewicz, Bruno et al. 1992). In addition, “classical” PLY-WT membrane pores with a suggested size of 260 Å should be PI-permeable (MW 650) (Iliev, Djannatian et al. 2007). However, no firm evidence that PI can penetrate fast enough through individual macropores to stain the chromatin could be found. Moreover, the possibility of transient pores can not be excluded and as there is no guarantee that PI could enter the cell through transient pores. Thus, the definition of lytic (permeabilised) and non-lytic (non-permeabilised) cells was chosen (Fortsch, Hupp et al. 2011). In addition, the ability to cause cell-lysis was investigated by measuring the release of lactate-dehydrogenase (LDH). As can be seen in Fig 18, only the PLY-WT was able to cause cell-lysis. Here, a 10-fold higher toxin concentration, than found in meningitis, was used. The variants PLY-W433F and PLY-Δ6 did not lead to cell lysis. This serves as one proof of the incapability of those variants to form pores. After challenge of primary mouse glial cells with physiological calcium concentrations (2 mM) and PLY-WT, the toxin showed a decreased toxic effect compared to the effect in medium deprived of calcium (Fig 33). Here, evidence for the dependence of the lytic capacity of PLY on the extracellular concentration of Ca^{2+} can be shown. Reduction of Ca^{2+}-concentration may have profound effects on PLY-WT neurotoxicity enhancement. Reduction of Ca^{2+}-concentration could transform sub-lytic pathophysiological concentrations into lytic concentrations, worsening the course of the

disease. Unfortunately, there is no systematic evidence for the dynamic changes of Ca^{2+}-concentration in the brain during the clinical course of pneumococcal meningitis.

The necessity of lytic pore formation for actin-dependent effects could be excluded, it remained unclear whether pore formation is needed at all or not. Evidence exists that PLY-WT builds a heterogenous population of pores, many of which have ion channel properties (Vikman, Backstrom et al. 2001). In these experiments, PLY-WT concentrations exceed physiological concentrations found in meningitis by a factor of 10 or more. In meningitis, values up to 0.2 µg per ml CSF were found (Spreer, Kerstan et al. 2003), while PLY-WT and non-pore forming variants (Korchev, Bashford et al. 1998; Kirkham, Kerr et al. 2006) were applied at concentrations up to 10 µg per ml in the experiments. In this work toxins were used in concentrations within the disease-relevant range (up to 0.2 µg/ml). Both mutants bound to the cell membranes in a manner similar to PLY-WT (Fig 20). This was further confirmed by biochemical spectrophotometric cholesterol-binding experiments by scanning for tryptophan-fluorescence (Fig 23). The binding capacity however, differed among the pneumolysin variants, therefore the concentration of the mutants was adjusted in all further experiments to fit exactly the PLY-WT binding. As expected, none of the mutants was lytic in the range of 0.1 to 0.5 µg/ml (Fig 18). Earlier experiments in artificial membranes and cell membrane patches show that PLY-W433F form big (presumably lytic) pores at concentrations of 5 µg/ml and more (Vikman, Backstrom et al. 2001; El-Rachkidy, Davies et al. 2008). They exceed, however, many times the physiological concentration of PLY in meningitis.

In primary glial culture in non-lytic conditions PLY-WT induced membrane depolarization Fig 22). Membrane polarity was analysed by using the oxonol dye $DiBAC_4$. This dye does not cause mitochondrial uncoupling and shows a linear fluorescence versus membrane penetration relationship (Epps, Wolfe et al. 1994). The fluorescence-emission of the dye increases when interacting with intracellular proteins, preferably with hydrophobic binding sites. Since PLY-WT pores are known to be predominantly cation-conductive (Korchev, Bashford et al. 1998; Vikman, Backstrom et al. 2001; El-Rachkidy, Davies et al. 2008), the occurrence of membrane depolarisation implies a role of sodium and/or calcium influx. However, it cannot be excluded that membrane depolarisation is

not related to direct effects of the PLY pores, but due to the involvement of endogenous ion channels as suggested previously (Iliev, Djannatian et al. 2007).

Consistent with the depolarisation experiments, the conductance of PLY-WT, PLY-W433F and PLY-Δ6 in planar lipid bilayer (PLB) as previously described was tested (Benz, Janko et al. 1978). In order to achieve an accelerated pore-formation, small amounts of oxidised cholesterol (about 30 % v/v) were added to the planar lipid bilayer. This is a well-known approach (Benz, Janko et al. 1978), but the exact molecular steps involved in improving the pore formation remain unclear. It is known, however, that the oxidised cholesterol dramatically improves both the elastic properties of artificial membranes (Benz, Beckers et al. 1979) and membrane fluidity (Wood, Igbavboa et al. 1995). Here, only PLY-WT was capable of forming big pores, most likely corresponding to lytic pores (Fig 24, arrow). Smaller oscillations (up to 25 pA) were also observed, showing an activity at the artificial membrane. Small conductance oscillations (not bigger than 5 pA) were seen with the PLY-W433F, although much smaller and infrequent than with PLY-WT at an equivalent toxin concentration. PLY-Δ6 did not lead to any conductance changes, i.e. no pore-forming capacity was present. Micropores caused by PLY-W433F as defined before (Vikman, Backstrom et al. 2001) could not be found, which may be due to the much lower toxin concentrations used and the presence of cholesterol in the PLB.

In artificial bilayer, the change in Ca^{2+}-concentrations did not affect the size or properties of individual PLY pores (Fig 25). The lack of effect of Ca^{2+} on ion conductance was surprising, because other studies have indicated the gating sensitivity of cation-selective PLY pores at higher-than-physiological bivalent ion concentrations (1–5 mM Zn^{2+} and 10–20 mM Ca^{2+}). This suggests that pore characteristics may be modulated by divalent cations (Vikman, Backstrom et al. 2001). Thus, it is possible that the enhanced binding of PLY-WT to membranes at low Ca^{2+}-conditions involves a similar change in membrane fluidity.

The ion selectivity of PLY micropores, derived from experiments with the PLB, indicates relative cation selectivity and sensitivity against closure by bivalent ions such as calcium (Ca^{2+}) and zink (“small” pores). PLY-WT alone is a factor, known to produce an increase in cellular Ca^{2+} (Stringaris, Geisenhainer et al. 2002), thus Ca^{2+}-selective micropores should be additionally considered, assuming that they exist and play a role in plasma Ca^{2+}-

elevation. Local increase of cytosolic Ca^{2+} contributes to cellular motility in electrical field stimulation model systems, which partially resembles the effects of PLY on membrane electrical phenomena (Onuma and Hui 1988; Ozkucur, Monsees et al. 2009). The major source of Ca^{2+}-influx into cells after PLY challenge is the extracellular environment (Stringaris, Geisenhainer et al. 2002), although Ca^{2+}-influx from intracellular stores, the biggest of which is the endoplasmic reticulum (ER) (Reyes and Parpura 2009), should also be considered.

Furthermore, it has been shown that the activation of Rac1 by PLY-WT in the human neuroblastoma cell SH-SY5Y is Ca^{2+}-influx-dependent (Iliev, Djannatian et al. 2007). This experimental setup, however, excludes the role of intracellular Ca^{2+}-depots, thus making it difficult to estimate the role of Ca^{2+}-influx for the initiation of cell shape changes. To answer the question about the initiating role of Ca^{2+}-influx in PLY-WT induced cell shape changes, the role of PLY-WT on astrocytes in Ca^{2+}-free medium was tested. LDH-release showed a higher toxicity of PLY-WT after depletion of extracellular Calcium (Fig 33) indicating a possible protective function of calcium on cells against PLY challenge.

This work provides evidence for the critical importance of the PLY pore forming capacity in cell shape changes. The mechanistic role of membrane depolarisation and Ca^{2+}-influx as pore-related cell shape change initiation factors can yet not be explained eintirely. However, the modulatory role in the cellular motility effects following the initial PLY challenge cannot be excluded. The possibility that other pore formation-related factors also play a role of the actin cytoskeleton effects of PLY exists. One of those is the interaction with plasmalemmal molecules or with molecules, positioned immediately under the membrane. This could play a role in cellular transport mechanisms which interactions would require the toxin molecules to be in a folded pore-like conformational state in order to interact, thus explaining the need of pore-forming capacity.

Although many bacterial toxin possess the feature of modulating actin cytoskeleton dynamics, mostly via small GTPase activation or inhibition (Aktories and Barbieri 2005), only few of these toxins possesses pore forming capacity. Our finding of small GTPase activation via PLY in human neuroblastoma cells (Iliev, Djannatian et al. 2007) suggests a possible role not only of pore formation, but of cholesterol sequestration and others. The pore forming capacity remains essential for the rapid cytoskeletal reorganization,

implying that PLY pore formation might play a much more complex role in the modulation of pathogen virulence than thought before.

5.2 From membrane to cellular trafficking

As observed, the PLY-WT, but not the non pore-forming variants, were internalised into the cell (Fig 34). The question remained, which mechanisms are involved and what the impact on the cell would be. Obviously, the interaction of the toxin with the membrane will involve not only the initial binding but also the following steps. As the membrane binding did not seem to have an effect on membrane depolarisation, discussed in the previous section, it could be assumed that the following observed effects would be due to an internalisation and not due to membrane binding or pore-formation.
Internalisation of a pore-forming toxin can have several alternative implications:
1.) cell protection, 2.) increased pathogenic response by internalisation of toxic components; 3.) improved transcytosis and 4.) artefacts.

To clarify these implications, the question of compartmentalisation and whether this compartment is the same as the ones that were enhanced by PLY-WT in the FM 1-43 assays, needed to be studied. The co-challenge of cells with inhibitors for myosin II and for dynamin prior to toxin challenge, led to a further discrimination which endocytotic pathway could be influenced by the toxin. Blebbistatin is known to be a specific inhibitor for non-muscle myosin II (Kovacs, Toth et al. 2004). Furthermore, myosin II plays a role in endocytotic processes e.g. fluid phase endocytosis. Here, the mechanism is regulated via the guanine exchange factor RhoGEF2 and thus is linked to actin cytoskeleton (Levayer, Pelissier-Monier et al. 2011). Dynamin plays an essential role e.g in clathrin-coated vesicle formation during endocytosis and thus is an important regulatory GTPase in endocytosis (Gu, Yaddanapudi et al. 2010). After blocking the cells with dynasore, inhibiting dynamin, and with inhibitors for dynamin and myosin II together, the rate of endocytosis after PLY challenge was blocked to a control level in live cell imaging.
FM 1-43 serves as a marker of overall endocytosis. It inserts into the outer leaflet of the membrane and gains its fluorescence properties in a hydrophobic milieu (Vida and Emr 1995; Murthy and Stevens 1998; Brumback, Lieber et al. 2004). Furthermore, it could be shown, that FM 1-43 follows a classical endocytic pathway as the increase in fluorescence

could not be observed after inhibition of endosomal acidification with Bafilomycin (Fig 28). The internalisation of FM 1-43 is inhibited by dynasore. This observation is consistent with the current knowledge on classical endosomes, namely where Dynamin plays a crucial part in the internalisation of classical endosomes. However, the inhibition of myosin II led to an increased overall uptake of FM 1-43 positive vesicles, whereas the internalisation on PLY-GFP seemed to be decreased (Fig 34). It is possible that these two different internalisation phenomena, FM 1-43- and PLY-GFP-internalisation, were uncoupled. Furthermore, these observations could mean that PLY is internalised in a dynamin and myosin II independent manner and thus caveolin- and clathrin dependent mechanisms can be ruled out (Fig 10).

Classical endocytotic pathways could be ruled out via immunocytochemical staining for different compartmental markers. The internalisation of albumin indicates a caveolin dependent endocytosis (Bento-Abreu, Velasco et al. 2009), transferrin a clathrin dependent endocytosis (Pearse and Robinson 1990) and dextran indicates phagocytosis (Costantini, Gilberti et al. 2011; Levayer, Pelissier-Monier et al. 2011). Internalised PLY-GFP showed no co-localisation with the used endocytic markers. Thus, the proposed mechanism of internalisation is most probably dynamin- and caveolin-independent pinocytosis leading the toxin to caveosomes. These caveosomes avoid the endosomes and lysosomes, so that the destination of the caveosome within the cell is not yet clear (Alberts 2008). This information suggests that the protein would not be degraded within the cell. The observation of an increased rate of endocytosis after toxin challenge might argue for a strategy of the cell to defend itself against the formation of micro- or macro-pores and thus avoid bacterial invasion. It has also been shown that cells use endo- and exocytosis as a strategy to eliminate pore-forming toxins from the cell surface (Husmann, Beckmann et al. 2009) in order to achieve a repair of the plasma membrane (Los, Kao et al. 2011). Previously, it has been shown, that bacterial protein toxins are internalised via different endocytotic pathways in order to enable bacteria to invade the cell (Lin and Guttman 2010). Exemplary the anthrax toxin binds to its receptor and upon oligomerisation is internalised via clathrin-dependent endocytosis. Upon acidification of the endosomes, a pore is formed in the endosomes releasing toxic factors into the cytosol (Young and Collier 2007). However, it has to be mentioned that the visible clusters of PLY-

GFP, which were detected by the microscopy used in this work, do not necessarily represent the entire pool of toxin used. It is possible that a small fraction, which would not be detecteable by methods used, is internalised in a dynamin- or blebbistatin-dependent mechanism. Such a concept would be supported by the experiments carried out with the dye $DiBAC_4$. If pneumolysin forms pores or micropores at the membrane, the membrane potential would change and the dye could enter the cytosol (Epps, Wolfe et al. 1994). As the treatment of cells with dynasore and both inhibitors showed a decrease of overall endocytosis (Fig 30), these micropores could stay for a longer time on the cell surface and thus lead to a higher degree of depolarisation compared to cells treated with blebbistatin alone. Here, the overall rate of endocytosis increased, thus internalising possible micropores more quickly and leading to a decrease in membrane depolarisation compared to samples, where no inhibitor was used. Another explanation would be that the cell increases the effort on other endocytic processes in order to compensate for the loss of the inhibited endocytic mechanisms. One question is, if the cell defends itself via these mechanisms, or if the bacteria also utilise pinocytic processes in order to invade into the cell or further tissue.

If injury is caused at the cell membrane, the cell uses repair-mechanisms, which are managed via endo- and exocytosis (Alberts 2008). Previously, it has been shown that sequential endocytosis and exocytosis serve as a mechanism to eliminate pore-forming (e.g. α-toxin from *S. aureus*) toxins from the cell without degrading them (Husmann, Beckmann et al. 2009). Furthermore, a dependency of these exocytotic repair mechanisms on calcium has been described (Bi, Alderton et al. 1995; Tam, Idone et al. 2010).

As previously mentioned, the lytic capacity of the PLY-WT has been tested under different calcium conditions (Fig 32). The absence of calcium, which is known to block large portions of endocytosis, showed a higher lytic capacity of PLY-WT compared to the physiological presence of 2 mM calcium. Contrary to other toxins the presence of calcium did not increase (Gekara, Westphal et al. 2007; Idone, Tam et al. 2008), but even decrease the rate of PLY-dependent endocytosis in FM 1-43 live-imaging (Fig 33). Again, in the description of exocytotic repair mechanisms calcium seems to have a crucial role. The

toxin has a far more toxic effect in calcium-free conditions than is has when extracellular calcium is available.

5.3 PLY and innate immunity

In the previous section, the internalisation of PLY-WT was discussed. The second, much more system-relevant question is why a bacterial toxin is internalised in a "non-classical" endocytotic manner and what the aim of the toxin-induced enhancement might be. Are the observed effects artefacts or a strategy of the cell to react to the toxin-stressor at the membrane? It has been shown previously that *S. pneumoniae* induces increased levels of TNF-α, IL-1β and IL-6 in rat brain, in the hippocampal formation and the prefrontal cortex, after meningitis (Dessing, Hirst et al. 2009; Barichello, dos Santos et al. 2010) and can initiate innate immune reactions, like TLR 2 and TLR 4-dependent responses (Paterson and Mitchell 2006). Furthermore, it has been discussed, whether PLY itself is recognised by TLR4 and thus leads to a direct activation of a TLR4-dependent answer (Weclewicz, Kristensson et al. 1994; Srivastava, Henneke et al. 2005; Paterson and Mitchell 2006; Marriott, Mitchell et al. 2008; Dogan, Zhang et al. 2011) or whether stimulation of the innate immunity is mediated by the action of stress kinases, such as MAPK, or oxidative stress caused by the complement system (Stringaris, Geisenhainer et al. 2002; Dessing, Hirst et al. 2009; Barichello, dos Santos et al. 2010; McNeela, Burke et al. 2010). Thus, another question that remained was, whether the cells would react to this possible stressor with a proinflammatory response.

Due to the observed endocytotic processes the original hypothesis was that the enhanced cellular trafficking can be linked to the signalling of the TLR 2 and 4. This led to the investigation of four proinflammatory cytokines (IL-1β, IL-6, IL-12(p40) and TNF-α) as shown in Fig 12.

In this work, the production of IL-1β, IL-12 and TNF-α was not increased. This contradicts the described findings from the previously described research.

Only IL-6 levels were elevated after treatment with PLY-WT (Fig 38). IL-6 serves as a key player in the production of acute phase proteins. Furthermore, it mediates T-cell activation, growth and differentiation (Borish and Steinke 2003). The production of no other proinflammatory cytokine was increased (Fig 36).

The non pore-forming variants, although they all bound to the membrane and did not lead to an increase in endocytotic rate, did not lead to a production of the pro-inflammatory cytokine IL-6. This led to the question, if the internalisation or the pore-forming capacity of the toxin would be the activating factor.

Since many of the TLR receptors require endocytotic events (Blasius and Beutler 2010) to achieve activation, the production of inflammatory cytokines upon PLY-WT treatment in combination with inhibitors for dynamin and myosin II was analysed. The inhibition of dynamin and myosin II did not affect the production of IL-6. This shows that the activation of IL-6 production is independent of dynamin and myosin II dependent endocytotic processes. A possible explanation for the raised levels of IL-6 could be that WT-PLY directly activates TLR 4, as reported previously (Weclewicz, Kristensson et al. 1994) (Dessing, Hirst et al. 2009) and thus leads to the IL-6 production (Lehnardt 2010; McGettrick and O'Neill 2010). Furthermore, an activation of TLR 4 by WT-PLY has been discussed (Dogan, Zhang et al. 2011).

Due to the lack of elevation of IL-6 after treatment with the PLY-Δ6 and PLY-W433F another possibility would be that the pore-forming capacity would be required for this activation.

In order to eliminate any possibility for off-target activation of TLR 4 via LPS, all toxin dilutions were pre-incubated with Polymyxin B. The toxins were expressed in *E. coli* and purified from this Gram negative bacterium, which could lead to small LPS traces despite thorough sample cleaning that would lead to an activation of TLR 4. Polymyxin B is supposed to eliminate most of the remaining LPS (Cardoso, Araujo et al. 2007). The pre-treatment of toxin dilutions with Polymyxin B, however, showed no difference in the production of the observed proinflammatory cytokines. Again, only IL-6 was elevated to the same extend as in treatment without Polymyxin B.

Another explanation for the raise of proinflammatory cytokines could be the activation of TLR 2 via peptidoglycane. For tackling this question, heat killed *S. pneumoniae* (HKSP) was added to the toxin dilutions. Fig 38 shows that again only the PLY-WT in combination with HKSP leads to an increased production of IL-6 in contrast to the variants, where no raise could be observed. However, the increase was lower

compared to treatment without HKSP. Thus, the effects observed can only be caused by PLY-WT and no co-stimulation by LPS or peptidoglycan would be necessary.

The discrepancy between the presented experiments and the data about inflammatory cytokine upregulation by PLY-WT can have several explanations. In studies described in literature, mice were treated either by nasopharyngeal injection (Dessing, Hirst et al. 2009; McNeela, Burke et al. 2010) with *S. pneumoniae* or with a direct injection into the 3rd ventricle (Barichello, dos Santos et al. 2010) of the brain. Overall infection with the Streptococcus ranged from 12-24 h and more. In the experiments shown in this work, astrocytes grown in the monolayer were treated with PLY-WT for 90 min. Following this incubation, the medium of cells was completely changed to complete medium and cells were left to rest for 21 h. The aim was to reduce the delayed apoptotic toxicity which was observed with PLY-WT after continuous incubation (Stringaris, Geisenhainer et al. 2002) to a minimum. Apoptotic cells could lead to a non-specific glial response like astrocytic reactive gliosis (Barreto, Gonzalez et al. 2011) and this could be the reason for the discrepancy between the findings of this work and the findings from previous papers that demonstrate an increase of IL-1β, TNF-α and others. Additionally, astrocytes represent the major source of IL-6 in CNS injury and neuroinflammation (Ma, Reynolds et al. 2010).

One can argue that this increase in proinflammatory cytokine IL-6 could lead to a clearance of the pathogen from the infected tissue. Previously, it has been discussed whether this proinflammatory response has a supporting or a damaging function in neurological disorders (Wee Yong 2010) and if the production of proinflammatory cytokines (e.g. IL-6) leads to neurodegeneration or neuroprotection (Lehnardt 2010).

In bacterial meningitis, the gene expression of the TLRs is upregulated and animals deprived of either TLR 2 or TLR 4 show a worsened course of infection with *S. pneumoniae* (Chin, Ifversen et al. 1994; Gerber and Nau 2010). Furthermore, an anti-inflammatory treatment in experimental bacterial meningitis caused a milder course of disease (Zysk, Bruck et al. 1996) and the inflammatory response by astrocytes or microglia might have a neurotoxic effect (Lehnardt 2010), which would enable bacteria to invade deeper into the brain. Here, neuroinflammation would lead to a worsened course of disease.

On the other hand it has been discussed that an inflammation of neural cells will lead to apoptosis, and thus serve as a mechanism of protection from invasive diseases (Srivastava, Henneke et al. 2005), neuroinflammation (Lehnardt, Massillon et al. 2003; McNeela, Burke et al. 2010) and neurodegeneration for example in multiple sclerosis or experimental allergic encephalomyelitis (Suzumura, Takeuchi et al. 2006).

Additionally, it has been shown that neuroinflammation could lead to an increased proliferation of neural cells in meningitis (Gerber, Bottcher et al. 2003; Gerber, Tauber et al. 2009). Thus, the question whether this inflammation serves as a support for bacteria to enhance invasion or as a defense of the cell against these pathogens remains open.

After Pneumolysin challenge primary mouse astrocytes showed changes compared to the variants and untreated control cells. Only the wildtype causes membrane depolarisation, pore-formation, membrane binding and cytoskeletal changes. This data shows that the pore-formation is critically important. The depolarisation seems to be secondary and not essential for cytoskeletal changes. The toxin only produces lysis on the cell surface leading to the idea that the internalisation could serve as a protective mechanism of the cell or establish the toxic function of pneumolysin. Apart from cell-lysis or shape-changes PLY-challenge could lead to the activation of TLR 2 and 4. Since TLR signalling can require endocytosis, the effect of pneumolysin on pro-inflammatory was thought to be linked to endocytotic events. Surprisingly, only IL-6 showed an increase compared to previous studies showing an influence of PLY on TNF-α and IL-1β. Additionally, this increase seemed to be independent of endocytosis. Furthermore, this work shows that neuroinflammatory responses are not directly linked to endocytotic events.

Future work should further investigate the exact role of PLY on downstream TLR and IL-6 signaling as well as the meaning of this IL-6 elevation on the course of meningitis.

6 REFERENCES

Abbott, N. J., L. Ronnback, et al. (2006). "Astrocyte-endothelial interactions at the blood-brain barrier." Nat Rev Neurosci **7**(1): 41-53.

Aktories, K. and J. T. Barbieri (2005). "Bacterial cytotoxins: targeting eukaryotic switches." Nat Rev Microbiol **3**(5): 397-410.

Alberts, B. (2008). Molecular biology of the cell. New York ; Abingdon, Garland Science.

Alouf, J. E. (2000). "Bacterial protein toxins. An overview." Methods Mol Biol **145**: 1-26.

Aspenstrom, P. (1999). "The Rho GTPases have multiple effects on the actin cytoskeleton." Exp Cell Res **246**(1): 20-25.

Baccala, R., R. Gonzalez-Quintial, et al. (2009). "Sensors of the innate immune system: their mode of action." Nature reviews. Rheumatology **5**(8): 448-456.

Bakhiet, M., T. Olsson, et al. (1993). "A Trypanosoma brucei brucei-derived factor that triggers CD8+ lymphocytes to interferon-gamma secretion: purification, characterization and protective effects in vivo by treatment with a monoclonal antibody against the factor." Scand J Immunol **37**(2): 165-178.

Balachandran, P., S. K. Hollingshead, et al. (2001). "The autolytic enzyme LytA of Streptococcus pneumoniae is not responsible for releasing pneumolysin." J Bacteriol **183**(10): 3108-3116.

Baraff, L. J., S. I. Lee, et al. (1993). "Outcomes of bacterial meningitis in children: a meta-analysis." Pediatr Infect Dis J **12**(5): 389-394.

Barichello, T., I. dos Santos, et al. (2010). "TNF-alpha, IL-1beta, IL-6, and cinc-1 levels in rat brain after meningitis induced by Streptococcus pneumoniae." J Neuroimmunol **221**(1-2): 42-45.

Barichello, T., J. S. Pereira, et al. (2011). "A kinetic study of the cytokine/chemokines levels and disruption of blood-brain barrier in infant rats after pneumococcal meningitis." J Neuroimmunol **233**(1-2): 12-17.

Barres, B. A. (2008). "The mystery and magic of glia: a perspective on their roles in health and disease." Neuron **60**(3): 430-440.

Barreto, G. E., J. Gonzalez, et al. (2011). "Astrocytic-neuronal crosstalk: implications for neuroprotection from brain injury." Neurosci Res **71**(2): 107-113.

Bento-Abreu, A., A. Velasco, et al. (2009). "Albumin endocytosis via megalin in astrocytes is caveola- and Dab-1 dependent and is required for the synthesis of the neurotrophic factor oleic acid." J Neurochem **111**(1): 49-60.

Benz, R., F. Beckers, et al. (1979). "Reversible electrical breakdown of lipid bilayer membranes: a charge-pulse relaxation study." J Membr Biol **48**(2): 181-204.

Benz, R., K. Janko, et al. (1978). "Formation of large, ion-permeable membrane channels by the matrix protein (porin) of Escherichia coli." Biochim Biophys Acta **511**(3): 305-319.

Benz, R., G. Stark, et al. (1973). "Valinomycin-mediated ion transport through neutral lipid membranes: influence of hydrocarbon chain length and temperature." J Membr Biol **14**(4): 339-364.

Berry, A. M., J. E. Alexander, et al. (1995). "Effect of defined point mutations in the pneumolysin gene on the virulence of Streptococcus pneumoniae." Infect Immun **63**(5): 1969-1974.

Berry, A. M., J. Yother, et al. (1989). "Reduced virulence of a defined pneumolysin-negative mutant of Streptococcus pneumoniae." Infect Immun **57**(7): 2037-2042.

Beutler, B. A. (2009). "TLRs and innate immunity." Blood **113**(7): 1399-1407.

Bi, G. Q., J. M. Alderton, et al. (1995). "Calcium-regulated exocytosis is required for cell membrane resealing." J Cell Biol **131**(6 Pt 2): 1747-1758.

Blasius, A. L. and B. Beutler (2010). "Intracellular toll-like receptors." Immunity **32**(3): 305-315.

Block, M. L., L. Zecca, et al. (2007). "Microglia-mediated neurotoxicity: uncovering the molecular mechanisms." Nat Rev Neurosci **8**(1): 57-69.

Borish, L. C. and J. W. Steinke (2003). "2. Cytokines and chemokines." J Allergy Clin Immunol **111**(2 Suppl): S460-475.

Bowman, E. J., A. Siebers, et al. (1988). "Bafilomycins: a class of inhibitors of membrane ATPases from microorganisms, animal cells, and plant cells." Proc Natl Acad Sci U S A **85**(21): 7972-7976.

Brumback, A. C., J. L. Lieber, et al. (2004). "Using FM1-43 to study neuropeptide granule dynamics and exocytosis." Methods **33**(4): 287-294.

Cardoso, L. S., M. I. Araujo, et al. (2007). "Polymyxin B as inhibitor of LPS contamination of Schistosoma mansoni recombinant proteins in human cytokine analysis." Microbial cell factories **6**: 1.

Chin, L. T., P. Ifversen, et al. (1994). "Human Th0-type T helper-cell clone supports antigen-specific immunoglobulin production in scid/beige-hu mice." Scand J Immunol **40**(5): 529-534.

Ciana, G., N. Parmar, et al. (1995). "Effectiveness of adjunctive treatment with steroids in reducing short-term mortality in a high-risk population of children with bacterial meningitis." J Trop Pediatr **41**(3): 164-168.

Clague, M. J. (1998). "Molecular aspects of the endocytic pathway." Biochem J **336 (Pt 2)**: 271-282.

Correale, J. and A. Villa (2009). "Cellular elements of the blood-brain barrier." Neurochem Res **34**(12): 2067-2077.

Costantini, L. M., R. M. Gilberti, et al. (2011). "The phagocytosis and toxicity of amorphous silica." PLoS One **6**(2): e14647.

Darzynkiewicz, Z., S. Bruno, et al. (1992). "Features of apoptotic cells measured by flow cytometry." Cytometry **13**(8): 795-808.

Dessing, M. C., R. A. Hirst, et al. (2009). "Role of Toll-like receptors 2 and 4 in pulmonary inflammation and injury induced by pneumolysin in mice." PLoS One **4**(11): e7993.

Dogan, S., Q. Zhang, et al. (2011). "Pneumolysin-induced CXCL8 production by nasopharyngeal epithelial cells is dependent on calcium flux and MAPK activation via Toll-like receptor 4." Microbes Infect **13**(1): 65-75.

Doherty, G. J. and H. T. McMahon (2009). "Mechanisms of endocytosis." Annu Rev Biochem **78**: 857-902.

El-Rachkidy, R. G., N. W. Davies, et al. (2008). "Pneumolysin generates multiple conductance pores in the membrane of nucleated cells." Biochem Biophys Res Commun **368**(3): 786-792.

Epps, D. E., M. L. Wolfe, et al. (1994). "Characterization of the steady-state and dynamic fluorescence properties of the potential-sensitive dye bis-(1,3-dibutylbarbituric acid)trimethine oxonol (Dibac4(3)) in model systems and cells." Chem Phys Lipids **69**(2): 137-150.

Erridge, C. (2010). "Endogenous ligands of TLR2 and TLR4: agonists or assistants?" J Leukoc Biol **87**(6): 989-999.

Fortsch, C., S. Hupp, et al. (2011). "Changes in astrocyte shape induced by sublytic concentrations of the cholesterol-dependent cytolysin pneumolysin still require pore-forming capacity." Toxins (Basel) **3**(1): 43-62.

Furyk, J. S., O. Swann, et al. (2011). "Systematic review: neonatal meningitis in the developing world." Trop Med Int Health **16**(6): 672-679.

Garcia-Suarez Mdel, M., M. D. Cima-Cabal, et al. (2004). "Protection against pneumococcal pneumonia in mice by monoclonal antibodies to pneumolysin." Infect Immun **72**(8): 4534-4540.

Gekara, N. O., K. Westphal, et al. (2007). "The multiple mechanisms of Ca2+ signalling by listeriolysin O, the cholesterol-dependent cytolysin of Listeria monocytogenes." Cell Microbiol **9**(8): 2008-2021.

Gerber, J., T. Bottcher, et al. (2003). "Increased neurogenesis after experimental Streptococcus pneumoniae meningitis." J Neurosci Res **73**(4): 441-446.

Gerber, J. and R. Nau (2010). "Mechanisms of injury in bacterial meningitis." Curr Opin Neurol **23**(3): 312-318.

Gerber, J., S. C. Tauber, et al. (2009). "Increased neuronal proliferation in human bacterial meningitis." Neurology **73**(13): 1026-1032.

Goldman, R. D., J. Swedlow, et al. (2010). Live cell imaging : a laboratory manual. Cold Spring Harbor, N.Y., Cold Spring Harbor Laboratory Press.

Gu, C., S. Yaddanapudi, et al. (2010). "Direct dynamin-actin interactions regulate the actin cytoskeleton." EMBO J **29**(21): 3593-3606.

Hart, C. A., L. E. Cuevas, et al. (1993). "Management of bacterial meningitis." J Antimicrob Chemother **32 Suppl A**: 49-59.

Herrmann, I., M. Kellert, et al. (2006). "Streptococcus pneumoniae Infection aggravates experimental autoimmune encephalomyelitis via Toll-like receptor 2." Infect Immun **74**(8): 4841-4848.

Husmann, M., E. Beckmann, et al. (2009). "Elimination of a bacterial pore-forming toxin by sequential endocytosis and exocytosis." FEBS Lett **583**(2): 337-344.

Idone, V., C. Tam, et al. (2008). "Two-way traffic on the road to plasma membrane repair." Trends Cell Biol **18**(11): 552-559.

Iliev, A. I., J. R. Djannatian, et al. (2007). "Cholesterol-dependent actin remodeling via RhoA and Rac1 activation by the Streptococcus pneumoniae toxin pneumolysin." Proc Natl Acad Sci U S A **104**(8): 2897-2902.

Janeway, C., P. Travers, et al. (1997). Immunobiology : the immune system in health and disease. London
New York ; London
Edinburgh ;, Current Biology ;
Garland ;
Churchill Livingstone.

Jedrzejas, M. J. (2001). "Pneumococcal virulence factors: structure and function." Microbiol Mol Biol Rev **65**(2): 187-207 ; first page, table of contents.

Kadioglu, A., J. N. Weiser, et al. (2008). "The role of Streptococcus pneumoniae virulence factors in host respiratory colonization and disease." Nat Rev Microbiol **6**(4): 288-301.

Kanclerski, K. and R. Mollby (1987). "Production and purification of Streptococcus pneumoniae hemolysin (pneumolysin)." J Clin Microbiol **25**(2): 222-225.

Kastenbauer, S. and H. W. Pfister (2003). "Pneumococcal meningitis in adults: spectrum of complications and prognostic factors in a series of 87 cases." Brain **126**(Pt 5): 1015-1025.

Kettenmann, H., U. K. Hanisch, et al. (2011). "Physiology of microglia." Physiol Rev **91**(2): 461-553.

Kim, K. S. (2010). "Acute bacterial meningitis in infants and children." Lancet Infect Dis **10**(1): 32-42.

Kirkham, L. A., A. R. Kerr, et al. (2006). "Construction and immunological characterization of a novel nontoxic protective pneumolysin mutant for use in future pneumococcal vaccines." Infect Immun **74**(1): 586-593.

Kleber, H. P., D. Schlee, et al. (1990). Biochemisches Praktikum. Jena. **5**.

Korchev, Y. E., C. L. Bashford, et al. (1998). "A conserved tryptophan in pneumolysin is a determinant of the characteristics of channels formed by pneumolysin in cells and planar lipid bilayers." Biochem J **329 (Pt 3)**: 571-577.

Kovacs, M., J. Toth, et al. (2004). "Mechanism of blebbistatin inhibition of myosin II." J Biol Chem **279**(34): 35557-35563.

Krieg, A. M. and J. Vollmer (2007). "Toll-like receptors 7, 8, and 9: linking innate immunity to autoimmunity." Immunol Rev **220**: 251-269.

Kristensson, K. (2011). "Microbes' roadmap to neurons." Nat Rev Neurosci **12**(6): 345-357.

Kuffler, S. W., A. R. Martin, et al. (1984). From neuron to brain : a cellular approach to the function of the nervous system. Sunderland, Mass., Sinauer Associates.

Laemmli, U. K. (1970). "Cleavage of structural proteins during the assembly of the head of bacteriophage T4." Nature **227**(5259): 680-685.

Lazo, J. S., K. Tamura, et al. (2001). "Antimitotic actions of a novel analog of the fungal metabolite palmarumycin CP1." J Pharmacol Exp Ther **296**(2): 364-371.

Lehnardt, S. (2010). "Innate immunity and neuroinflammation in the CNS: the role of microglia in Toll-like receptor-mediated neuronal injury." Glia **58**(3): 253-263.

Lehnardt, S., L. Massillon, et al. (2003). "Activation of innate immunity in the CNS triggers neurodegeneration through a Toll-like receptor 4-dependent pathway." Proc Natl Acad Sci U S A **100**(14): 8514-8519.

Levayer, R., A. Pelissier-Monier, et al. (2011). "Spatial regulation of Dia and Myosin-II by RhoGEF2 controls initiation of E-cadherin endocytosis during epithelial morphogenesis." Nat Cell Biol **13**(5): 529-540.

Lin, A. E. and J. A. Guttman (2010). "Hijacking the endocytic machinery by microbial pathogens." Protoplasma **244**(1-4): 75-90.

Los, F. C., C. Y. Kao, et al. (2011). "RAB-5- and RAB-11-dependent vesicle-trafficking pathways are required for plasma membrane repair after attack by bacterial pore-forming toxin." Cell Host Microbe **9**(2): 147-157.

Ma, X., S. L. Reynolds, et al. (2010). "IL-17 enhancement of the IL-6 signaling cascade in astrocytes." J Immunol **184**(9): 4898-4906.

Malmgren, L., Y. Olsson, et al. (1978). "Uptake and retrograde axonal transport of various exogenous macromolecules in normal and crushed hypoglossal nerves." Brain Res **153**(3): 477-493.

Marriott, H. M., T. J. Mitchell, et al. (2008). "Pneumolysin: a double-edged sword during the host-pathogen interaction." Curr Mol Med **8**(6): 497-509.

McGettrick, A. F. and L. A. O'Neill (2010). "Localisation and trafficking of Toll-like receptors: an important mode of regulation." Curr Opin Immunol **22**(1): 20-27.

McNeela, E. A., A. Burke, et al. (2010). "Pneumolysin activates the NLRP3 inflammasome and promotes proinflammatory cytokines independently of TLR4." PLoS Pathog **6**(11): e1001191.

Mierke, C. T. (2009). "The role of vinculin in the regulation of the mechanical properties of cells." Cell Biochem Biophys **53**(3): 115-126.

Mook-Kanamori, B. B., M. Geldhoff, et al. (2011). "Pathogenesis and pathophysiology of pneumococcal meningitis." Clin Microbiol Rev **24**(3): 557-591.

Murthy, V. N. and C. F. Stevens (1998). "Synaptic vesicles retain their identity through the endocytic cycle." Nature **392**(6675): 497-501.

O'Brien, K. L., L. J. Wolfson, et al. (2009). "Burden of disease caused by Streptococcus pneumoniae in children younger than 5 years: global estimates." Lancet **374**(9693): 893-902.

Oliver, T., J. Lee, et al. (1994). "Forces exerted by locomoting cells." Semin Cell Biol **5**(3): 139-147.

Onuma, E. K. and S. W. Hui (1988). "Electric field-directed cell shape changes, displacement, and cytoskeletal reorganization are calcium dependent." J Cell Biol **106**(6): 2067-2075.

Ortqvist, A., J. Hedlund, et al. (2005). "Streptococcus pneumoniae: epidemiology, risk factors, and clinical features." Semin Respir Crit Care Med **26**(6): 563-574.

Ozkucur, N., T. K. Monsees, et al. (2009). "Local calcium elevation and cell elongation initiate guided motility in electrically stimulated osteoblast-like cells." PLoS One **4**(7): e6131.

Paterson, G. K. and T. J. Mitchell (2006). "Innate immunity and the pneumococcus." Microbiology **152**(Pt 2): 285-293.

Pearse, B. M. and M. S. Robinson (1990). "Clathrin, adaptors, and sorting." Annu Rev Cell Biol **6**: 151-171.

Pollard, T. D. and G. G. Borisy (2003). "Cellular motility driven by assembly and disassembly of actin filaments." Cell **112**(4): 453-465.

Pollard, T. D. and J. A. Cooper (2009). "Actin, a central player in cell shape and movement." Science **326**(5957): 1208-1212.

Qazi, S. A., M. A. Khan, et al. (1996). "Dexamethasone and bacterial meningitis in Pakistan." Arch Dis Child **75**(6): 482-488.

Reyes, R. C. and V. Parpura (2009). "The trinity of Ca2+ sources for the exocytotic glutamate release from astrocytes." Neurochem Int **55**(1-3): 2-8.

Ridley, A. J. (2001). "Rho GTPases and cell migration." J Cell Sci **114**(Pt 15): 2713-2722.

Ridley, A. J. (2006). "Rho GTPases and actin dynamics in membrane protrusions and vesicle trafficking." Trends Cell Biol **16**(10): 522-529.

Rosado, C. J., A. M. Buckle, et al. (2007). "A common fold mediates vertebrate defense and bacterial attack." Science **317**(5844): 1548-1551.

Rosado, C. J., S. Kondos, et al. (2008). "The MACPF/CDC family of pore-forming toxins." Cell Microbiol.

Rossjohn, J., G. Polekhina, et al. (2007). "Structures of Perfringolysin O Suggest a Pathway for Activation of Cholesterol-dependent Cytolysins." J. Mol. Biol. **367**: 1227-1236.

Shemesh, T., A. B. Verkhovsky, et al. (2009). "Role of focal adhesions and mechanical stresses in the formation and progression of the lamellipodium-lamellum interface [corrected]." Biophys J **97**(5): 1254-1264.

Shepard, L. A., A. P. Heuck, et al. (1998). "Identification of a membrane-spanning domain of the thiol-activated pore-forming toxin Clostridium perfringens perfringolysin O: an alpha-helical to beta-sheet transition identified by fluorescence spectroscopy." Biochemistry **37**(41): 14563-14574.

Siegel, G. J., R. W. Albers, et al. (2006). "Basic neurochemistry : molecular, cellular, and medical aspects." 7th.

Smith, P. K., R. I. Krohn, et al. (1985). "Measurement of protein using bicinchoninic acid." Anal Biochem **150**(1): 76-85.

Solovyova, A. S., M. Nollmann, et al. (2004). "The solution structure and oligomerization behavior of two bacterial toxins: pneumolysin and perfringolysin O." Biophys J **87**(1): 540-552.

Sonnen, A. F., A. J. Rowe, et al. (2008). "Oligomerisation of pneumolysin on cholesterol crystals: Similarities to the behaviour of polyene antibiotics." Toxicon **51**(8): 1554-1559.

Spreer, A., H. Kerstan, et al. (2003). "Reduced release of pneumolysin by Streptococcus pneumoniae in vitro and in vivo after treatment with nonbacteriolytic antibiotics in comparison to ceftriaxone." Antimicrob Agents Chemother **47**(8): 2649-2654.

Squire, L. R. and M. J. Zigmond (2003). Fundamental neuroscience. San Diego, Calif. ; London, Academic.

Srivastava, A., P. Henneke, et al. (2005). "The apoptotic response to pneumolysin is Toll-like receptor 4 dependent and protects against pneumococcal disease." Infect Immun **73**(10): 6479-6487.

Steinborn, M., K. C. Seelos, et al. (1999). "MR findings in a patient with Kernicterus." Eur Radiol **9**(9): 1913-1915.

Stringaris, A. K., J. Geisenhainer, et al. (2002). "Neurotoxicity of pneumolysin, a major pneumococcal virulence factor, involves calcium influx and depends on activation of p38 mitogen-activated protein kinase." Neurobiol Dis **11**(3): 355-368.

Suzumura, A., H. Takeuchi, et al. (2006). "Roles of glia-derived cytokines on neuronal degeneration and regeneration." Ann N Y Acad Sci **1088**: 219-229.

Tam, C., V. Idone, et al. (2010). "Exocytosis of acid sphingomyelinase by wounded cells promotes endocytosis and plasma membrane repair." J Cell Biol **189**(6): 1027-1038.

Thiery, J., D. Keefe, et al. (2010). "Perforin activates clathrin- and dynamin-dependent endocytosis, which is required for plasma membrane repair and delivery of granzyme B for granzyme-mediated apoptosis." Blood **115**(8): 1582-1593.

Tilley, S. J., E. V. Orlova, et al. (2005). "Structural basis of pore formation by the bacterial toxin pneumolysin." Cell **121**(2): 247-256.

Tweten, R. K. (2005). "Cholesterol-dependent cytolysins, a family of versatile pore-forming toxins." Infect Immun **73**(10): 6199-6209.

Vida, T. A. and S. D. Emr (1995). "A new vital stain for visualizing vacuolar membrane dynamics and endocytosis in yeast." J Cell Biol **128**(5): 779-792.

Vikman, K. S., E. Backstrom, et al. (2001). "A two-compartment in vitro model for studies of modulation of nociceptive transmission." J Neurosci Methods **105**(2): 175-184.

Vivian, J. T. and P. R. Callis (2001). "Mechanisms of tryptophan fluorescence shifts in proteins." Biophys J **80**(5): 2093-2109.

Weclewicz, K., K. Kristensson, et al. (1994). "Rotavirus causes selective vimentin reorganization in monkey kidney CV-1 cells." J Gen Virol **75 (Pt 11)**: 3267-3271.

Wee Yong, V. (2010). "Inflammation in neurological disorders: a help or a hindrance?" Neuroscientist **16**(4): 408-420.

Wippel, C., C. Fortsch, et al. (2011). "Extracellular calcium reduction strongly increases the lytic capacity of pneumolysin from streptococcus pneumoniae in brain tissue." The Journal of infectious diseases **204**(6): 930-936.

Wood, W. G., U. Igbavboa, et al. (1995). "Cholesterol oxidation reduces Ca(2+)+MG (2+)-ATPase activity, interdigitation, and increases fluidity of brain synaptic plasma membranes." Brain Res **683**(1): 36-42.

Young, J. A. and R. J. Collier (2007). "Anthrax toxin: receptor binding, internalization, pore formation, and translocation." Annu Rev Biochem **76**: 243-265.

Zhang, Y. and B. A. Barres (2010). "Astrocyte heterogeneity: an underappreciated topic in neurobiology." Curr Opin Neurobiol **20**(5): 588-594.

Zou, J., Y. X. Wang, et al. (2010). "Glutamine synthetase down-regulation reduces astrocyte protection against glutamate excitotoxicity to neurons." Neurochem Int **56**(4): 577-584.

Zysk, G., W. Bruck, et al. (1996). "Anti-inflammatory treatment influences neuronal apoptotic cell death in the dentate gyrus in experimental pneumococcal meningitis." J Neuropathol Exp Neurol **55**(6): 722-728.

7 ACKNOWLEDGEMENTS

I would like to thank…

…Dr. Asparouh Iliev for giving me the opportunity to work on this great project and for joining his group in Würzburg. I am very glad for the patience and great personal and scientific support in the last years. Furthemore, I am very thankful for the many occasions to present our data.

…Prof. Roland Benz for supervising my project and for giving me the opportunity to work with his group and to work with the planar lipid bilayer. I am very grateful for the fruitful discussions and ideas.

…Prof. Timothy Mitchell for his supervision, the lovely invitation to Glasgow and the impulse to also look for immunological parameters.

…Alexandra Bohl for her excellent, patient, friendly and very supportive technical assistance and her friendship.

…Elke Maier and all members of Prof. Benz's Group in Würzburg and in Bremen. Thank you for your help while working at the bilayer and for the great times.

…the members of the Iliev Group. Your honesty, your great humor, our trips and tips at work (high-throughput) made the time in Würzburg worth remembering.

…Prof. Martin Lohse and the members of the institute for pharmacology and toxicology for fruitful discussions. Especially M. Adler, S. Vogl, A. Seifried, J. Baetz, J. Wagner, S. Ramm, H. Popa-Henning and P. Bellwon. For asking the right questions at the right time and for the kindness to discuss scienftific and non-scientific issues while having a cup of coffee…

…Andreas Schäfer. For reading the thesis with helpful comments, although you are from a completely different background. For your partnership, love and loyalty.

…my parents and siblings. Danke für die jahrelange Unterstützung. Ohne Euch würde ich nicht da stehen, wo ich jetzt bin. Ohne Euch hätte ich dieses Ziel niemals verfolgt. Danke!

8 APPENDIX

8.1 Fold changes of IL-6

Table 14: Fold-changes of IL-6 production after Toxin challenge. Raises in IL-6 are either compared to the corresponding control or to the control of treated cells without HKSP.

	values normalised (CTRL corresponding)	values normalised (CTRL without HKSP)
PLY n.i.		2,06
PLY D		1,35
PLY B		1,88
Δ6 n.i.		0,85
Δ6 D		0,78
Δ6 B		0,99
W433F n.i.		0,93
W433F D		0,94
W433F B		0,92
PLY n.i. HKSP	1,50	1,34
PLY D HKSP	1,48	1,15
PLY B HKSP	1,47	1,87
Δ6 n.i. HKSP	0,92	0,83
Δ6 D HKSP	0,92	0,71
Δ6 B HKSP	0,80	1,02
W433F n.i. HKSP	0,85	0,76
W433F D HKSP	1,03	0,80
W433F B HKSP	0,83	1,06
CTRL HKSP n.i.	-	0,89
CTRL HKSP D	-	0,78
CTRL HKSP B	-	1,27

8.2 Protein ladders

Protein	Approximate Molecular Weights (kDa)				
	Tris-Glycine	Tricine	NuPAGE® MES	NuPAGE® MOPS	NuPAGE® Tris-Acetate
Myosin	250	210	188	191	210
Phosphorylase	148	105	98	97	111
BSA	98	78	62	64	71
Glutamic Dehydrogenase	64	55	49	51	55
Alcohol Dehydrogenase	50	45	38	39	41
Carbonic Anhydrase	36	34	28	28	n/a
Myoglobin Red	22	17	17	19	n/a
Lysozyme	16	16	14	14	n/a
Aprotinin	6	7	6	n/a	n/a
Insulin, B Chain	4	4	3	n/a	n/a

NuPAGE® Novex
Bis-Tris 4-12% Gel

IM-1008F 072602